HHS Public Access

Author manuscript

Neurosci Biobehav Rev. Author manuscript; available in PMC 2016 December 01.

Published in final edited form as:

Neurosci Biobehav Rev. 2015 December ; 59: 16–52. doi:10.1016/j.neubiorev.2015.09.007.

Neuroimaging of Parkinson's Disease: Expanding views

Carol P. Weingarten[a], **Mark H. Sundman**[b], **Patrick Hickey**[c], and **Nankuei Chen**[b,d]

Carol P. Weingarten: carol.weingarten@duke.edu

[a]Department of Psychiatry and Behavioral Sciences, Duke University School of Medicine

[b]Brain Imaging and Analysis Center, Duke University Medical Center

[c]Department of Neurology, Duke University School of Medicine

[d]Department of Radiology, Duke University School of Medicine

Abstract

Advances in molecular and structural and functional neuroimaging are rapidly expanding the complexity of neurobiological understanding of Parkinson's disease (PD). This review article begins with an introduction to PD neurobiology as a foundation for interpreting neuroimaging findings that may further lead to more integrated and comprehensive understanding of PD. Diverse areas of PD neuroimaging are then reviewed and summarized, including positron emission tomography, single photon emission computed tomography, magnetic resonance spectroscopy and imaging, transcranial sonography, magnetoencephalography, and multimodal imaging, with focus on human studies published over the last five years. These included studies on differential diagnosis, co-morbidity, genetic and prodromal PD, and treatments from L-DOPA to brain stimulation approaches, transplantation and gene therapies. Overall, neuroimaging has shown that PD is a neurodegenerative disorder involving many neurotransmitters, brain regions, structural and functional connections, and neurocognitive systems. A broad neurobiological understanding of PD will be essential for translational efforts to develop better treatments and preventive strategies. Many questions remain and we conclude with some suggestions for future directions of neuroimaging of PD.

Keywords

Parkinson's disease; Brain imaging; Neuroimaging; PET; SPECT; MRS; MRI; TCS; MEG; DTI; fMRI; Magnetic resonance imaging; Positron emission tomography; Diffusion tensor imaging; Functional connectivity

1. Introduction

Parkinson's Disease (PD) is the second most common neurodegenerative disorder and is increasing in importance as the population ages (Burke & O'Malley, 2013; Schapira, 2013).

40 Duke Medicine Circle, Room 414: BIAC, Durham, NC 27710, Tel.: +1 828 329 3268; fax: +1 919 681 7033.

The most well known neurobiological model of PD has provided a simplified schema for how changes in neurotransmitters and brain regions and networks can be the basis of motor symptoms in PD. The model is centered on the role of decreased availability of the neurotransmitter dopamine in regions and pathways of the cortico-basal ganglia-thalamocortical motor circuit (Delong, 1990; Galvan & Wichmann, 2008). However, it has long been known that PD also involves cognitive, mood, sleep, olfactory, and autonomic disorders in addition to motor dysfunction; neurotransmitters and other neurochemicals in addition to dopamine; and neuropathological findings in widespread regions of the brain, brainstem, spinal cord, and peripheral nervous system (Goedert et al., 2013; Langston, 2006; Smith et al., 2012; Sulzer & Surmeir, 2013). Thus it is important to examine a wide range of factors to better understand the neurobiological mechanisms of PD and its treatments, which can be accomplished in part through a wide array of neuroimaging techniques applied to the study of PD. We have reviewed a broad range of these neuroimaging studies of PD.

The first goal of this review was to provide an introduction to the variety and complexity of PD neurobiology (section 2). This knowledge serves as a foundation for interpreting neuroimaging findings that may further lead to more integrated and comprehensive understanding of PD (sections 3 and 4). To facilitate understanding of the diverse neuroimaging findings and their implications for PD research, the relevant background on brain regions, circuits, and neurochemistry in PD will be more systematically discussed (sections 2.2 to 2.4) than in most previous PD neuroimaging reviews.

Our second goal was to broadly review diverse areas of PD neuroimaging (section 3), including positron emission tomography (PET) (section 3.1), single photon emission computed tomography (SPECT) (section 3.1), magnetic resonance spectroscopy (MRS) (section 3.2), magnetic resonance imaging (MRI) (section 3.3), transcranial sonography (TCS) (section 3.4), magnetoencephalography (MEG) (section 3.5), and multimodal imaging (section 3.6). These modalities probe different features of the neurobiological involvement of PD and, collectively, are producing an increasingly complex set of findings about brain regions, neurochemicals, metabolism, blood flow, functional activation, and structural and functional connections and networks in PD. This review was performed with a focus on human studies published over the last five years (section 4), which included studies on PD molecular neuroimaging (sections 4.2 and 4.3), structural and functional neuroimaging (sections 4.4 and 4.5), PD differential diagnosis (section 4.6), co-morbid syndromes (section 4.6), genetic and prodromal PD (section 4.7), and treatments ranging from L-DOPA (levodopa) to brain stimulation approaches, transplantation and gene therapies (section 4.8).

A third goal was to systematically discuss the neuroimaging findings of changes in neurotransmitters and other neurochemicals, structure, function, neuronal circuitry, etc. in PD from two complementary perspectives: 1) a methodological perspective focused on how neuroimaging approaches have been used to address various clinical questions (sections 4.2 to 4.5); and 2) a clinical perspective focused on how a clinical topic has been investigated with various neuroimaging approaches (sections 4.6 to 4.8). Both perspectives are valuable and provide different insights into the contributions of neuroimaging to neurobiological understanding of PD.

Pubmed literature searches were used to identify neuroimaging studies of PD published in English. The neuroimaging modalities used in each study were identified and representative examples were selected, with a focus on major publications of human studies over the past five years. The final list of selected studies represents a wider range of neuroimaging studies of PD than has appeared in previous reviews.

2. Parkinson's Disease

We begin with description of motor features of Parkinsonism, other diagnoses that may be considered in the differential diagnosis of PD, and the importance of nonmotor co-morbid syndromes (section 2.1). Brain regions, structural pathways, and neurotransmitters of the most well known model of motor involvement in PD – the cortico-basal ganglia-thalamocortical motor circuit – will then be presented (section 2.2). Neuropathology of PD will be discussed centered on Braak's staging of PD, which describes the progression of pathological abnormalities in regions throughout the brain (section 2.3). Finally, biochemistry of neurotransmitter systems involved in PD will be summarized (section 2.4). These topics are a useful foundation for understanding and interpreting PD neuroimaging findings (sections 3 and 4).

2.1. Symptoms and diagnosis of PD

Parkinsonism (Parkinson's syndrome) comprises the motor symptoms of bradykinesia (slow movements), rigidity, tremor at rest, and postural instability (Hickey & Stacy, 2011). PD or idiopathic PD is the most common disorder presenting as Parkinsonism. Other diagnoses presenting with Parkinsonism include atypical parkinsonian syndromes such as corticobasal degeneration (CBD), dementia with Lewy bodies (DLB), multiple system atrophy (MSA), and progressive supranuclear palsy (PSP) (Stamelou & Hoeglinger, 2013). Parkinsonism may also be secondary to genetic mutations (Klein & Westenberger, 2012), side effects of medications (e.g. antipsychotic medications, amphetamine) (Ham et al., 2015), traumatic brain injury (Bhidayasiri et al., 2012), and toxins such as Mn (Criswell et al., 2011), etc. (Ali & Morris, 2014). Current validation of a diagnosis of PD is based on neuropathological findings. A recent study using post mortem neuropathological confirmation of PD indicated that clinical diagnostic accuracy was only 53% for patients with < 5 years disease duration, although 88% accuracy for patients with > 5 years duration (Adler et al., 2014). Thus development of neuroimaging for diagnosis of PD has been an important line of inquiry in PD neuroimaging (section 4.6).

There are also many nonmotor symptoms and co-morbid syndromes in PD. These include cognitive disorders, depression, olfactory dysfunction, sleep disorders, constipation, genitourinary dysfunction, etc. (Langston, 2006; O'Sullivan et al., 2008; Schapira & Tolosa, 2010). Cognitive dysfunction may appear in 15–20% of even early stage, untreated PD patients and eventually be found in over 80% of patients during long-term follow-up (Calabresi et al., 2013; Hely et al., 2008; Lin & Wu, 2015). Depression has been reported in 45 to 75% of PD patients (Jaunarajs et al., 2011; Lemke, 2008). Around 80% of patients with idiopathic rapid eye movement sleep behavior disorder (RBD) may convert to PD or atypical parkinsonian syndromes within 10 to 15 years (Mayer et al., 2015). Nonmotor symptoms, such as RBD, often pre-date motor symptoms - 98% of all de novo PD patients

report at least one nonmotor symptom at diagnosis (Erro et al., 2013). This suggests that neurodegeneration starts outside of the motor system, may involve nondopaminergic neurons, and has implications for diagnosis and development of preventive strategies.

Nonmotor symptoms can sometimes become more distressing to patients than motor symptoms. For example, depression has been described as “the single most important factor in PD patients’ reported quality of life, above disease severity and motor complications of L-DOPA therapy” (Jaunarajs et al., 2011: 2). Thus there is need for more understanding of both motor and nonmotor aspects of PD, and both have been the focus of many neuroimaging studies.

2.2. Classic model of cortico-basal ganglia-thalamocortical motor circuit in PD

Figure 1 shows a simplified schema of some key brain regions and pathways involved in the most well known model of motor dysfunction in PD. These are regions of the cortico-basal ganglia-thalamocortical circuit and the direct and indirect pathways (Delong, 1990; Honey et al., 2003; Lanciego et al., 2012). The basal ganglia comprise the dorsal striatum or the caudate and putamen above the internal capsule, globus pallidus externa, globus pallidus interna, subthalamic nucleus, substantia nigra pars compacta and substantia nigra pars reticularis, and the ventral striatum comprising the nucleus accumbens and caudate and putamen below the internal capsule. The major input to the basal ganglia is from the cortex to the dorsal striatum in the corticostriate pathway. Projection neurons of the corticostriate pathway use the excitatory neurotransmitter glutamate. Main outputs from the basal ganglia are projection neurons from the globus pallidus interna and substantia nigra pars reticularis to the thalamus. Both are inhibitory pathways employing the inhibitory neurotransmitter γ-aminobutyric acid (GABA). Thalamocortical excitatory glutamatergic projection neurons then complete the circuit back to the cortex.

Within the basal ganglia there are important pathways between the dorsal striatum and globus pallidus interna: (i) direct pathway, which is a monosynaptic connection from the dorsal striatum to globus pallidus interna; and (ii) indirect pathway, which is a polysynaptic connection from the dorsal striatum to globus pallidus externa to subthalamic nucleus to globus pallidus interna. Output from globus pallidus interna to thalamus is via inhibitory GABAergic pathways, i.e. the globus pallidus interna inhibits thalamic activity. Because thalamic output to the cortex excites the motor cortex, inhibition of thalamic activity leads to decreased motor activation.

Nigrostriatal connections lead from the substantia nigra pars compacta to the dorsal striatum, while striatonigral connections lead from the dorsal striatum to the substantia nigra pars reticularis. The neurotransmitter dopamine is synthesized in dopaminergic neurons whose cell bodies are located in substantia nigra pars compacta. The nigral dopaminergic projection neurons synapse with two kinds of dopamine receptors in the dorsal striatum, D1 and D2. D1 receptors modulate activity of medium spiny neurons that project to globus pallidus interna in the direct pathway, while D2 receptors modulate activity of medium spiny neurons that project to globus pallidus externa in the indirect pathway.

Dopaminergic input into the direct pathway via D1 receptors activates medium spiny neurons and leads to inhibition of globus pallidus interna. Inhibition of globus pallidus interna then diminishes its inhibition of the thalamus. This in turn leads to increased excitatory output from the thalamus to the cortex, i.e. activation of motor regions of the cortex. On the other hand, dopaminergic input into the indirect pathway via D2 receptors leads to inhibition of medium spiny neurons whose output normally inhibits globus pallidus externa. Thus the activity of globus pallidus externa is increased, which inhibits the subthalamic nucleus. When subthalamic nucleus activity is inhibited there is decreased activation of globus pallidus interna. From here the consequences follow the schema of the direct pathway described above: globus pallidus interna's inhibition of the thalamus is diminished; the thalamus activates the cortex; and motor regions are activated.

Degeneration of the substantia nigra pars compacta and, therefore, decreased dopaminergic output from substantia nigra pars compacta to the dorsal striatum has been the most highlighted neurobiological alteration in PD. According to the model in Figure 1, given that nigral dopaminergic output to the dorsal striatum promotes activation of the motor cortex, then loss of nigral dopaminergic output will lead to decreased motor activation. Thus this model explains cardinal motor features of PD as a hypokinetic disorder, e.g. bradykinesia and rigidity. Because it depends on alterations in the activity or firing rates of neurons it is known as the ""rate model" of movement disorders" (Wichmann & Dostrovsky, 2011:235).

This cortico-basal ganglia-thalamocortical circuit model defines a core set of brain regions, neurotransmitters, and structural connections that may be altered in PD. Many neuroimaging studies of neurotransmitters, brain regions, and connectivity networks in PD have drawn from this model and provided evidence for validity of many of its components.

However, the model also has inconsistencies with empirical evidence. For example, increased globus pallidus interna or decreased globus pallidus externa or thalamic activity does not always lead to parkinsonian motor dysfunction predicted by the model (Galvan & Wichmann, 2008). Importantly, "thalamotomy procedures did not result in worsening of parkinsonism" (Wichmann & Dostrovsky, 2011: 235). Further, although deep brain stimulation (DBS) of the subthalamic nucleus can be an effective PD treatment, subthalamic nucleus stimulation is "thought to increase GPi (globus pallidus interna) output to the thalamus," and according to the model this stimulation "should worsen rather than ameliorate parkinsonism" (Galvan & Wichmann 2008: 1463). The model ignores many brain regions, connections, and neurotransmitter systems known to be important in PD.

It also does not explain a key finding in the Parkinsonian state: abnormal beta oscillations in the brain's electrophysiological activity, such as local field potentials, in the beta range around 12–30 Hz (Galvan &Wichmann, 2008; Little & Brown, 2014; McCarthy et al., 2011). In PD, beta oscillations appear in regions of the cortico-basal ganglia-thalamocortical circuit, for example, frontal cortex, subthalamic nucleus, globus pallidus externa, and globus pallidus interna. Beta oscillations decrease after treatment with L-DOPA or subthalamic DBS, as well as after movement, and the decreases can correlate with improvement in bradykinesia and rigidity.

One model of beta oscillations in PD was based on a dynamic causal model (DCM) of the cortico-basal ganglia-thalamocortical circuit with direct and indirect pathways, along with the hyperdirect pathway and reciprocal pathways between globus pallidus externa and subthalamic nucleus (Figure 2a) (Moran et al., 2011). The hyperdirect pathway is a direct pathway between the subthalamic nucleus and the cortex. Studies of PD patients using DBS electrode electrophysiological measures have indicated that effective connectivity between the subthalamic nucleus and globus pallidus externa, globus pallidus interna, and cortex (hyperdirect pathway) may promote beta oscillations in the L-DOPA OFF state (Figure 2b) (Marreiros et al., 2013). Although beta oscillations are important in PD they have been difficult to study using neuroimaging. However, neuroimaging studies are now able to examine connectivities of some key pathways in models of beta oscillations, such as the hyperdirect pathway (section 4).

2.3. PD neuropathology: beyond the cortico-basal ganglia-thalamocortical motor circuit

There are numerous other brain regions beyond the classic cortico-basal ganglia-thalamocortical circuit that have been implicated in PD, particularly for non-motor symptoms. Table 1 lists some brain regions that have been highlighted in neuropathological studies of Lewy bodies and neurites in PD (Braak et al., 2004; Goedert et al., 2013). Lewy bodies and neurites are cellular inclusions that are aggregates of the protein α-synuclein and appear in neuron cell bodies or neuron cell processes (e.g. axons) respectively. Post mortem neuropathological investigations conducted by Braak and colleagues have described six stages of PD pathology in the brain. These describe spread of inclusion bodies from early (Stage 1) to late (Stage 6) stages in PD. Some brain regions involved in these stages are noted in Table 1. Note that the substantia nigra pars compacta in the midbrain, usually highlighted as the basis of dopaminergic and motor dysfunction in PD (e.g. Figure 1), is only one of many involved brainstem regions. The substantia nigra is also not the earliest region involved. Indeed, inclusion bodies appear first in the medulla in the dorsal motor nucleus of the vagus and in the olfactory cortex. Eventually “inclusion body pathology gradually overruns the entire neocortex” (Braak et al., 2004: 131). Some regions in Braak staging are the locations of cell bodies of projection neurons of major neurotransmitters in the brain, such as acetylcholine, dopamine, norepinephrine, and serotonin (Table 1). Note that some regions involved with nondopaminergic neurotransmitters show neuropathological involvement before nigral involvement.

Although it is outside the scope of this review, it is apparent that α-synuclein deposition extends outside the brain to involve the peripheral nervous system, including the spinal cord, enteric nervous system, adrenal medulla, and cardiac conduction system (Goedert et al., 2013; Sulzer & Surmeier, 2013). Indeed, the model of Braak and colleagues suggests that in the central nervous system, α-synuclein pathology starts from the dorsal motor nucleus of the vagus and spreads to rostral structures. This suggests that the gut could be a nidus, and the dorsal motor nucleus of the vagus a portal, for α-synuclein entrance to the CNS. Furthermore, there is increasing evidence that this spread then proceeds in a prion-like fashion throughout the brain (Goedert et al., 2013). Although these proposals are speculative, they may have important implications for the development of neuroprotective

strategies, as well as imaging of neural function outside the CNS in PD (Gjerløff et al., 2015; Stoessl, 2015).

PD becomes clinically manifest when neuropathological findings reach Braak Stages 3–4 and α-synuclein inclusions have reached the substantia nigra pars compacta. Some investigations have indicated that motor symptoms appear when there has been loss of approximately 30% of substantia nigra dopamine neurons or 50 to 70% of nigrostriatal dopaminergic axonal terminals in the striatum, although other studies have suggested that motor symptoms may appear with more preservation of dopamine neurons and striatal dopamine terminals than previously understood (Burke & O'Malley, 2013; Tabbal et al., 2012). Further, although Braak staging has drawn attention to α-synuclein inclusions in the substantia nigra and, therefore, degeneration of neuron cell bodies (soma) in the substantia nigra, it is possible that degeneration of neuron axon terminals in the striatum may progress more rapidly than degeneration of nigral cell bodies. Indeed, attention is now being given to the importance of axonal degeneration in the neuropathophysiology of PD. For example, Lewy neurites in axonal processes appear before Lewy bodies in neuron cell bodies. In particular, it has been proposed that axonopathy precedes cell body death of nigral dopaminergic projection neurons. This is referred to as "dying-back degeneration" (Burke & O'Malley, 2013: 73). Note that axons in the brain, both myelinated and unmyelinated, traverse the brain in white matter. Some implications of this axonal degeneration are that neuroimaging of white matter and white matter tracts, as well as functional connectivity networks, would be expected to show changes in PD, including in early stages. Many examples of such changes have been observed (Tables 3 and 5) and will be discussed in section 4.

2.4. Neurotransmitters in PD

Six small molecule neurotransmitters are the most important neurotransmitters in PD: acetylcholine, γ-aminobutyric acid, glutamate, dopamine, norepinephrine, and serotonin (5-hydroxytryptamine or 5-HT). All have been investigated in PD neuroimaging studies.

2.4.1. Glutamate and γ-aminobutyric acid—As described above, corticostriate and thalamocortical pathways are excitatory glutamatergic projections (Figure 1). Within the basal ganglia, projections from the subthalamic nucleus to globus pallidus externa or interna are also glutamatergic. However, GABA is the most common neurotransmitter of the basal ganglia nuclei; neuronal output from caudate, putamen, globus pallidus, and substantia nigra pars reticularis all comprise inhibitory GABAergic projections. These GABAergic outputs include the main output regions of the basal ganglia, which are the globus pallidus interna and substantia nigra pars reticulata. Glutamatergic and GABAergic pathways play central roles in the cortico-basal ganglia-thalamocortical circuit and the rate model of PD described in section 2.2 (Figure 1).

GABAergic neurons of the striatum are the subject of intensive study (Lanciego et al., 2012; Rice et al., 2011). There are two types of neurons in the striatum, with approximately 90% as projection neurons and 10% interneurons. The projection neurons (striatofugal) are medium spiny neurons and they are all GABAergic and, therefore, inhibitory. Medium spiny

neurons are differentiated by several characteristics including two different types of dopamine receptors, dopamine receptor subtype D_1 or subtype D_2. Dopaminergic projections from the substantia nigra pars compacta that synapse with D_1 or D_2 receptors lead to excitation or inhibition respectively of medium spiny neurons. Medium spiny neurons with D_1 receptors project to globus pallidus interna (direct pathway) and substantia nigra pars reticulata and co-express the large molecule neurotransmitters substance P and dynorphin, while medium spiny neurons with D_2 receptors project to the globus pallidus externa (indirect pathway) and release or co-express the large molecule neurotransmitter enkephalin (Levesque & Parent, 2005).

With respect to the other 10% of striatal neurons, these are mainly two types of interneurons. There are cholinergic interneurons that synthesize the neurotransmitter acetylcholine. There are also GABAergic interneurons. Although cholinergic and GABAergic interneurons may comprise only small percentages of striatal neurons they may have important roles in PD (Calabresi et al., 2006; Dehorter et al., 2009).

Recent MRI neuroimaging studies have indicated the importance of glutamate and GABA in predicting the strength of functional connectivity networks in normal persons (Kapogiannis et al., 2013) or resting motor network (Stagg et al., 2014). GABA may also play a special role in neurobiological mechanisms of negative functional connectivity and anticorrelated functional connectivity networks, such as those observed in some neuroimaging studies of PD (e.g. Di Martino et al., 2008; Hacker et al., 2012; Kelly et al., 2009; Liang et al., 2011; Liu, H. et al., 2013; Yu et al., 2013).

2.4.2. Dopamine—Dopamine is synthesized in neurons projecting from several regions of the brain including the substantia nigra pars compacta and ventral tegmental area (Düzel et al., 2009; Kwon & Jang, 2014). It is the neurodegeneration of the substantia nigra pars compacta and loss of dopaminergic input to the striatum that has been central to the classic model of PD and its treatment. Thus the production of dopamine and the integrity of these dopaminergic inputs to the striatum are critically relevant to studies of PD.

Dopamine is synthesized from the amino acid tyrosine (hydroxyphenylalanine) in dopaminergic neurons (Hammoud et al., 2007) (Figure 3). The first step takes place in the cytoplasm as tyrosine is converted to dihydroxyphenylalanine (DOPA) using the enzyme tyrosine hydroxylase. DOPA is then converted to dopamine using the enzyme aromatic l-amino acid decarboxylase (AAAD), also known as DOPA decarboxylase. Dopamine is then stored in cytoplasmic vesicles employing a vesicular monoamine transporter (VMAT). During neurotransmission dopamine is released from the vesicles into the synaptic cleft or extrasynaptic space. Though there are 5 types of dopamine receptors to which the released dopamine can bind, D1 and D2 are of primary importance in PD. Dopamine action ends in several ways. There is reuptake back into the neuron by way of a dopamine transporter (DAT) and then transport into vesicles for reuse. Alternatively, dopamine is catabolized with the enzymes monoamine oxidase (MAO) or catechol-O-methyltransferase (COMT).

The most important treatment approach for PD has been the pharmacotherapeutic agent L-3,4-dihydroxyphenylalanine or L-DOPA, a precursor of dopamine (Hickey & Stacy,

2011; Smith et al., 2012). Dopamine cannot cross the blood-brain barrier while L-DOPA can. Thus L-DOPA can be taken up by cells in the brain and then converted to dopamine by AAAD. L-DOPA is also converted to dopamine in the peripheral nervous system, which can lead to significant side effects. To counteract the peripheral conversion of L-DOPA to dopamine, a DOPA decarboxylase inhibitor such as carbidopa is given along with L-DOPA. Another approach to reverse the decrease in dopaminergic function in PD is use of dopamine agonists, such as ropinirole, rotigotine, and pramipexole. Inhibition of the catabolism of dopamine in the CNS is also possible using MAO inhibitors (e.g. selegiline and rasagiline) or COMT inhibitors (e.g. entacapone).

The main model of PD has been based on alterations in dopaminergic projections from the substantia nigra to the dorsal striatum in the motor loop. However, there is increasing attention to other dopaminergic projections to the striatum, especially for understanding nonmotor symptoms and side effects of treatments. The striatum is divided into the dorsal striatum and ventral striatum. The dorsal striatum and ventral striatum have been thought to receive dopaminergic afferents from the substantia nigra pars compacta and ventral tegmental area respectively. (However, see section 4.1 and Kwon & Jang (2014) for another view.) The pathway between the ventral tegmental area and nucleus accumbens is the center of the reward circuit and the mesolimbic system, which also includes dopaminergic projections from ventral tegmentum to the olfactory tubercle, hippocampus, amygdala, etc. This circuit is involved in reward-related perceptions, learning, memory, motivation, synaptic plasticity, attachment (social bonds), and mood disorders.

Figure 4 describes four pathways between the frontal cortex and striatum and a fifth direct connection between the frontal cortex and ventral tegmentum (Calabresi et al., 2013; Fuente-Fernandez, 2012; O'Callaghan et al., 2014). The motor loop - involving mainly the putamen that is also the first area of the striatum to lose dopamine in PD - has already been described above (Figure 1). Dysfunction of the motor loop has been used to explain the hypokinetic motor symptoms of PD of bradykinesia and rigidity. The other loops are especially helpful for explaining PD nonmotor symptoms and some treatment side effects. These other loops also feed into the globus pallidus, substantia nigra pars reticularis, and thalamus as described for the motor loop. However, this is a simplified schema and the mesolimbic and mesocortical loops have additional complex anatomical and functional features.

The hallmark of PD cognitive decline is in executive function, in contrast to Alzheimer's Disease (AD) for which memory decline is the hallmark (Narayanan et al., 2013). As PD progresses, dopamine depletion expands from the putamen to the dorsal caudate, which is connected to the dorsolateral prefrontal cortex and a key region in executive function. Executive function includes planning, attention, working memory, and task set-shifting. Involvement of the cortico-basal ganglia-thalamocortical dorsolateral prefrontal cortex loop can be a mechanism for important aspects of decline in executive function. It may also contribute to difficulties in motoric behaviors dependent on habit formation (O'Callaghan et al., 2014).

Additionally, it is notable that the hippocampus, a node in mesolimbic loops, has complex dopamine interactions (Calabresi et al., 2013; Russo and Nestler, 2013). The hippocampus degenerates in later stages of PD and leads to memory impairment and other cognitive dysfunction. There may also be hippocampal dysfunction from degeneration of cholinergic nuclei. All of these mechanisms may contribute to why cognitive dysfunction and dementia become increasingly important in later stages of PD.

Although the ventral striatum/nucleus accumbens and ventral tegmental area are spared in early PD, they, too, are eventually affected, with 60% loss of dopamine in the ventral striatum (Fuente-Fernandez, 2012). The orbitofrontal cortex and anterior cingulate cortex loops may be considered together as limbic loops. They are involved in apathy, anxiety, pain, and depression. Such psychiatric symptoms may be experienced by 75% of patients. One important feature of the limbic loops is that in earlier stages of PD they may be overstimulated by dopaminergic therapies given to treat motor symptoms. Recall that striatal dysfunction begins with dopamine depletion in the putamen while ventral striatal dopaminergic function remains intact. Thus dopaminergic treatments given to treat motor dysfunction and putaminal depletion in earlier stages may overdose the ventral striatal pathways. This can lead to impairments of the limbic loops, including impaired reversal-learning and reward-based cognitive functioning. It can also lead to emergence of impulse control disorders (ICD) (pathological gambling, hypersexuality, etc.) as a distressing behavioral side effect of treatment of motor dysfunction; ICDs may appear in 14% or more of PD patients on dopaminergic treatments (Weintraub et al., 2013).

Finally, the direct connection between the ventral tegmental area and frontal cortex also becomes impaired later than the motor loop, again suggesting that this pathway may be overstimulated from dopaminergic treatments in earlier stages. One consequence of hyperstimulation of this and limbic loops may be the prevalence of visual hallucinations and psychosis during dopaminergic treatments. Note that increased dopamine function has been implicated in schizophrenia and psychosis (Carlsson et al., 2000).

2.4.3. Norepinephrine—Norepinephrine in the brain is mainly synthesized in projection neurons of the locus coeruleus region of the pons. Locus coeruleus noradrenergic neurons project to the spinal cord, cerebellum, diencephalon (thalamus, hypothalamus), hippocampus and amygdala, and the entire neocortex (Figure 5). Norepinephrine is synthesized from dopamine, within cytoplasmic vesicles (see above), by the enzyme dopamine β-hydroxylase. Thus both dopamine and norepinephrine synthesis depend on activity of aromatic acid decarboxylase. Norepinephrine is released from the vesicles into the synaptic cleft where it binds to noradrenergic receptors. There are multiple types of noradrenergic receptors with the two main subtypes as α and β noradrenergic receptors. Norepinephrine action is terminated with reuptake into neurons via a norepinephrine transporter (NET) or catabolism using MAO or COMT. In PD, there is neurodegeneration of the locus coeruleus and decreased norepinephrine output.

Norepinephrine and serotonin have been central to many theories and treatments of affective disorders. This includes depression in PD (Bomasang-layno et al., 2015; Jaunarajs et al., 2011; Lewitt, 2012; Troeung et al., 2013). Degeneration of the locus coeruleus, the source of

noradrenergic projection neurons in the brain, occurs in PD relatively early in Braak Stage 2 (Table 1) (Goedert et al., 2013).

2.4.4. Serotonin—Serotonin synthesis also depends on aromatic acid decarboxylase and several steps similar to dopamine and norepinephrine. Serotonin is synthesized from the essential amino acid tryptophan in the raphe nuclei of the medulla and pons. The first step is conversion to 5-hydroxytryptophan using tryptophan hydroxylase. This is then converted to 5-hydroxytryptamine (5-HT) - serotonin - using aromatic acid decarboxylase. Serotonin is transported into vesicles using VMAT and then released from the vesicles into the synaptic cleft where it can bind with at least seven types of serotonin receptors. Reuptake into the neuron is conducted using a serotonin transporter (SERT), and serotonin is catabolized by MAO. Serotonergic projection neurons project to multiple regions in the brain, including the entire neocortex, substantia nigra, dorsal striatum, globus pallidus, thalamus, hippocampus, amygdala, and nucleus accumbens, and cerebellum (Figure 5). In PD there is neurodegeneration of the raphe nuclei and decreased serotonin output.

Along with norepinephrine, serotonin has been central to many theories and treatments of affective disorders including depression in PD. And similar to pathology of the noradrenergic locus coeruleus, degeneration of the raphe nuclei, the source of serotonergic projection neurons in the brain, begins in PD relatively early in Braak Stage 2 (Table 1) (Goedert et al., 2013).

Dyskinesias are abnormal, involuntary, distressing muscle movements that appear after long-term treatment of PD using L-DOPA or dopamine neural transplantations (Politis et al., 2012). Dyskinesias are also side effects of some antipsychotic pharmacotherapies (Tinazzi et al., 2014). The cause of dyskinesias in PD is not well understood. Increased activity of striatal glutamatergic systems has been implicated (Ahmed et al., 2011; Dupre et al., 2008), as well as nitric oxide activity, glial activation, and neuroinflammation (Bortolanza et al., 2015).

However, there is also evidence that serotonin function is involved in emergence of dyskinesias from treatment of PD. Aromatic acid decarboxylase, which is a key enzyme for synthesis of serotonin, norepinephrine, and dopamine, also catalyzes the conversion of L-DOPA to dopamine. The rationale of L-DOPA treatment in PD is to increase dopamine function in dopaminergic pathways to the striatum. However, L-DOPA can also be taken up by serotonergic projection neurons, including from SERT transporters, and converted to dopamine in serotonergic pathways. Some serotonergic projection neurons innervate the striatum. Thus it has been proposed that uptake of L-DOPA and conversion to dopamine in serotonergic projection neurons may lead to “aberrant” release of dopamine by serotonergic neurons in striatal pathways, i.e. as a “false neurotransmitter” (Politis et al., 2014: 1340). The aberrant release of dopamine in the striatum may then lead to dysfunction in the motor loop that appears as dyskinesia.

2.4.5. Acetylcholine—The final small molecule neurotransmitter is acetylcholine. In the central nervous system, acetylcholine is synthesized by projection neurons of the nucleus basalis of Meynert and septal nuclei that innervate the cerebral cortex, amygdala,

hippocampus, and thalamus; and pedunculopontine nucleus that innervate the substantia nigra pars compacta, thalamus, hypothalamus, and cerebellar nuclei (Figure 5) (Calabresi et al., 2006; Pahapill & Lozano, 2000). Acetylcholine is also synthesized by striatal interneurons in caudate, putamen, and nucleus accumbens. Acetylcholine is synthesized in the cytoplasm from choline and acetyl-CoA by choline acetyltransferase. Acetylcholine is then transported into vesicles by vesicle-associated transporter (VAT). Acetylcholine is released into the synaptic cleft and can bind to two main types of receptors, nicotinic (nAchR) or muscarininc (mAchR) receptors. Acetylcholine is inactivated in the synaptic cleft by acetylcholinesterase. In PD there is neurodegeneration of nucleus basalis of Meynert, septal nuclei, and pedunculopontine nucleus leading to decreased cholinergic output.

Dopamine and acetylcholine balance is an important factor in PD. When dopaminergic function declines in the striatum, a relative hyperactivity of cholinergic versus dopaminergic function develops in the striatum due to sparing of striatal cholinergic interneuron function, which is not affected in PD (Figure 5). This striatal interneuron cholinergic imbalance may play a role in the generation of abnormal beta oscillations in PD according to some models (McCarthy et al., 2011). Imbalance between dopamine and acetylcholine in the striatum can affect all the loops in the cortico-basal ganglia-thalamocortical circuits (Figure 4). In the motor loop this can increase motor dysfunction that may be ameliorated by anticholinergic treatments that block effects of the relative excess of cholinergic activity in the striatum. When dopaminergic depletion progresses from the dorsal to ventral regions there can also be cholinergic dependent dysfunction in executive function and limbic loops (Figure 4).

Finally, degeneration of the nucleus basalis of Meynert and pedunculopontine nucleus lead to depletion of cortical acetylcholine, which can also contribute to cognitive decline. (Mesulam, 2004). Also note that in the cerebral cortex, which is innervated by cholinergic projection neurons from the nucleus basalis of Meynert and dopaminergic projections from the ventral tegmental area (Figure 5), a relative hypoactivity of cholinergic versus dopaminergic function may further develop in some stages of PD since the nucleus basalis of Meynert cholinergic projection neurons degenerate before ventral tegmental area dopaminergic projection neurons to the cerebral cortex (Calabresi et al., 2006). This relative cholinergic hypoactivity in the cortex may be exacerbated by anticholinergic treatments given to ameliorate the relative cholinergic hyperactivity in the striatum involving cholinergic interneurons described above.

2.4.6. Other neurotransmitters—There are many other important neurotransmitters/neuromodulators in the neuropathophysiology of PD (see Rice et al. (2011) for a review). Large molecule neuroactive peptides include substance P and the endogenous opioid peptides dynorphin and encephalin. These help modulate basal ganglia neurotransmission. For example, as described above, medium spiny neurons of the dorsal striatum use GABA as their neurotransmitter. However, medium spiny neurons can also release substance P, dynorphin, or enkephalin (Lanciego et al., 2012). As another example, dopamine release in the nucleus accumbens (ventral striatum) from neurons from the ventral tegmental area may be modulated by dynorphins and enkephalins. Other neurotransmitters important in understanding PD include the endocannabinoids, adenosine, nitric oxide, and hydrogen

peroxide (H_2O_2). Cannabinoid receptors are found in the basal ganglia. There is some evidence that presynaptic cannabinoid receptors can modulate GABA release and medium spiny neuron activity. Adenosine is a neuromodulator with at least four subtypes of receptors A_1, A_{2a}, A_{2b}, A_3. A_{2a} receptors are found in the basal ganglia and interact with the dopamine receptor D_2 (Mishina et al., 2011). A_{2a} receptors are a major target of research into nondopaminergic compounds that affect basal ganglia function (Hickey & Stacy, 2011). H_2O_2, produced by dopamine neurons in the substantia nigra pars compacta may modulate somatodendritic release of dopamine in the substantia nigra pars compacta but not in the ventral tegmental area; this may be a factor in the greater involvement and degeneration of neurons in the substantia nigra versus ventral tegmental area in PD. NO produced by striatal interneurons may also modulate axonal release of dopamine.

3. Neuroimaging methods

This section will introduce neuroimaging methods that have been applied to PD. It begins with the molecular imaging modalities PET, SPECT, and MRS. These will be followed by MRI, TCS, MEG, and multimodal approaches.

3.1. Positron emission tomography and single photon emission computed tomography

PET and SPECT are molecular imaging methods that employ exogenous, radiolabeled agents (Hammoud et al., 2007; Niethammer et al., 2012; Price, 2012). In general, PET methods have better spatial resolution and sensitivity than SPECT. PET employs radioisotopes such as ^{11}C, ^{18}F, and ^{15}O that have relatively short half-lives and require a nearby cyclotron to provide the necessary radioisotopes. On the other hand, SPECT employs radioisotopes such as ^{123}I or ^{99m}Tc that have longer half-lives and do not require an on-site cyclotron. SPECT is less expensive and more widely available than PET and is a valuable imaging modality for many PD applications.

Tables 2 and 5 provide examples of radioligands that have been used to study PD. Politis (2014) has listed over 100 possibly useful radioligands and more are in development (Appel et al., 2015; Bagchi et al., 2013; Boassa et al., 2013; Bu et al., 2014; Coakeley & Strafella, 2015; Kiessling, 2014). Many radioligands probe neurotransmitter systems and depend on sophisticated application of the biochemistry of neurotransmitters (Brooks, 2005; Brooks & Pavese, 2011; Hammoud et al., 2007). Neurotransmitters (or neuromodulators) that have been investigated in PD include acetylcholine, adenosine, cannabinoid, dopamine, GABA, glutamate, norepinephrine, and serotonin.

One common approach to the study of neurotransmitters uses ^{18}F-FDOPA (fluoro-dihydroxyphenylalanine) PET imaging to target activity of aromatic acid decarboxylase, the enzyme that catalyzes the last step in synthesis of the monoamines dopamine, norepinephrine, and serotonin (see section 2). ^{18}F-FDOPA is a substrate for aromatic acid decarboxylase. Thus the uptake of ^{18}F-FDOPA can reflect the activity of aromatic acid decarboxylase, as well as transport and vesicular storage of synthesized dopamine, norepinephrine, and serotonin. Because the three monoamines are synthesized in different brain regions, and their projection neurons are also unique, the pattern of ^{18}F-FDOPA findings can be used to understand the three monoamines:^{18}F-FDOPA findings in the dorsal

and ventral striatum can be used for dopamine function; locus coeruleus for norepinephrine function; and raphe nuclei for serotonin function (e.g. Pavese et al., 2010).

Other aspects of neurotransmitter function investigated using PET or SPECT radioligands include vesicular transporters, reuptake transporters, neurotransmitter receptors, and enzymes that catabolize neurotransmitters such as acetylcholinesterase (Table 2) (section 2). For example, transport of dopamine into vesicles can be probed using radioligands such as ^{18}F-DTBZ and ^{18}F-F-AV to target vesicular monoaminergic transporter VMAT. Both D1 and D2/D3 receptor functions can be targeted using radioligands such as ^{11}C-NNC, ^{123}I-IBZM, and ^{11}C-RAC. The transporter that mediates reuptake of dopamine back into the neuron after dopamine has been released, i.e. dopamine transporter DAT, can be investigated using several radioligands including SPECT or PET imaging of versions of ioflupane or ^{123}I-FP-CIT, ^{18}F-FP-CIT, ^{99m}Tc-TRODAT, etc.

There are neurochemicals other than neurotransmitters/neuromodulators that can also be imaged using PET/SPECT (Tables 2, 5). These often target neurodegenerative processes in the brain. The radioligand ^{11}C-PIB has been used to image β-amyloid plaques, which are found in Alzheimer's disease and also approximately 40% of PD patients with dementia (Edison et al., 2013). Several radioligands have been used to image tau protein aggregates, which appear in disorders such as Alzheimer's disease, chronic traumatic encephalopathy, and PD and some atypical parkinsonian disorders (Coakeley et al., 2015; Villemagne et al., 2015). Another valuable PET radioligand is ^{11}C-(R)PK11195, which has been used as a marker for mitochondrial translocator protein (TSPO, tryptophan-rich sensory protein) found in microglia (Iannaccone et al., 2013). Microglia are activated in the brain's inflammatory response, which can include upregulation of TSPO and then increased binding of ^{11}C-(R)PK11195.

Note that although α-synuclein deposits (Lewy bodies) are the neuropathological hallmark of PD, there is no current method for human in vivo neuroimaging of α-synuclein (Vernon et al., 2010).

Finally, PET/SPECT is used for functional imaging of the brain (Tables 2, 5). Physiological cerebral glucose metabolism can be measured with ^{18}F-FDG (fluorodeoxyglucose) PET, and cerebral blood flow (CBF) or perfusion measured using ^{15}O-H_2O PET. Perfusion studies have also been performed using SPECT with the radiotracer ^{99m}Tc-ECD (ethylene cysteine dimer). PET/SPECT measures of cerebral metabolism or CBF have been employed for functional imaging of brain activity during motor and other tasks (section 4.5). These approaches have also been used to assess several types of spatial covariance patterns in the resting-state in PD (Ma et al., 2007; Eidelberg, 2009) (e.g. sections 4.6 and 4.8).

Use of PET/SPECT includes invasive administration of radioactive compounds, which can limit some applications especially for repeated or longitudinal studies or study of younger populations. Nonetheless, current PET/SPECT methods can be conducted safely and these modalities have been widely used for study of patients and normal subjects. The capabilities of PET/SPECT imaging to investigate the brain at molecular levels through use of numerous biochemical probes is currently unmatched by other neuroimaging modalities. Although the

temporal resolution of PET/SPECT (minutes) is lower than fMRI (seconds), PET/SPECT functional imaging provides relatively direct measures of metabolism and CBF in comparison with functional MRI (fMRI), which is based on a more indirect measure of brain function. Thus PET/SPECT functional imaging of glucose or oxygen metabolism or CBF in resting-state or task-based studies is very valuable. PET/SPECT approaches can also be less sensitive to motion artifacts than MRI, an important consideration in the study of movement disorders.

3.2. Magnetic resonance spectroscopy

Magnetic resonance spectroscopy is a magnetic resonance modality (see MRI below) that allows for relatively direct imaging of many biochemical compounds (Dager et al., 2009; Posse et al., 2013; Sharma et al., 2013; Tuite et al., 2013) (Table 2). These methods include single voxel MRS as well as MRS imaging (MRSI). Proton ^{1}H-MRS and MRSI have been used to investigate a wide range of endogenous neurochemicals in PD, such as the neurotransmitters dopamine, GABA, and glutamate (Emir et al., 2012; Gröger et al., 2014). Additional neurochemicals are investigated as markers of neurodegeneration in PD, such as N-acetylaspartate as a marker of healthy neurons, creatine moieties as a marker of energy metabolism, and glutathione as a marker of oxidative stress. MRS of a different nucleus, ^{31}P, can be used to investigate energy metabolism by imaging high energy phosphate (phosphocreatine, adenosine triphosphate) and low energy free phosphate (free phosphate) moieties in the brain (Weiduschat et al., 2014). MRS can also be used to assess glycerophosphocholine and glycerophosphoethanolamine as markers of membrane catabolism, or myoinositol as a marker of glial activity or osmotic status.

The spatial and temporal resolution of MRS is less than PET/SPECT and other MRI methods. However, MRS can image important biochemicals relatively directly, noninvasively, without radiation exposure, and probe some biochemical systems that cannot be investigated using other (PET/SPECT) molecular imaging approaches.

3.3. Magnetic resonance imaging

MRI uses magnetic fields to create images of the body by detecting spin properties of nuclei. Most MRI studies are based on ^{1}H nuclei of hydrogen atoms – protons – found endogenously throughout the body. Structural MRI, perfusion MRI, diffusion weighted imaging (DWI) or diffusion tensor imaging (DTI), and functional MRI have been used in PD neuroimaging (Pyatigorskaya et al., 2013; Tuite et al., 2013; Zhang & Liu, 2013). Many applications of these MRI approaches to PD can be found in studies listed in Tables 3 and 5 and discussions in section 4 below.

Morphometric studies of sizes and shapes of brain regions in PD have been performed using anatomical *T1-weighted imaging* (T1 is the spin-lattice relaxation time). Recently, a neuromelanin sensitive T1-weighted imaging method has been developed for improved imaging of substantia nigra pars compacta and locus coeruleus based on presence of neuromelanin in dopaminergic neurons (Garcia-Lorenzo et al., 2013). *T2- or T2*-weighted imaging* can also be used for structural imaging of PD (T2 is the spin-spin relaxation time and T2* is a function of T2 and also magnetic field inhomogeneities). Note that T2- and

T2*- [or the transverse relaxation rate R2* where R2*= (1/T2*)] weighted MRI are sensitive to the presence of paramagnetic iron, which is found in the substantia nigra. Because of this sensitivity to iron, T2 and T2* weighted imaging of the substantia nigra were among the earliest MRI studies of PD (Tuite et al., 2013). Another MRI method that is sensitive to the presence of iron is *susceptibility weighted imaging.* These studies have shown refined imaging of the substantia nigra, including the nigrosomes (e.g. Schwarz et al., 2014). *Quantitative susceptibility mapping (QSM)* has also shown improved imaging of the subthalamic nucleus and globus pallidus interna (Liu, T. et al., 2013).

Although hydrogen protons are found in biochemical molecules throughout the body, most MRI methods are primarily sensitive to hydrogen belonging to freely mobile water molecules rather than hydrogen associated with biochemical macromolecules and tissue microstructural elements such as myelin, membranes, or proteins, which have highly restricted and slow motions. However, two MRI methods have sensitivity to protons with characteristics of the macromolecular pool: *magnetization transfer (MT)* (Henkelman et al., 2001; Tambasco et al., 2015), and *rotating frame adiabatic $R_1\rho$ relaxation* (Andronesi et al., 2014). Because of their sensitivity to the macromolecular pool of protons, these methods may be useful for assessment of alterations in tissue microstructure and integrity in PD.

Arterial spin labeling (ASL) is based on magnetic labeling of water molecules in blood, which can then be imaged as a tracer for blood flow (Detre et al., 2012). ASL can be used to assess cerebral perfusion and may be useful as an MRI alternative to PET/SPECT measurements of cerebral perfusion in PD (Ma et al., 2010a; Melzer et al., 2011). ASL neuroimaging results have compared favorably with ^{15}O-H_2O PET perfusion and also ^{18}F-FDG PET glucose metabolic patterns in PD (Ma et al., 2010a).

Diffusion weighted MRI is based on effects of diffusion of water molecules on MRI images (Alexander et al., 2007; Hagmann et al., 2006; Le Bihan, 2003). Diffusion of water molecules depends, in turn, on microstructural characteristics of the tissues through which the water molecules diffuse. For example, water molecules can diffuse more rapidly in the cerebrospinal fluid (CSF) of the ventricles than in gray matter regions of the brain. One measure of diffusion is the diffusion coefficient, which in tissues is approximated by the apparent diffusion coefficient (ADC). Diffusion weighted MR imaging can be used to map ADCs in different regions of the brain. Another characteristic of diffusion is whether molecules move isotropically, i.e. equally in all directions, or anisotropically, i.e. unequally in different directions. Water molecules in a compartment like a neuron's soma (body) may be able to move relatively equally in all directions, but in a neuron's axon may have hindered motion in the direction perpendicular to the long axis of the axon and myelin fibers. *Diffusion tensor imaging* is sensitive to the anisotropy of diffusion. DTI measures include fractional anisotropy (FA), a measure of the anisotropy of diffusion, and also mean diffusivity (MD), axial diffusivity (AD), and radial diffusivity (RD) (Alexander et al., 2007; Le Bihan, 2003; Madden et al., 2012). Both white matter and gray matter can be assessed using DTI measures (Table 3). Of special note is that DTI can be used to reconstruct white matter axonal tracts, including the large-scale structural connections of the brain (Abhinav et al., 2014; Bach et al., 2014; Farquharson et al., 2013; Wakana et al., 2004).

Functional MRI was developed to study brain activations associated with specific tasks. It is based on the blood oxygenation-level dependent (BOLD) MRI method, which is sensitive to localized changes in levels of blood oxygenation in brain regions that are activated. The relationship between neural activation or inhibition and BOLD MRI signals is complex and continues to be investigated (Logothetis, 2008). The current standard model for BOLD signals is that neural activation involves a local neurovascular response that leads to localized increase of blood flow and oxygenated hemoglobin levels, which then leads to a localized increase in fMRI BOLD signal.

Although fMRI signals typically increase during task performance in activated regions of the brain, fMRI signals also show spontaneous fluctuations or oscillations at approximately 0.01 to 0.1 Hz. These low frequency signal fluctuations, in different regions of the brain, can be synchronized or temporally correlated (Biswal et al., 2010; Di et al., 2013; Du et al., 2014). This synchronized activity reflects functionally connected brain regions or networks. Functional connectivity can be assessed during tasks or in the resting state. Current interest is especially focused on resting-state studies (Tables 3, 5). Resting-state functional connectivity (rsfc) may be referred to as intrinsic functional connectivity, and functional connectivity networks as intrinsic connectivity networks. Many intrinsic connectivity networks have been described, such as the default mode, executive, sensorimotor, salience, dorsal attention, visual, and auditory networks (Fox et al., 2005; Raichle, 2011; Shine et al., 2014; Van den Heuvel et al., 2010). The spontaneous fluctuations in fMRI BOLD signals can also be characterized by their regional homogeneity (ReHo) in a cluster of voxels, which may reflect how well neural function is synchronized in the region (Wu et al., 2009). Another important measure of these fluctuations is their amplitude, as amplitude of low frequency fluctuations (ALFF) or fractional ALFF (fALFF) (Aiello et al., 2015; Biswal et al., 2010).

Graph theoretical analyses of connectivity networks describe the organization of connectivity networks as nodes joined by edges. Baggio et al.'s (2014) graph theoretical analysis of functional connectivity networks in PD patients includes helpful introductions to common terms used in graph theory analyses: nodes, edges, betweenness, characteristic path length, clustering coefficient, degree, global efficiency, hubs, local efficiency, modularity, small world topology, etc.

MRI in PD investigations is a noninvasive approach and does not expose subjects to radiation. This safety profile, along with excellent spatial and temporal resolution and wide availability, has led to widespread applications of MRI for structural and functional neuroimaging investigations of PD.

3.4. Transcranial sonography

TCS is a noninvasive ultrasound imaging method that is being developed for structural imaging of some brain regions in PD and has potential use in the clinical diagnosis of PD (Alonso-Canovas et al., 2014; Bouwmans et al., 2013; Mehnert et al., 2010; Politis, 2014; Sahuquillo et al., 2013; Stenc et al., 2015). Most TCS studies of PD have focused on echogenicity of the substantia nigra, but other brain regions have also been assessed, such as the lenticular nucleus, raphe nuclei, and ventricles.

So far TCS has been applicable for study of only a few brain regions in PD. TCS also depends on an adequate acoustic window through the skull: some patients lack this window and are, therefore, unsuitable for examination using TCS. Further, TCS is very dependent on operator skill and can be difficult to employ reliably (Alonso-Canovas et al., 2014; Miller & O'Callaghan, 2015). Nonetheless, TCS is much less expensive than MEG, MRI, PET, and SPECT modalities. This could be an important advantage for clinical applications of TCS if adequate clinical validity and reliability are demonstrated.

3.5. Magnetoencephalography

MEG is a functional neuroimaging technology that detects electromagnetic fields primarily associated with neuronal currents of pyramidal cells of the cerebral cortex (Stam, 2010). MEG has overlap with electroencephalography applications. Oscillations in different frequency bands (e.g. alpha, beta, etc.) and synchronization of oscillations between different brain regions can be assessed. MEG has been used to study cortico-muscular coherence (Airaksinen et al., 2015) and predict dementia in PD (Olde Dubbelink et al., 2014b). MEG has also been used to study functional connectivity alterations in PD (Olde Dubbelink et al., 2013, 2014a; Ponsen et al., 2013).

MEG is noninvasive and can more directly measure neural function than PET/SPECT or MRI. It also has superior temporal resolution (milliseconds) compared with other neuroimaging modalities used to study PD such as PET/SPECT or MRI, while having useful spatial resolution (Meyer-Lindenberg, 2010). However, MEG is more costly than other methods in several ways, which has so far resulted in less availability for investigational purposes or clinical utility.

3.6. Multimodal neuroimaging

Any single imaging modality will have benefits and limitations in comparison with other imaging modalities. Multimodal imaging combines imaging from complementary modalities to enhance the benefits of imaging. Multimodal imaging can refer to imaging platforms that allow for acquisition of imaging data from more than one modality sequentially or simultaneously (Price, 2012). Hybrid SPECT/CT and PET/CT platforms were the earliest examples of these platforms and allowed for improved integration of structural (CT) and metabolic (PET/SPECT) imaging data (Basu & Alavi, 2008). Some PD studies have employed hybrid ^{18}F-FP-CIT or ^{18}F-FDOPA PET/CT (Bhidayasiri et al., 2012; Park et al., 2014; Song et al., 2014) or ^{123}I-FP-CIT SPECT/CT (Sydoff et al., 2013)

Technological advancements with more complex PET/MRI platforms are beginning to make it possible for simultaneous MRI structural or functional and PET molecular imaging (Jadvar & Colletti, 2014; Riedl et al., 2014). Hybrid PET/MRI has been used to compare ^{18}F-FDG PET and fMRI ALFF, ReHo, and functional connectivity degree of centrality measures in normal subjects (Aiello et al., 2015). Applications to the study of PD are still in developmental stages, although use of PET/MRI with ^{18}F-Florbetan amyloid PET and structural MRI to diagnose a Lewy body dementia has been reported (Werner et al., 2015).

Multimodal imaging may also refer to methods that utilize data acquired separately from different modalities. Several combinations of PET and MRI results have been applied to PD: dopaminergic PET imaging and fMRI to understand striatal dopamine modulation of functional connectivity networks (Baik et al., 2014; Lebedev et al., 2014); ^{18}F-FDG PET and structural MRI to assess metabolic and morphometric changes in the brain after mesenchymal stem cell treatment for MSA (Lee et al., 2012); ^{18}F-FDOPA PET, TCS of the substantia nigra, and DTI of the olfactory tract and hyposmia in PD (Scherfler et al., 2013); and ^{11}C-PiB PET, ^{18}F-FDG PET, and structural MRI for differential diagnosis of DLB from Alzheimer's disease (Kantarci et al., 2012). The term multimodal has also been used for MRI studies that combine structural, functional connectivity, and diffusion weighted imaging in a single study (e.g. Aquino et al., 2014; Garcia-Lorenzo et al., 2013; Long et al., 2012; Yao et al., 2014). These studies demonstrate the potential value of integration of different neuroimaging approaches to improve neurobiological understanding of PD.

4. Neuroimaging of PD

To help illustrate the variety and complexity of PD neuroimaging studies we will now focus on several topics for more detailed discussions. We begin with some recent neuroimaging studies that have probed PD relevant neural systems in healthy participants (section 4.1). These studies are making important contributions to understanding of the normal state of brain regions, connections, and neurotransmitter functions that may be altered in PD and its treatments. This will be followed by several topics from neuroimaging of PD patients. These topics were chosen from two complementary perspectives: 1) a methodological perspective focused on how neuroimaging approaches have been used to address various clinical questions (sections 4.2 to 4.5), followed by 2) a clinical perspective focused on how a clinical topic has been investigated with various neuroimaging approaches (sections 4.6 to 4.8). The methodological perspective includes discussions of molecular neuroimaging of neurotransmitter systems and other neurochemicals; structural, perfusion, and diffusion weighted MRI; and functional imaging of PD. These discussions will primarily draw from comparisons of PD patients with healthy controls. We will then take up clinical perspectives on neuroimaging of differential diagnosis of PD and co-morbid syndromes; genetic PD and prodromal syndromes; and treatment effects. Some studies will be described in more depth to provide examples of more detailed illustration of these complex investigations. Summaries of some key results from neuroimaging studies of PD are provided in Tables 2, 3, and 5.

Note that the focus of our review was human studies. Thus all studies in discussions that follow were human studies unless identified as an animal study; also, all studies in Tables 2 to 5 were human studies. The majority of PD neuroimaging studies have been conducted in the resting-state. Thus neuroimaging studies in discussions that follow or are listed in Tables 2 to 5 were resting-state studies unless noted to be task-based. Finally, results from neuroimaging studies of PD treatments presented in our discussions or Table 5 were focused on longitudinal studies.

4.1. PD relevant normal brain structure and function

Much of our understanding of brain structure and function relevant to PD was derived from animal studies or human lesion or post mortem studies rather than observations in vivo in humans. Figure 6 shows white matter pathways that have been imaged only recently for the first time in vivo in humans using DTI. These include the nigrostriatal, nigrothalamic, pallidothalamic, subthalamopallidal, striatopallidal (Lenglet et al., 2012), and hyperdirect pathways (Brunenberg et al., 2012) in normal subjects; and cerebellar subthalamopontocerebellar and dentatothalamic tracts in PD patients (Sweet et al., 2014).

Our understanding of how midbrain dopaminergic neurons project to the striatum, with dopaminergic neurons from substantia nigra pars compacta mainly projecting to dorsal striatum while those from the ventral tegmental area project to ventral striatum and frontal cortex (Figures 4 and 5), was also derived primarily from animal studies (Düzel et al., 2009). However, DTI studies have now indicated that the substantia nigra pars compacta in humans actually has more structural connectivity with the ventral striatum and frontal cortex than does the ventral tegmental area (Kwon & Jang, 2014). If valid these findings will alter understanding of key regions and connectivity networks involved in PD.

Another aspect of the normal brain that is important in PD is organization of the basal ganglia. Recent neuroimaging studies of structural and functional connectivity of the basal ganglia (Barnes et al., 2010; Di Martino et al., 2008; Draganski et al., 2008; Kim, D. et al., 2013; Lenglet et al., 2012; Postuma et al., 2006; Tziortzi et al., 2014) have been largely consistent with earlier models of segregated parallel loops between the basal ganglia and cortex (Fuente-Fernandez, 2012; O'Callaghan et al., 2014) (Figure 4). Refinements to these models include some overlap between loops and information about smaller subregions.

An understanding of the role of dopamine in the normal brain is also critical to understanding PD and its treatment with dopaminergic agents. For example, Kelly et al. (2009) administered L-DOPA to healthy subjects and observed that functional connectivity increased between putamen and cerebellum and midbrain ventral brainstem, but decreased between right dorsal caudate and default mode network. Further, functional connectivity between the inferior ventral striatum and ventrolateral prefrontal cortex (task-positive network) or posterior cingulate cortex (default mode network) was increased or decreased by L-DOPA respectively. L-DOPA also decreased functional connectivity within the default mode network. In another study, Cole et al. (2013) compared administration of L-DOPA, the dopamine antagonist haloperidol, and placebo in normal subjects. Results included that functional connectivity between a basal ganglia limbic network (BGLN) and precentral and postcentral gyri (motor cortex) was increased by dopamine but decreased by haloperidol relative to placebo (L-DOPA > placebo > haloperidol). However, BGLN functional connectivity with anterior/mid cingulate region was higher in placebo than either L-DOPA or haloperidol. Default mode network functional connectivity with several cortical regions showed variable results for the three agents. Results indicated complex linear and nonlinear dopaminergic modulation of different functional connectivity networks.

Because dopamine is synthesized in humans from the amino acid tyrosine (Figure 3), it is possible to manipulate dietary sources of tyrosine to deplete dopamine within a few hours.

Carbonell et al. (2014) used this approach to assess resting-state functional connectivity in normal subjects in a dopaminergic depleted state. Observations included that the normal segregation of task positive and default mode networks, as well as functional connectivity within the task positive network, were impaired in the lowered dopamine state; these may be factors for cognitive impairment in PD.

Finally, Tzioritzi et al. (2014) conducted a multimodal study that combined PET imaging of D2/D3 receptors with diffusion weighted MRI to investigate amphetamine induced dopamine release in the striatum in normal subjects. They concluded that approximately 80% of cortical connections to the striatum were from the frontal lobe, followed by the parietal lobe, then temporal lobe, and only 2% from the occipital lobe. With respect to frontal cortical connections with the striatum, approximately 50% of connections were from executive frontal regions (e.g. dorsolateral prefrontal cortex), 20% from limbic regions, and rostral and caudal motor regions comprised only approximately 9+/− 5 and 4 +/− 3% respectively. Thus: “executive projections occupy a large portion of the striatum, and this finding contradicts the concept that striatum is primarily a motor functional region” (Tziortzi et al., 2014: 1173). Advances are also being made regarding the normal role of GABA in motor networks. For example, Stagg et al. (2014) conducted a multimodal study that combined MRS and fMRI to show that GABA levels in the primary motor cortex were negatively correlated with resting-state functional connectivity in the motor network. In addition, transcranial direct current stimulation to the primary motor cortex, which is known to decrease GABA levels, resulted in increased functional connectivity in the motor network.

Overall, these studies of normal brain structure and function show that much remains to be known about the normal state of the brain that may be altered by PD and its treatments. They also point to experimental approaches that could be applied to PD patients.

4.2. Molecular neuroimaging of neurotransmitter function

The most frequently investigated neurotransmitter system in PD has been dopamine. One of the most repeated observations is that PD patients compared with healthy controls show decreased dopamine function in the striatum (caudate and putamen) (Bajaj et al., 2013; Brooks & Pavese, 2011; Suwijn et al., 2015). This has been observed in PET/SPECT studies of aromatic acid decarboxylase activity, dopamine receptors, and dopamine and vesicular monoamine transporters (Table 2). Further, there is a gradient of dopaminergic dysfunction with earliest and greatest decrease in function occurring in the posterior putamen, followed by the anterior putamen, and then the caudate (Brooks and Pavese, 2011; Gröger et al., 2014; Hacker et al., 2012; Zhang & Liu, 2013). Dopaminergic dysfunction in the striatum, especially in the posterior putamen which is the striatal region with more connectivity with motor cortical region, is consistent with the clinical importance of motor impairment.

Although most dopaminergic studies have assessed striatal dopaminergic function, alterations in other regions of the brain have also been observed. For example, PD patients compared with controls have shown increased dopamine transporter function in the extrastriatal region of the ventromedial prefrontal cortex (Lee, J.-Y. et al., 2014). This is part of the mesolimbic dopaminergic system, which has implications for dopaminergic treatment

side effects such as impulse control disorders in PD. Another example is from Gröger et al. (2014), who recently used MRSI to make the first direct in vivo observations of dopamine depletion in the substantia nigra in PD. Rostral and caudal portions of the substantia nigra, approximating the substantia nigra pars reticulata and compacta respectively, showed decreased dopamine levels in PD, with lower levels in caudal than rostral substantia nigra. This is consistent with pathological observations of nigral degeneration in PD (Braak et al., 2004).

There have been multimodal studies of PET imaging of dopaminergic function combined with fMRI for functional connectivity networks in PD. For example, Baik et al. (2014) observed positive correlations between posterior putamen dopaminergic function and functional connectivity of the caudate with postcentral/precentral regions, anterior putamen with dorsolateral frontal regions, and posterior putamen with cerebellar cortices or dorsolateral frontal regions. Negative correlations were observed between posterior putamen dopaminergic function and connectivity of anterior putamen with mesiofrontal regions, and connectivity of posterior cingulate cortex with anterior prefrontal or parietal regions. Results indicated a variety of associations between putaminal dopaminergic function and connectivity networks with implications for PD symptoms and dopaminergic treatment effects.

There are also molecular neuroimaging studies of all the other major neurotransmitters. For example, with respect to cholinergic function, Meyer et al. (2009) observed that patients with PD compared with healthy controls showed decreased nicotinic receptor binding in the midbrain, pons, anterior cingulate cortex, frontoparietal cortex, and cerebellum. Suggested mechanisms for the decline of cholinergic receptor binding included degeneration of nigrostriatal dopaminergic neurons that also have cholinergic receptors, mesocorticolimbic dopaminergic neurons, cholinergic projection neurons from the basal nucleus of Meynert, pedunculopontine nucleus, or striatal cholinergic interneurons. However, a more recent study of nicotinic receptor function in early stage PD showed nicotinic receptor density that was “higher in the putamen, the insular cortex, and the supplementary motor area and lower in the caudate nucleus, the orbitofrontal cortex, and the middle temporal gyrus” (Isaias et al., 2014: 1). Increased receptor density indicated compensatory upregulation of cholinergic function in some regions. The investigators remarked that their study was the first to observed increased nicotinic receptor binding in PD and suggested that the discrepancy could be due to differences in patient characteristics or, that in their study, patients had been off dopaminergic pharmacotherapy for a much longer (72 hours) period at the time of scanning than in other studies. Although neuroimaging of the peripheral nervous system is outside the scope of this review, we note that a recent study of PD by Gjerløff et al. (2015) applied PET imaging of cholinergic function to the study of organs other than the brain. They observed decreased ^{11}C-donepezil binding as a measure of acetylcholinesterase function that indicated parasympathetic denervation of the small intestine and pancreas in PD patients.

^{18}F-FDOPA PET imaging has been used to study norepinephrine and serotonin function in addition to dopaminergic function (Pavese et al., 2010, 2011, 2012). Advanced stage PD compared with healthy controls showed decreased norepinephrine and serotonin function in

locus coeruleus and midbrain raphe respectively (Pavese et al., 2010). However, a longitudinal study of early stage PD indicated that, at baseline, serotonin function in the midbrain raphe was significantly increased while norepinephrine function in the locus coeruleus was insignificantly increased (Pavese et al., 2011). After three years there were decreases in both norepinephrine and serotonin function. Results suggested possible compensatory mechanisms for serotonin and norepinephrine. Another study of serotonergic and dopaminergic function in PD used ^{123}I-FP-CIT SPECT imaging (Joutsa et al., 2015). Results indicated that the striatum and ventral midbrain had decreased dopaminergic function but the thalamus and raphe nuclei had increased serotonergic function indicating compensatory upregulation.

With respect to glutamatergic and GABAergic function in PD, ^{1}H-MRS studies have observed increased glutamate in the substantia nigra in PD by Gröger et al. (2014), but not Emir et al. (2012). Increased GABA has been observed in pons and putamen (Emir et al., 2012) or substantia nigra in PD (Gröger et al., 2014). The GABA increases are consistent with some human and animal studies of PD, such as Mn toxicity induced parkinsonian syndromes that showed increased GABA levels in striatum in ^{1}H MRS studies in men exposed to Mn (Dydak et al., 2011). Note that GABAergic neurons in the striatum include medium spiny neurons that are the source of GABA striatofugal pathways in the classic cortico-basal ganglia-thalamocortical model of PD (Figure 1), as well as a small population (< 5%) of GABAergic interneurons (Lanciego et al., 2012). Animal studies have suggested that both populations of GABAergic neurons could be altered under conditions of dopamine depletion such as occurred in PD (Dehorter et al., 2009).

With respect to neuromodulators, PET imaging of adenosine A_{2A} receptor binding in PD patients (without levodopa induced dyskinesias) did not show differences with healthy controls (Mishina et al., 2011; Ramlacksingh et al., 2011). However, PET imaging of cannabinoid receptors in PD has shown several significant differences with controls: cannabinoid receptor availability was decreased in midbrain region of the substantia nigra, but increased in putamen, prefrontal cortex, midcingulate, anterior insula, and hippocampus (Laere et al., 2012). Increased cannabinoid receptor availability suggested compensatory mechanisms in basal ganglia, mesocortical, and mesolimbic function.

4.3. Molecular neuroimaging of other neurochemicals

Several other neurochemicals that can be markers of neurodegenerative processes have been investigated with PET or MRS imaging in PD (Table 2).

PET studies of ^{11}C-PIB for presence of amyloid observed no significant differences between PD and controls (Campbell et al., 2013) or only minor findings (Edison et al., 2013). However, PET studies of ^{11}C-PK11195 for neuroglial activation found significantly increased ^{11}C-PK11195 binding in temporo-parietal and occipital regions (Edison et al., 2013), or in the putamen and substantia nigra (Iannaccone et al., 2013) in PD patients compared with healthy controls. PET studies of ^{18}F-FDDNP as a marker for tau have observed increased binding in midbrain, thalamic, and cerebellar regions that distinguished PSP compared with PD (Kepe et al., 2013).

^{1}H-MRS studies have found differences between PD (or DLB) patients and controls in levels of N-acetylaspartate, glutathione, myo-inositol, and creatine moieties indicating alterations in neuronal health, oxidative stress, gliosis, and energy metabolism respectively (Graff-Radford et al., 2014; Gröger et al., 2014; Levin et al., 2012).

Finally, alterations in energy metabolites in men and women in PD have been studied using ^{31}P-MRS. Evidence has suggested that men are more prone to experience non-motor symptoms related to dopaminergic therapy and carry a greater disease burden and suffer lower quality of life (Lubomski et al., 2014; Picillo et al., 2014). Also, lifelong exposure to estrogen may be protective against PD (Gatto et al., 2014). Weiduschat et al. (2014) (Table 2) observed that in the striatum and temporo-parietal gray matter, men with PD had lower amounts of high energy phosphate compounds than women with PD, while normal men and women did not show these differences. Because energy metabolism takes place in the mitochondria, this suggested that men with PD may have greater mitochondrial dysfunction, perhaps due to estrogen's ability to increase oxidative phosphorylation and decrease adenosine triphosphatase.

4.4. Structural, perfusion, and diffusion MRI

Many structural MRI investigations of PD have been conducted in conjunction with DTI or fMRI studies listed in Table 3 (e.g. Cherubini et al., 2014; Luo et al., 2014b; Shine et al., 2014). Other investigations have focused on structural MRI per se (e.g. Biundo et al., 2015; Fioravanti et al., 2015; Höglinger et al., 2014; Lee, E. et al., 2014; Lee, J.E. et al., 2014; Morelli et al., 2014; Salvatore et al, 2014). Most of these studies reported atrophy in some cortical, basal ganglia, or brainstem regions in PD compared with healthy controls, generally consistent with widespread pathological findings in the brain in PD. Other types of structural MRI findings have included 7 Tesla T2*-weighted imaging of the substantia nigra that have shown diminished smoothness of substantia nigra borders (Cho et al., 2011) or absence of hyperintense nigrosome 1 (Blazejewska et al., 2013) in PD. Susceptibility weighted imaging at 3 Tesla has also been able to detect absence of nigrosomes in PD (Schwarz et al., 2014). Susceptibility mapping has shown increased magnetic susceptibility in the substantia nigra, consistent with increased iron content in PD (Loftipour et al., 2012; Murakami et al., 2015). Susceptibility mapping in PD patients has also shown improved imaging of the subthalamic nucleus and globus pallidus internus, both important regions for neurosurgical placement of electrodes for DBS (Liu, T. et al., 2013). Decreased magnetization transfer has been observed for substantia nigra in PD suggesting diminished structural integrity (Bunzeck et al., 2013). Alterations in rotating frame adiabatic R1 rho mapping have also been observed in the brainstem in PD indicating neurodegenerative changes (Tuite et al., 2012). Finally, neuromelanin sensitive imaging has observed decreased volumes of substantia nigra pars compacta and locus coeruleus (Castellanos et al., 2015), or decreased signals in locus coeruleus (Garcia-Lorenzo et al., 2013), indicating loss of dopaminergic neuromelanin containing neurons in these regions in PD.

Several ASL perfusion studies of PD have appeared. Al-Bachari et al. (2014) examined neurovascular status in PD through ASL measures of arterial arrival time (AAT). Widespread regions of the brain showed prolongation of AAT. A combined ASL and

morphometric study observed a pattern of “parietal cortical thinning and reduced precuneus perfusion” that appeared even in mild PD (Madhyastha et al., 2015: 1). A novel ASL perfusion approach has also been used to examine functional connectivity of the subthalamic nucleus in PD and indicated subthalamic nucleus hyperconnectivity with primary motor cortex and precuneus regions (Fernandez-Seara et al., 2015).

The number of DTI studies of PD are large and growing rapidly (Table 3). Two meta-analyses have recently appeared. Cochrane & Ebmeier (2013: 859) assessed studies of “parkinsonian syndromes and related dementias” and “consistently detected an alteration in anisotropy of at least 1 region.” The strongest result, based on a meta-analysis of nine studies comparing PD patients with healthy controls, was for decreased FA in the substantia nigra. However, in another meta-analysis of DTI of the substantia nigra comparing PD with controls, Schwarz et al. (2013) did not observe any significant changes in FA of the substantia nigra but did observe a significant increase in MD in the substantia nigra. Their results showed a much larger variation in results than observed by Cochrane & Ebmeier (2013) and their meta-analyses of either MD or FA changes in the substantia nigra showed insignificant disease effects. They concluded: “results of the meta-analysis of nigral FA changes question the stability and validity of this measure as a PD biomarker” (Schwarz et al., 2013: 481).

Although these two meta-analyses are quite recent, many DTI studies have appeared since their publication. Indeed, none of the diffusion weighted studies in Table 3 of this review were included in Cochrane & Ebmeier (2013) or Schwarz et al. (2013). These studies often reported decreased FA and/or increased MD in gray and white matter regions and tracts in many cortical, subcortical, brainstem, and cerebellar regions. Decreased FA and increased MD indicate loss of microstructural integrity and, therefore, these results are generally consistent with neuropathological findings in widespread regions in gray and white matter in PD. Also note that correlations between FA or MD with measures of clinical function (e.g. unified Parkinson’s disease rating scale (UPDRS), cognitive measures) suggest that better microstructural integrity correlates with better clinical function, such as FA positively correlated with executive function in multiple white matter tracts (Rae et al., 2012). An example of an exception to this type of result is Garcia-Lorenzo et al.’s (2013) observation of increased FA in the midbrain tegmentum and rostral pons in PD patients with REM sleep behavior disorder compared with healthy controls. Possible reasons for increased FA in this result included degeneration of a crossing fiber tract in these regions, or other expressions of disease progression particular to this patient population.

Note that DTI studies can have complex results. For example, Kim, H. et al. (2013) examined white matter tracts in PD patients compared with healthy controls. Although no significant differences in FA were observed, increased MD in many white matter tracts was observed, including the corticofugal tracts (corona radiata, internal capsule, cerebral peduncle); cingulum, uncinate fasiculus, crus fornix stria terminalis, corpus callosum, external capsule, superior longitudinal fasiculus, posterior thalamic radiation, superior cerebellar peduncle, and tracts near the precuneus and supramarginal gyrus. The investigators noted that the corona radiata and internal capsule are traversed by the corticostriatal, corticospinal, corticopontine, and corticobulbar tracts. The corticostriatal

pathway is a component of the cortico-basal ganglia-thalamocortical circuit; and the corticospinal and corticopontine and corticobulbar (cranial nerves) tracts contain the pyramidal projection pathways essential for motor function. The cingulum, uncinate fasiculus and external capsule are pathways of cholinergic projection neurons from the nucleus basalis of Meynert, which begin to show pathological changes relatively early in PD Braak stage 2. These cholinergic afferents are important for cognitive function, which is often impaired in PD. Involvement of many of these regions has been observed for visuospatial as well as motor functions. By way of summary, deficits were observed in many white matter tracts that subserve motor and nonmotor symptoms PD.

As another example, Zheng et al. (2014) examined correlations between five domains of cognitive function and FA and MD maps of white matter tracts in PD. The five cognitive domains were executive function, linguistic performance, attention, short-term memory, and long-term memory. Performance in all five domains showed positive correlations with FA and negative correlations with MD in some regions, consistent with expectations that FA decreases and MD increases with neurodegeneration and neurocognitive dysfunction. The anterior corona radiata appeared in results for executive, linguistic, attention, and long-term memory domains, suggesting that motor function subserved by pathways of the anterior corona radiata may influence assessments of cognitive function across domains.

4.5. Functional neuroimaging

PET/SPECT studies of glucose metabolism and cerebral blood flow have been the most frequently used methods to study patterns of brain activity during rest (Tables 2 and 5). MRI has been the most frequently used modality to study brain activity during tasks or functional connectivity networks during rest or tasks (Table 3).

4.5.1. Brain activity during rest—^{18}F-FDG PET imaging of regional cerebral glucose metabolism has been used to assess resting-state spatial covariance patterns of metabolic activity in PD (Eidelberg, 2009; Ma et al., 2007). The most important PD related metabolic pattern (PDRP) has been identified in association with motor symptoms. PDRP can be characterized by relatively decreased metabolism, in PD patients compared with healthy controls, in “parietal association cortex, visual cortex, and lateral premotor and prefrontal association cortices” and increases “in the pons, bilateral thalamus, pallidum, dorsal putamen, primary motor cortex, and supplementary motor area” (Teune et al., 2013: 550) (Tang et al., 2010). A similar pattern has been observed in a nonhuman primate model of parkinsonism (Ma et al., 2012). PDRP has also been assessed using ^{15}O-H_2O PET or ^{99m}Tc-ECD SPECT imaging of cerebral blood flow (Eckert et al., 2007; Hirano et al., 2008; Holtbernd et al., 2014).

MRI can also image patterns of regional brain activity in the resting-state in PD (Tables 3 and 5). Continuous arterial spin labeling measures have been used to assess spatial covariance patterns of perfusion in PD. A direct comparison between ^{18}F-FDG-PET and CASL spatial covariance patterns in PD observed good overlap (Ma et al., 2010a; Teune et al., 2014). Other MRI studies have used ALFF or ReHo analyses of fMRI BOLD signals. For example, a PDRP pattern derived from ALFF (PDRP-ALFF) comprised decreases in

"striatum, supplementary motor area, middle frontal gyrus, and occiptal cortex" and increases in "thalamus, cerebellum, precuneus, superior parietal lobule, and temporal cortex" (Wu et al., 2015: 1). Some PDRP-ALFF results were similar to ^{18}F-FDG PET derived PDRP, e.g. in supplementary motor area, thalamus, cerebellum, but others were different, e.g. in striatum. Also, there were some similarities and differences between these PDRP-ALFF results and other ALFF studies of PD (Hou et al., 2014; Skidmore et al., 2013a; Zhang et al., 2013) (Table 3).

4.5.2. Brain activity during tasks—The most frequently studied tasks in PD neuroimaging have been motor tasks. Herz et al. (2014) conducted a meta-analysis of 24 functional neuroimaging studies (three PET, 21 fMRI) of motor tasks in PD. Finger and hand motor tasks showed decreased activation in the right posterior putamen but increased activation in left superior parietal lobule. Further, in the OFF medication state during externally but not internally driven motions, PD patients showed decreased activation in the left primary motor cortex and increased activation in the left inferior parietal cortex and superior parietal lobule. The 24 studies also showed some inconsistent results. For example, studies of presupplementary motor area activity in PD patients versus controls described both increased and decreased activation. Inconsistent results were also observed for ON versus OFF dopaminergic medication comparisons in the right putamen and middle frontal gyrus; some studies showed increases while others showed decreases.

Additional functional neuroimaging studies of tasks (Tables 2, 3, and 5) have been of motor or motor sequence learning (Burciu et al., 2015; Gonzalez-Garcia et al., 2011; Herz et al., 2015; Jahanshahi et al., 2010; Ko et al., 2013; Mure et al., 2012; Van Nuenen et al., 2009; Weiss et al., 2015; Wu et al., 2011a, 2011b, 2012), selection (MacDonald et al., 2011), affective face processing (Anders et al., 2012), virtual reality gait (Shine et al., 2013), visuomotor tracking (Palmer et al., 2010), visual tasks that can identify patients with hallucinations (Shine et al., 2014), and the ictal period of REM sleep in PD patients with REM sleep behavior disorder (Mayer et al., 2015) (section 4.7). Overall, changes have been observed in widely distributed regions of the brain, brainstem, and cerebellum in PD for many types of tasks.

4.5.3. Functional connectivity—Resting-state fMRI based functional connectivity studies comprise the vast majority of functional connectivity studies of PD (Tables 3, 5). Many of these have shown alterations to motor networks. An early study was by Helmich et al. (2010) on functional connectivity of corticostriatal networks. In both PD and healthy controls, the posterior putamen was functionally connected with motor cortex (e.g. primary motor, primary somatosensory, supplementary motor area); anterior putamen with pre-supplementary motor area and anterior cingulate cortex; and caudate with dorsomedial and dorsolateral prefrontal cortex. However, PD patients compared with controls showed decreased functional connectivity between posterior putamen with cingulate motor area, postcentral gyrus and inferior parietal cortex, and increased functional connectivity between anterior putamen and inferior parietal cortex. Further, a dissociation was observed for a region in the inferior parietal cortex, for which healthy controls showed connectivity with posterior putamen but PD patients showed connectivity with anterior putamen. Finally, in

controls both precentral gyrus and inferior parietal cortex were connected with the posterior putamen, but in PD patients the precentral gyrus was connected with posterior putamen while the inferior parietal cortex connected with the anterior putamen (Helmich et al., 2010: 1181). These results suggested that compensatory alterations or "remapping" occur in PD that increase the role of the anterior putamen versus the posterior putamen, consistent with the posterior putamen's earlier and greater dopaminergic dysfunction in PD (Brooks & Pavese, 2011). Functional connectivity between the precentral gyrus and inferior parietal cortex were also decreased in PD, indicating that "cortico-striatal remapping may also impair cortico-cortico processing" (ibid: 1181).

More recent striatal connectivity studies have supported some of these findings, such as decreased corticostriatal functional connectivity with the putamen in PD (Luo et al., 2014). However, there have also been important differences. For example, Hacker et al. (2012) highlighted decreased functional connectivity between the striatum and extended brainstem – thalamus, midbrain, pons, and cerebellum – in PD. As another example, Luo et al. (2014b) observed decreased functional connectivity in corticostriatal and mesolimbic-striatal networks but did not observe any increased functional connectivity in PD. The investigators suggested that differences in patient characteristics, such as study of early stage medication naive patients by Luo et al. (2014b) but more advanced stage patients by Helmich et al. (2010) and Hacker et al. (2012), or methodological differences might be the basis for differences in results.

Functional connectivity studies of PD have highlighted other networks in addition to striatal networks. Baudrexel et al. (2011) observed increased connectivity between subthalamic nucleus and bilateral primary motor, premotor, supplementary motor area, and primary sensory regions. These results suggested increased engagement of the hyperdirect pathway in PD. Increased functional connectivity between the subthalamic nucleus and cortex in PD has also been observed more recently by Fernandez-Seara et al. (2015) and Kahan et al. (2014).

With respect to core brain networks, Tessitore et al. (2012b) found decreased functional connectivity between the medial temporal lobe and inferior parietal cortex regions of the default mode network. Further, although PD patients did not have diagnoses of mild cognitive impairment, functional connectivity of the medial temporal lobe was positively correlated with memory scores, while connectivity of the inferior parietal lobule positively correlated with visuospatial function. Results indicated a role for disruption of the default mode network in cognitive dysfunction in PD. Gorges et al (2013) investigated the default mode network and a subtype of motor impairment, namely, oculomotor motor dysfunction in PD. They found decreased functional connectivity between the medial prefrontal cortex and posterior cingulate cortex, and increased connectivity between the right and left hippocampi. There was also a negative correlation between saccadic accuracy and functional connectivity between posterior cingulate cortex and medial temporal lobe, but positive correlation between vertical saccadic accuracy and functional connectivity of the right hippocampus to left inferior parietal lobe and left hippocampus to right inferior parietal lobule. It was suggested that increased connectivity between bilateral hippocampi, involved in memory, might help compensate for cognitive dysfunction.

In the normal brain, the default mode and central executive networks are typically anticorrelated while the salience and central executive networks are positively correlated. Recently, Putcha et al. (2015) described alterations to coupling between these networks in PD. The default mode and central executive networks were observed to be positively coupled rather than anticorrelated. Also, there was decreased coupling between the salience and central executive networks. Functional connectivity between the salience network and the striatum was also negatively correlated with motor function. Results indicated disruption of the normal function of core connectivity networks that may explain aspects of motor and cognitive dysfunction in PD.

Application of graph theoretical perspectives to brain functional connectivity networks in PD has also shown widespread alterations in network function. Skidmore et al. (2011) found decreased mean global efficiency in PD, as well as decreased efficiency for many nodes including precuneus/cuneus, middle frontal gyrus, supplementary and precentral regions, calcarine and secondary visual regions, and cerebellum. Göttlich et al. (2013) also observed decreased global efficiency and increased characteristic path length in PD. Further, they found that the visual network had a lower degree (number of connections) and sensorimotor network had a higher degree in PD patients versus controls. The increased connectivity of the sensorimotor module suggested a possible compensatory mechanism. Finally, Zhang et al. (2015) observed decreased functional connectivity density in the ventral visual pathway and increased connectivity density in precuneus and posterior cingulate regions, overlapping some results from Göttlich et al. (2013).

An important question is whether there is a relationship between structural and functional connectivity alterations in PD and other disorders. Sharman et al. (2013) conducted a multimodal study of both structural and functional connectivity in PD. Structural connectivity was decreased between the sensorimotor cortical region and putamen and thalamus, along with decreased connectivity in pallidothalamic and nigrothalamic connections. Functional connectivity was decreased in connections of the sensorimotor cortex with thalamus; globus pallidus with putamen and thalamus; and substantia nigra with globus pallidus, thalamus, and putamen; but increased in connections of thalamus with associative cortex, limbic cortex, and putamen (Sharman et al., 2013: 452). Thus structural and functional connectivity changes overlapped in connections from “thalamus to sensorimotor cortex, globus pallidus, and SN (substantia nigra)” (ibid: 452) and indicated “a possible link between brain structure and function” for “dysfunction of the sensorimotor circuit in PD” (ibid: 447). The increased functional connectivity in some thalamic connections suggested compensatory mechanisms.

4.6. Differential diagnosis and co-morbid syndromes

Currently there is one approved neuroimaging agent to aid in the diagnosis of parkinsonian syndromes, namely, the radioligand ^{123}I-FP-CIT (also known as ^{123}I-fluopane or DaTSCAN) that is used for SPECT imaging of the dopamine transporter (Bajaj et al., 2013). Patients with parkinsonian syndromes show decreased FP-CIT binding in the striatum (Table 2). This finding can help differentiate parkinsonian syndromes (i.e. PD, multiple system atrophy, progressive supranuclear palsy) from essential tremor, or dementia with

Lewy bodies (which overlaps diagnosis of PD) from Alzheimer's disease (Bajaj et al., 2013; Gerasimou et al., 2012; Oliveira et al., 2015; Thiriez et al., 2015). However, it is important to realize that decreased ^{123}I -FP-CIT identifies the loss of dopaminergic neurons, which is not specific for PD. This highlights the many diagnostic needs that are unaddressed by currently available techniques. The development of neuroimaging to improve PD diagnosis continues to be a major topic in PD neuroimaging (Politis, 2014; Zhang & Liu, 2013).

Another important molecular imaging approach for differential diagnosis in PD is ^{18}F-FDG PET imaging of resting-state cerebral glucose metabolism (described in section 4.5 above). This has been used to identify differences in regional cerebral glucose metabolism that can differentiate PD from healthy controls, CBD, DLB, MSA-C, MSA-P, and PSP (Table 2). For example, resting-state spatial covariance patterns can discriminate between PD (PDRP), MSA (MSARP), and PSP (PSPRP) (Eckert et al., 2008; Tang et al., 2010). Resting-state spatial covariance patterns have also been obtained from ^{15}O-H_2O PET or ASL MRI perfusion imaging and ALFF fMRI. Although further studies are needed, note that Wu et al.'s (2015) study of ALFF resting-state spatial covariance patterns showed promise for differentiating PD patients from healthy controls at the individual level, and may have potential clinical advantages over ^{18}F-FDG PET approaches because of the wider availability and safety profile of MRI.

There are also many structural MRI studies relevant to diagnosis of PD, including many of the structural MRI studies presented above (section 4.4). These have involved voxel based morphometric analyses of cortical, basal ganglia, and brainstem regions to look for atrophic changes secondary to neurodegeneration in PD. They have also involved an expanding list of advanced MRI methods, such as T2, T2*, susceptibility weighted imaging, magnetization transfer, neuromelanin sensitive imaging, etc., to image the substantia nigra and midbrain with sufficient detail to discriminate pathological changes of PD. A meta-analysis of 39 voxel-based morphometry studies of PD, MSA-P, CBD, and PSP has indicated that there are patterns of atrophy that can differentiate these disorders from each other (Yu et al., 2015). Other recent structural MRI studies not included in this meta-analysis were a volumetric study of the midbrain tegmentum to differentiate PD versus PSP (Kim et al., 2015); a support vector machine learning algorithm for classification of PD, PSP, and healthy controls using T1-weighted MRI (Salvatore et al., 2014); and susceptibility weighted imaging of the putamen to differentiate PD and MSA-P (Yoon et al., 2015). DTI also has potential for differentiating PD from atypical parkinsonian syndromes (Cherubini et al., 2014; Haller et al., 2012; Prodoehl et al., 2013) (Table 3).

Another important neuroimaging topic in PD diagnosis is differentiation of PD from Alzheimer's disease and other dementias or taupathies (Petrou et al., 2015; Politis, 2014). Examples are PET ^{11}C-PiB imaging of amyloid for comparison of PD and Alzheimer's disease (Campbell et al., 2013), PET ^{18}F-FDDNP imaging of tau deposits for comparison of PSP and PD (Kepe et al., 2013), and ^{1}H-MRS metabolites and MRI morphometric studies for comparison of Alzheimer's disease, dementia with Lewy bodies, and controls (Graff-Radford et al., 2014) (Table 2).

Finally, there are numerous co-morbid syndromes in PD that are being studied with neuroimaging. The results are highly heterogeneous, complex, particular to specific co-morbid syndromes, and often include examples of inconsistent findings. Thus it is not possible to adequately discuss them in our review. Here we will call attention to the range of neuroimaging studies of PD co-morbid syndromes, examples of which are given in Tables 2, 3, and 5; and recent reviews of PD co-morbid syndromes that included discussions of neuroimaging studies. These can be useful background for further inquiry.

Cognitive dysfunction/dementia is one of the most common co-morbid syndromes in PD. Discussions of neuroimaging of cognitive dysfunction in PD have been included in reviews by Calabresi et al. (2006), Duncan et al., 2013; Lin & Wu (2015), Mak et al. (2015), and Petrou et al. (2015). Neuroimaging studies relevant to understanding cognitive dysfunction in PD have examined PD with dementia, PD with mild cognitive impairment, and neuroimaging correlates of cognitive function in patients with PD who did not have a diagnosed cognitive disorder (e.g. Weintraub et al., 2012; Yarnall et al., 2014). Significant findings related to cognitive dysfunction have included alterations in dopaminergic and cholinergic function, amyloid, MRS metabolites, ^{18}F-FDG PET cognitive related PDCP pattern, atrophy observed using structural MRI, DTI abnormalities in gray and white matter and white matter tracts, and fMRI assessment of deficits in functional connectivity networks, ReHo, and ALFF findings. As one example of a recent PET study of PD with co-morbid cognitive dysfunction, Lucero et al. (2015) observed that binding of ^{11}C-PiB PET correlated with cognitive decline in PD patients with less than 16 years of education but not in those with 16 or more years of education, suggesting that “education may protect PD patients’ cognition against cortical amyloid pathology” (ibid: 899) (Table 2).

Depression is another very common co-morbid syndrome of PD that is beginning to be studied with neuroimaging. Vriend et al. (2014a) reviewed neuroimaging studies of depression in PD and highlighted decreased dopaminergic function in the ventral striatum. MRI studies of co-morbid depression in PD have also shown alterations in ALFF and morphometric result although they are notable for some inconsistent results in ALFF results (Luo et al., 2014a; Skidmore et al., 2013b; Wen et al., 2013) and morphometric studies (Surdhar et al., 2012; van Mierlo et al., 2015).

Three other PD co-morbid syndromes that have been the focus of recent reviews are visual hallucinations (Lenka et al., 2015), impulse control disorders (Jimenez-Urbieta et al., 2015; Vriend et al., 2014a), and dyskinesias (Jimenez-Urbieta et al., 2015). Note that Vriend et al. (2014a) reviewed both depression and impulse control disorders in PD, while Jimenez-Urbieta et al. (2015) reviewed both impulse control disorders and levodopa induced dyskinesias, as disorders with related neurobiological mechanisms. Finally, co-morbid olfactory dysfunction, REM sleep behavior disorder, and tremor are also being investigated with neuroimaging (Tables 2, 3, 5).

4.7. Genetic PD and prodromal PD

Neuroimaging of genetic PD can increase understanding of pathways from specific genetic and biochemical alterations to alterations in structure and function of the brain (Table 4).

Studies of genetic PD also provide unique opportunities to investigate changes occurring in the presymptomatic period in asyptomatic carriers.

Asymptomatic carriers of Parkin and PINK1 mutations have shown decreased ^{18}F-FDOPA uptake in the striatum, especially in the putamen, a key striatal region for motor deficits in PD (Eggers et al., 2010; Hilker et al., 2012; Pavese et al., 2010). For example, homozygous PINK1 carriers have shown a 60% decrease in ^{18}F-FDOPA uptake in caudate and putamen, while heterozygous carriers showed a 20% decrease in the putamen (Eggers et al., 2010). As another example, Pavese et al. (2010) observed that asymptomatic heterozygote Parkin carriers showed decreased ^{18}F-FDOPA uptake in caudate and putamen in comparison with healthy controls. However, Parkin PD patients showed decreases in additional regions of the ventral striatum, locus coeruleus, midbrain raphe, and pallidum. Idiopathic PD patients showed decreases in even more regions, including the hypothalamus, thalamus, and pineal. PINK1 patients showed reductions in caudate, putamen, and ventral striatum. Thus results indicated alterations in monoaminergic function that differed between asymptomatic carriers and patients, and between genetic and idiopathic forms of PD. Results also showed evidence of abnormal dopaminergic, noradrenergic (locus coeruleus), and serotonergic (midbrain raphe) function in genetic Parkin and idiopathic PD.

McNeill et al. (2013) examined patients with GBA, SNCA, LRRK2, PINK1, and Parkin PD with ^{123}I-FP-CIT SPECT imaging to assess asymmetry of uptake in caudate and putamen. Parkin, PINK1, and SNCA PD showed relatively symmetric decreases in ^{123}I-FP-CIT uptake, while GBA and LRRK2 showed relatively asymmetric decreases in uptake. Investigators suggested that the symmetry of Parkin, PINK1 and SNCA alterations were consistent with deficits that would be expressed from birth. On the other hand, the asymmetric alterations of GBA and LRRK2 could be more consistent with the later onset of these disorders and involvement of endogenous or environmental factors for PD to manifest.

Several studies of genetic PD have indicated compensatory mechanisms in tasks. An fMRI study of finger tapping motor tasks in asymptomatic carriers of Parkin or PINK1 mutations showed increased activation in motor regions of the rostral supplementary motor area and dorsal premotor cortex in comparison with healthy controls, suggestive of a compensatory mechanism (Van Nuenen et al., 2009). A neuroimaging study of an affective face processing task in asymptomatic carriers showed increased activation in the right ventrolateral premotor cortex/inferior frontal gyrus pars opercularis and decreased activity in the left lateral orbitofrontal cortex (Anders et al., 2012). The inferior frontal gyrus pars opercularis is the putative site of mirror neurons, suggesting compensatory recruitment for this social affective processing task.

Resting-state functional connectivity studies have also shown evidence of compensatory mechanisms in SCA2 parkinsonism (Wu et al., 2013). Both asymptomatic carriers and patients showed decreased functional connectivity between the posterior putamen and many regions of the basal ganglia, cortex, and thalamus. However, asymptomatic carriers also showed increased functional connectivity between the posterior putamen and M1, postcentral gyrus, precuneus, parietal lobule, anterior cingulate cortex, prefrontal cortex, and pons. With respect to functional connectivity with the pre-supplementary motor region,

asymptomatic carriers showed increased connectivity with motor cortical areas such as M1, caudate, pons, and cerebellum, while patients showed increased connectivity with M1 but decreased connectivity with basal ganglia, pons, cerebellum, etc. These results indicated that there are resting state functional connectivity decreases in basal ganglia networks that already occur in asymptomatic states of SCA2 carriers, along with compensatory increases in other connectivity networks such as with M1 that could explain the lack of motor symptoms.

Compensatory mechanisms have also been observed using DTI in a study by Thaler et al. (2014) on asymptomatic carriers of the G2019S mutation in the leucine-rich repeat kinase 2 (LRRK2) gene, which is the most common mutation that causes PD. Carriers compared to noncarriers did not show significant differences in FA, MD, RD, or AD values in gray matter regions of the basal ganglia or thalamus or white matter tracts. However, there was a trend towards significance for increased FA and decreased MD in the bilateral anterior thalamic radiations and corticospinal tracts, and right superior longitudinal fasiculus, inferior fronto-occipital fasiculus, cingulate, and forceps major (Thaler et al., 2014: 3). Because decreased FA and increased MD indicate neurodegeneration, this trend towards increased FA and decreased MD might “indicate structural remodeling as a mechanism of compensation” (Thaler et al., 2014:3).

Neuroimaging of prodromal syndromes is another important way to study how the brain may be altered before PD is clinically manifest. REM sleep behavior disorder, which may appear 10 to 15 years earlier in patients with PD (Mayer et al., 2015), has been studied with many types of neuroimaging approaches in Tables 2 and 3. Kotagal et al. (2012) used PET to examine acetylcholinesterase, vesicular monoamine transporter, and serotonin transporter activity and observed decreased cholinergic function in the neocortex without change in dopaminergic or serotonergic function in PD patients with RBD. A ^{18}F-DOPA PET study of dopaminergic function in patients with RBD with depression but without PD showed decreased dopaminergic function in the putamen and caudate (Wing et al., 2015). As these patients also showed olfactory dysfunction the evidence suggested that the patients may represent a prodromal stage of PD. An MRI study employed neuromelanin sensitive imaging, diffusion weighted ADC mapping, and DTI measures and showed that PD patients with RBD had decreased intensity in the locus coeruleus/subcoeruleus (Garcia-Lorenzo et al., 2013). Using ^{18}F-FDG PET, Holtbernd et al. (2014) observed that patients with RBD showed elevated PDRP patterns. Further, follow-up after around 5 years showed that 8 out of 17 subjects converted to PD or DLB and that conversion was predicted by PDRP expression and age at the time of PET imaging. Finally, Mayer et al. (2015) conducted ^{99m}Tc-ECD SPECT imaging during ictal REM sleep in one patient with RBD, one with PD-RBD, and two with narcolepsy and RBD. All patients showed similar activation patterns in cortical, brainstem, and cerebellum regions. There was also no evidence of basal ganglia involvement, indicating that the motor activity of RBD did not involve the basal ganglia, unlike motor activity in the waking state.

4.8. Treatment effects

Most neuroimaging studies of treatment effects in Table 5 have been of idiopathic PD, with one study each of SCA2 genetic PD, MSA, and parkinsonism associated with schizophrenia. Several studies have included investigation of levodopa induced dyskinesias. Although to our knowledge no articles have yet appeared on effects of treatment for patients with PD and depression, one study has assessed PD patients with L-DOPA associated mood fluctuations (Black et al., 2005). Patients have been assessed as early as the asymptomatic carrier state of a genetic mutation (SCA2), early stage, drug naive PD, advanced stages of PD after DBS electrodes have been implanted, or 13 to 16 years after dopamine grafting.

All neuroimaging studies of treatment of PD in Table 5 have shown significant results, usually in the direction of normalization of abnormal findings. Here we give examples of a few of the many interesting results.

Many PET/SPECT treatment studies examined changes in neurotransmitter function after treatment, including adenosine, dopamine, glutamate, norepinephrine, and serotonin. The most frequently investigated neurotransmitter systems have been dopamine and serotonin, and several studies have investigated both neurotransmitter systems. Serotonin function has been of special interest in patients with levodopa induced dyskinesias (Politis et al., 2012, 2014; Smith et al., 2015). For example, there have been two PET studies of neurotransmitter function after dopamine grafts (Ma et al., 2010b; Politis et al., 2012). Both of these examined dopaminergic function with ^{18}F-DOPA PET imaging and showed improved dopaminergic function in the basal ganglia after grafting. In addition, Politis et al. (2012) also examined norepinephrine function with ^{18}F-DOPA PET and serotonin function with ^{11}C-DASB PET. Results indicated that although norepinephrine (^{18}F-DOPA binding in the locus coeruleus region) function appeared normal, serotonergic function in the raphe region declined and, therefore, was not improved by the dopamine graft. As another example, Politis et al. (2014) studied effects of L-DOPA along with the serotonin agonist buspirone as treatments for PD with levodopa induced dyskinesias. Patients with PD and dyskinesia showed abnormally increased striatal release of dopamine from L-DOPA. Buspirone pretreatment before administration of L-DOPA resulted in decreased striatal dopamine release, as well as decreased dyskinesias. L-DOPA effects have also been investigated in patients with parkinsonism associated with schizophrenia (Tinazzi et al., 2014). In these patients, abnormal dopaminergic function in the dorsal striatum predicted motor impairment and also response to L-DOPA treatment.

Study of cerebral metabolic and blood flow spatial covariance patterns are making important contributions to understanding of a wide range of treatments, including effects of L-DOPA, DBS, AAV-GAD, and sham surgery treatments. An ^{18}F-FDG PET study of AAV-GAD gene therapy examined expression of PDRP and PDCP, which were elevated at baseline, and showed that there was decreased expression of PDRP but not PDCP after treatment (Feigin et al., 2007). Other studies examined L-DOPA and DBS treatments and observed that they had different effects, for example, for a normal movement related pattern (Ko et al., 2013), motor sequence learning related pattern (Mure et al., 2012), and motor related PD patterns (Hirano et al., 2008). Note that the study by Hirano et al. (2008) included both ^{18}F-FDG PET metabolic and ^{15}O-H_2O PET CBF assessments that revealed an interesting

dissociation: L-DOPA decreased metabolic but increased CBF PDRPs, while DBS decreased both metabolic and CBF PDRPs.

One of the most interesting PET studies of spatial covariance patterns was of sham burr hole surgery (SHAM) in a double-blind 12 month longitudinal study of AAV-GAD gene therapy (Ko et al., 2014). Under the blind, patients who received SHAM treatment and showed clinical motor improvement revealed a sham-related metabolic covariance pattern (SSRP) characterized by increased activity in the anterior cingulate, subgenual cingulate, inferior temporal cortex, hippocampus, amygdala, and posterior cerebellar vermis. SSRP expression correlated with motor scores. Motor outcomes for SHAM and AAV-GAD responders were not significantly different under the blind, although SSRP expression differed. When patients were unblinded, SHAM expression in responders decreased. Baseline SSRP expression predicted motor outcomes under blinded conditions at 6 months. One conclusion was that results indicated that baseline SSRP expression might be useful as a way to identify SHAM placebo responders when selecting subjects for randomized trials.

Another important neuroimaging approach for the study of PD treatments is fcMRI based functional connectivity studies. The earliest study was by Kwak et al. (2010), who observed increased resting-state functional connectivity in corticostriatal connections in PD that was decreased by L-DOPA. However, Esposito et al. (2013) observed decreased functional connectivity in the sensorimotor network in PD patients OFF medication that increased and normalized after L-DOPA administration. Further, PD patients showed “rhythm specific modulation of the sensorimotor network” by L-DOPA (Esposito et al., 2013: 710). For example, L-DOPA led to increased oscillations in the 0.02–0.03 Hz, but not in 0.015–0.020 Hz, band in the sensorimotor network. Regarding differences between their results and Kwak et al. (2010), the investigators noted differences in patients (medication naive patients versus treated patients withdrawn from medication) as well as different analytic approaches, such as ICA versus seed-based connectivity networks respectively (Esposito et al., 2013: 721). More recently, decreased resting-state functional connectivity in the basal ganglia network has been observed in PD patients OFF medication, which improved after administration of their own medications (Szewczyk-Krolikowski et al., 2015). Other studies have observed that L-DOPA increased functional connectivity of regions in the cerebellum and brain stem (Jech et al., 2013); between substantia nigra pars compacta and multiple regions of the cerebral cortex, basal ganglia, thalamus, cerebellum, and pons (Wu et al., 2012); and between putamen and thalamo-cortical and cerebellar circuits and cortical motor networks in asymptomatic and symptomatic SCA2 carriers (Wu et al., 2013).

FcMRI has also been used to investigate effects of subthalamic DBS (Kahan et al., 2014). A simplified version of the DCM model was used (Figure 2c). DBS increased the strength of cortico-striatal, striato-thalamic (direct pathway), and thalamo-cortical connections; but decreased cortico-subthalamic (hyperdirect), striato-subthalamic, and subthalamic-thalamic connections. Connectivity strengths in several connections were able to predict motor impairment, with three connections that were predictive both on and off DBS stimulation: hyperdirect, striato-subthalamic, and direct pathways (Figure 2c). Increasing connectivity strength in the direct and hyperdirect pathways predicted decreased motor impairment, while

increasing connectivity strength in the striato-subthalamic pathway predicted increased motor impairment. These three connections also predicted response to DBS treatment.

Overall, the complexity of current neuroimaging findings on treatments of PD demonstrates the valuable contributions being made from many different types of neuroimaging studies, and that much work remains to develop understanding of the neural mechanisms involved in treatments of PD.

5. Overall summary and future directions

Our understanding of PD has long been informed by a model of the cortico-basal ganglia-thalamocortical motor circuit that describes how decreased dopaminergic input into the motor loop of the circuit alters neuronal activity in direct and indirect pathways and thus leads to diminished motor function. Neuroimaging investigations have helped to validate some aspects of this model.

The white matter structural connections of the nigrostriatal, subthalamopallidal, pallidothalamic, and striatopallidal pathways of the simplified model of the corticobasal ganglia-thalamocortical circuit in PD have recently been imaged in vivo in humans for the first time, helping to validate pathways that previously had only been observed in animal or human post mortem studies or sometimes group MRI studies (Figures 1, 6). With respect to the model's role for dopamine, numerous PET and SPECT radioligand studies have demonstrated decline in dopaminergic function in the dorsal striatum, the target of substantia nigra pars compacta projection neurons that degenerate in PD (Table 2). A meta-analysis of functional MRI studies of motor tasks in PD has also shown that patients OFF dopaminergic medication have decreased putaminal activity associated with motor tasks and increased likelihood of decreased putaminal activity with increasing motor impairment. ^{1}H-MRS studies have been able to observe a decline in dopamine levels in the substantia nigra per se in PD. The model also predicts that there will be alterations in pathways of the cortico-basal ganglia-thalamocortical circuit in PD. Many neuroimaging studies have observed alterations in structure and function of regions and connections of this circuit in PD. Finally, the model predicts that dopaminergic replacement therapies will improve function of the cortico-basal ganglia-thalamocortical circuit; many neuroimaging studies have observed this.

Although many aspects of the model have been validated, neuroimaging studies are also providing evidence for ways to modify the model. One such modification is importance of the hyperdirect pathway between the cortex and subthalamic nucleus in PD neuropathophysiology and treatments. Structural connectivity studies have now provided in vivo neuroimaging evidence for the hyperdirect pathway in humans. Several studies have observed alterations to the hyperdirect pathway, such as increased functional connectivity (hyperconnectivity) of the hyperdirect pathway in PD. In addition, neuroimaging studies are beginning to provide evidence for a critical role of the hyperdirect pathway in the emergence of beta oscillations that are not explained by the classic rate model. Further, neuroimaging studies have indicated that L-DOPA and DBS treatments can modulate the connectivity of the hyperdirect pathway.

Another possible modification is inclusion of the cerebellum (Wu & Hallett, 2013). The cerebellum is absent from the classic model of PD although neuroimaging studies frequently observe its involvement in PD (Tables 2, 3, and 5). Although the cerebellum has been an infrequent target of molecular neuroimaging neurotransmitter studies, ^{18}F-FDG PET and ^{15}O-H_2O PET or ^{99m}Tc-ECD SPECT studies of cerebellar glucose metabolism and cerebral blood flow, respectively, have often observed alterations in PD and atypical parkinsonian syndromes. Functional MRI studies of PD have shown increased activation of the cerebellum associated with motor tasks or REM ictal periods for RBD, while resting-state functional connectivity studies have shown alterations in cerebellar functional connectivity in PD that tended to normalize after administration of L-DOPA. Imaging of two white matter tracts to the cerebellum that may be important in PD and DBS treatment have also recently been imaged for the first time in vivo in humans and the studies suggested the importance of the dentatothalamic tracts for DBS tremor control.

There are numerous other neurotransmitters, neurochemicals, brain regions, and connectivity networks that show involvement in PD and its treatments as this review has shown. Alterations of all the major neurotransmitters of the brain, as well as other neuromodulators such as adenosine, and other neurochemicals such as the neurodegenerative marker TPSO, bioenergetic metabolites, and amyloid, are being revealed by molecular neuroimaging. There are also alterations in many brain regions and networks beyond the motor loop of the cortico-basal ganglia-thalamocortical circuit, from the lower brainstem to cerebellum and all the lobes of the cerebral cortex. Current trends towards use of data driven analytic methods that can reveal findings throughout the brain and are not limited by model dependent hypotheses may be facilitating expansion of knowledge about PD beyond the classic model. Many of these more wide ranging findings involve neurocognitive systems for nonmotor systems and symptoms, such as the limbic and executive loops of the cortico-basal ganglia-thalamocortical circuit, default mode network, cognitive impairment and dementia, depression, olfactory or visual functions, etc.

Although there has been great expansion in the number of PD neuroimaging studies much work remains. First, there are discrepancies in the current literature that await further investigation and understanding. Perlmutter & Norris' (2014) review of neuroimaging biomarkers in PD provided several examples of discrepancies. Additional examples of discrepancies were described in this review. Possible reasons for discrepancies include heterogeneous methods and analytical approaches (e.g. Gröger et al., 2014; Hacker et al., 2012; Rae et al., 2012). However, imaging and analytical approaches employed in PD studies have, in general, contributed to understanding of many neurocognitive systems in healthy individuals and neuropsychiatric disorders.

Another possible factor is the heterogeneity of PD patients in studies (Duncan et al., 2013). PD patients may have heterogeneous etiologies (idiopathic, genetic, etc.) and diagnoses that include atypical Parkinsonian syndromes; stages from early stage medication naïve to advanced PD; akinetic rigid or tremor dominant forms; history or not of levodopa induced dyskinesias, mood fluctuations, or impulse control disorders; dominant left or right sided motor symptoms; presence or not of co-morbid depression or cognitive impairment; age; gender; etc. Any of these differences could be predicted to show differentiable neuroimaging

findings, with potential combinations and interactions between various factors adding to the complexity. Thus a second direction for future studies is better characterization and selection of patient groups that would provide more homogeneous groups for investigations, as well as analytical approaches that can better probe heterogeneous populations. Many studies are beginning to target more specific subtypes of PD patients according to factors such as rigidity/akinesia, tremor, depression, cognitive impairment, dyskinesias, men versus women, etc., and these results can contribute to understanding effects of heterogeneous participants. Note that study of genetic PD may allow for especially homogeneous participant groups and findings, since genetic PD emerges from a specific genetic variation and biochemical alteration and, further, participants may be assessed from asymptomatic (including heterozygotic and homozygotic carriers) through advanced stages. Application of analytical approaches to address heterogeneity has begun (Holiga et al., 2013). Methods such as behavior-based connectivity analysis that can address multiple behavioral measures may be helpful (Chen et al., 2009).

Third, improved methods for motion correction in MRI studies may diminish effects of head motion that could lead to systematic errors in comparisons of ON versus OFF treatment conditions, since motion artifacts would be expected to be greater in the OFF condition in movement disorders such as PD. Improved motion correction may also lead to decreased variance in either ON or OFF conditions.

Fourth, development of the clinical value of neuroimaging will continue to be an important area of endeavor as the clinical value of neuroimaging has been limited (Perlmutter & Norris, 2014; Politis, 2014). So far the additive value of neuroimaging over a good history and physical exam has not been very useful for clinical purposes (e.g. Hellwig et al., 2013). For example, although many neuroimaging studies of PD cited in this review refer to one or more of their neuroimaging findings as a biomarker or potential biomarker, currently there are no established neuroimaging biomarkers for clinical use in PD (Duncan et al., 2013; Miller & O'Callaghan, 2015; Perlmutter & Norris, 2014; Schapira, 2013; Sharma et al., 2013). Further, it is possible that any single measure, neuroimaging or otherwise, may not be sufficiently useful as a clinical biomarker of PD (Schapira, 2013). Thus future work on biomarkers may include studies that explore combinations of measures, perhaps including combinations of neuroimaging biomarkers.

Fifth, a key direction for future studies is the advancement of current and novel neuroimaging methods to improve investigation of the neurodegenerative changes in PD. Neuroimaging approaches that could better reveal the nature of neurodegenerative changes, especially in prodromal and early stages, could help advance understanding of neurodegenerative processes and may lead to new approaches for treatments and, hopefully, preventive strategies. The ability to image α-synuclein would be of particular importance as α-synuclein deposits in Lewy bodies and neurites are the neuropathological signature of PD. Efforts to image α-synuclein are underway (Perlmutter & Norris, 2014; Vernon et al., 2010). A better understanding of the biochemical and cellular pathways that lead to neurodegeneration may also open up new imaging targets to facilitate early detection and disease staging (e.g. NO and glial activation (Bortolanza et al., 2015); axonal degeneration

(Burke & O'Malley, 2013); prion-like mechanisms (Goedert et al., 2013; Surmeier & Sulzer, 2013).

Overall, neuroimaging of PD is likely to continue to reveal a complex picture of neural involvement consistent with the extensive brain regions and neurobiological systems involved in PD, with many neurodegenerative changes already present when patients first begin to seek medical attention and which then further expand as the disorder progresses. These changes potentially include all the major regions of the brain and multiple neurotransmitter systems. Thus future advances in neuroimaging that allow for more refined imaging of brain structure and function seem likely to lead to even more complexity. Hopefully this complexity will converge with development of more individualized neuroimaging and personalized medicine approaches for assessment, treatment, and prevention of PD.

Finally, Gjerløff et al.'s (2015) PET study of parasympathetic denervation in PD reminds us that "neuroimaging" extends far beyond the brain (Stoessl, 2015). The Braak hypothesis supports the pattern of a "gut-to-brain" propagation of Lewy pathology, and indeed symptoms of peripheral nervous system dysfunction are common amongst *de novo* PD patients. Future neuroimaging studies targeted to the peripheral nervous system may allow identification of PD in its earliest (preclinical) stages, improve our understanding of disease pathogenesis and progression, and enable the design of clinical trials to test treatments that might prevent or delay the onset of motor and other central nervous system features of PD.

In conclusion, much work will be needed to develop better treatments and preventive strategies. A description of PD and effects of L-DOPA treatment was once given by a patient: "'who likened the glow of the levodopa awakening to the switching on of a light and the equally abrupt return of the parkinsonian darkness to the light going off' (Lees, 1989; Duvoisin, 1974) (sic)" (Black et al., 2005: 590). Neuroimaging is bringing more light to the previously hidden landscape of the neuropathophysiological alterations occurring in PD and its treatments. In this way it is hoped that neuroimaging will also help bring more light to where it is most needed, in the lives of those with PD.

Acknowledgements

Grateful acknowledgement is given to anonymous reviewers for their indispensable assistance. Our research was supported by Grant Number R01NS074045 from the National Institute of Neurological Disorders and Stroke. The content is solely the responsibility of the authors and does not necessarily represent the official views of the National Institute of Neurological Disorders and Stroke or the National Institutes of Health.

References

Abhinav K, Yeh FC, Pathak S, Suski V, Lacomis D, Friedlander RM, Fernandez-Miranda JC. Advanced diffusion MRI fiber tracking in neurosurgical and neurodegenerative disorders and neuroanatomical studies: a review. Biochim Biophys Acta. 2014; 1842:2286–2297. [PubMed: 25127851]

Adler CH, Beach TG, Hentz JG, Shill HA, Caviness JN, Driver-Dunckley E, … Dugger BN. Low clinical diagnostic accuracy of early vs advanced Parkinson disease: clinicopathologic study. Neurology. 2014; 83:406–412. [PubMed: 24975862]

Agosta F, Canu E, Stefanova E, Sarro L, Tomic A, Spica V, … Filippi M. Mild cognitive impairment in Parkinson's disease is associated with a distributed pattern of brain white matter damage. Hum Brain Mapp. 2014; 35:1921–1929. (**significant contribution). [PubMed: 23843285]

Ahmed I, Bose SK, Pavese N, Ramlackhansingh A, Turkheimer F, Hotton G, … Brooks DJ. Glutamate NMDA receptor dysregulation in Parkinson's disease with dyskinesias. Brain. 2011; 134:979–986. [PubMed: 21371994]

Aiello M, Salvatore E, Cachia A, Pappata S, Cavaliere C, Prinster A, … Quarantelli M. Relationship between simultaneously acquired resting-state regional cerebral glucose metabolism and functional MRI: A PET/MRI hybrid scanner study. Neuroimage. 2015; 113:111–121. (*special interest). [PubMed: 25791784]

Airaksinen K, Mäkelä JP, Nurminen J, Luoma J, Taulu S, Ahonen A, Pekkonen E. Cortico-muscular coherence in advanced Parkinson's disease with deep brain stimulation. Clin Neurophysiology. 2015; 126:748.

Al-Bachari S, Parkes LM, Vidyasagar R, Hanby MF, Tharaken V, Leroi I, Emsley HCA. Arterial spin labeling reveals prolonged arterial arrival time in idiopathic Parkinson's disease. Neuroimage: Clin. 2014; 6:1–8. [PubMed: 25379411]

Alexander AL, Lee JE, Lazar M, Field AS. Diffusion tensor imaging of the brain. Neurotherapeutics. 2007; 4:316–329. [PubMed: 17599699]

Alexander GE, DeLong MR, Strick PL. Parallel organization of functionally segregated circuits linking basal ganglia and cortex. Ann Rev Neurosci. 1986; 9:357–381. [PubMed: 3085570]

Ali K, Morris HR. Parkinson's disease: chameleons and mimics. Pract Neurol. 2015; 15:14–25. [PubMed: 25253895]

Alonso-Canovas A, Lopez-Sendon JL, Buisan J, deFelipe-Mimbrera A, Guillan M, Garcia-Barragan N, … Walter U. Sonography for diagnosis of Parkinson disease- from theory to practice. J Ultrasound Med. 2014; 33:2069–2074. [PubMed: 25425362]

Anders S, Sack B, Pohl A, Münte T, Pramstaller P, Klein C, Binkofski F. Compensatory premotor activity during affective face processing in subclinical carriers of a single mutant *Parkin* allele. Brain. 2012; 135:1128–1140. [PubMed: 22434215]

Andronesi OC, Bhat H, Reuter M, Mukherjee S, Caravan P, Rosen BR. Whole brain mapping of water pools and molecular dynamics with rotating frame MR relaxation using gradient modulated low-power adiabatic pulses. Neuroimage. 2014; 89:92–109. [PubMed: 24345390]

Appel L, Jonasson M, Danfors T, Nyholm D, Askmark H, Lubberink M, Sörensen J. Use of 11C-PE21 PET in differential diagnosis of parkinsonian disorders. J Nucl Med. 2015; 56:234–242. [PubMed: 25593112]

Aquino D, Contarino V, Albanese A, Minati L, Farina L, Grisoli M, … Chiapparini L. Substantia nigra in Parkinson's disease: a multimodal MRI comparison between early and advanced stages of the disease. Neurol Sci. 2014; 35:753–758. [PubMed: 24337946]

Auning E, Kjaervik VK, Selnes P, Aarsland D, Haram A, Bjørnerud A, … Fladby T. White matter integrity and cognition in Parkinson's disease: a cross-sectional study. BMJ Open. 2014; 4:e003976.

Bach M, Laun FB, Leemans A, Tax CMW, Biessels GJ, Stieltjes B, Maier-Hein KH. Methodological considerations on tract-based spatial statistics (TBSS). Neuroimage. 2014; 100:358–369. [PubMed: 24945661]

Bagchi DP, Yu L, Perlmutter JS, Xu J, Mach RH, Tu Z, Kotzbauer PT. Binding of the radioligand SIL23 to α-synuclein fibrils in Parkinson disease brain tissue establishes feasibility and screening approaches for developing a Parkinson disease imaging agent. PLOS ONE. 2013; 8(2):e55031.10.1371/journal.pone.0055031 [PubMed: 23405108]

Baggio HC, Sala-Llonch R, Segura B, Marti MJ, Valldeoriola F, Compta Y, … Junque C. Functional brain networks and cognitive deficits in Parkinson's disease. Hum Brain Mapp. 2014; 35:4620–4634. [PubMed: 24639411]

Baik KW, Cha J, Ham JH, Baek GM, Sunwoo MK, Hong JY, … Lee PH. Dopaminergic modulation of resting-state functional connectivity in de novo patients with Parkinson's disease. Hum Brain Mapp. 2014; 35:5431–5441. (**significant contribution). [PubMed: 24938993]

Bajaj N, Hauser RA, Grachev ID. Clinical utility of dopamine transporter single photon emission CT (DaT-SPECT) with (^{123}I) ioflupane in diagnosis of parkinsonian syndromes. J Neurol Neurosurg Psychiatry. 2013; 84:1288–1295. [PubMed: 23486993]

Barnes KA, Cohen AL, Power JD, Nelson SM, Dosenbach YBL, Miezin FM, … Schlagger BL. Identifying basal ganglia divisions in individuals using resting-state functional connectivity MRI. Front Syst Neuroscience. 2010; 4,18:1–10.

Basu S, Alavi A. Unparalleled contribution of ^{18}F-FDG PET to medicine over 3 decades. J Nucl Med. 2008; 49:17N–37N.

Baudrexel S, Witte T, Seifried C, Von Wegner F, Beissner F, Klein JC, … Hilker R. Resting state fMRI reveals increased subthalamic nucleus-motor cortex connectivity in Parkinson's disease. Neuroimage. 2011; 55:1728–1738. (**significant contribution). [PubMed: 21255661]

Bhidayasiri R, Chotipanich C, Joutsa J, Tepmongkol S, Wannachi N, Johansson J, … Rinne JO. Boxing and Parkinson disease: a link or a myth? An ^{18}F-FDOPA PET/CT study in retired Thai traditional boxers. Parkinsonism Rel Disord. 2012; 18:694–696. (*special interest).

Biswal BB, Mennes M, Zuo XN, Gohel S, Kelly C, Smith SM, … Milham MP. Toward discovery science of human brain function. Proc Natl Acad Sci. 2010; 107:4734–4739. [PubMed: 20176931]

Biundo B, Weis L, Facchini S, Formento-Dojot P, Vallelunga A, Pilleri M, … Antonini A. Patterns of cortical thickness associated with impulse control disorders in Parkinson's disease. Mov Disord. 2015; 15:688–695. (*special interest). [PubMed: 25649923]

Black KJ, Hershey T, Hartlein JM, Carl JL, Perlmutter JS. Levodopa challenge neuroimaging of levodopa-related mood fluctuation in Parkinson's disease. Neuropsychopharmacol. 2005; 30:590–601. (*special interest).

Blazejewska A, Schwarz ST, Pitiot A, Stephenson MC, Lowe J, Bajaj N, … Gowland PA. Visualization of nigrosome 1 and its loss in PD: pathoanatomical correlation and in vivo 7 T MRI. Neurology. 2013; 81:534–540. (*special interest). [PubMed: 23843466]

Boassa D, Berlanga ML, Yang ML, Terada M, Hu J, Bushong EA, … Ellisman MH. Mapping the subcellular distribution of alpha-synuclein in neurons using genetically encoded probes for correlated light and electron microscopy: implications for Parkinson's disease pathogenesis. J Neurosci. 2013; 33:2605–2615. [PubMed: 23392688]

Bohnen NI, Müller MLTM. In vivo neurochemical imaging of olfactory dysfunction in Parkinson's disease. J Neural Transm. 2013; 120:571–576. [PubMed: 23263541]

Bohnen NI, Müller MLTM, Zarzhevsky N, Koeppe RA, Bogan CW, Kilbourn MR, … Albin RL. Leucoaraiosis, nigrostriatal denervation and motor symptoms in Parkinson's disease. Brain. 2011; 134:2358–2365. [PubMed: 21653540]

Bomasang-Layno E, Fadlon I, Murray AN, Himelhoch S. Antidepressive treatments for Parkinson's disease: a systematic review and meta-analysis. Parkinsonism Rel Disord. 2015; 21:833–842. (**significant contribution).

Borghammer P, Hansen SB, Eggers C, Chakravarty M, Vang K, Aanerud J, … Gjedde A. Glucose metabolism in small subcortical structures in Parkinson's disease. Acta Neurol Scand. 2012; 125:303–313. [PubMed: 21692755]

Borroni B, Premi E, Formenti A, Turrone R, Alberici A, Cottini E, … Padovani A. Structural and functional imaging study in dementia with Lewy bodies and Parkinson's disease dementia. Parkinsonism Rel Disord. 2015; 21:1049–155.

Bortolanza M, Cavalcanti-Kiwiatkoski R, Padovan-Neto FE, da-Silva CA, Mitkovski M, Raisman-Vozari R, Del-Bel E. Glial activation is associated with L-DOPA induced dyskinesia and blocked by a nitric oxide synthase inhibitor in a rat model of Parkinson's disease. Neurobiol Disease. 2015; 73:377–387.

Bouwmans AEP, Vlaar AMM, Mess WH, Kessels A, Weber WE. Specificity and sensitivity of the transcranial sonography of the substantia nigra in the diagnosis of Parkinson's disease: prospective cohort study in 196 patients. BMJ Open. 2013; 3:e002613.

Braak H, Ghebremedhin E, Rüb U, Bratzke H, Del Tredici K. Stages in the development of Parkinson's disease-related pathology. Cell Tissue Res. 2004; 318:121–134. (**significant contribution). [PubMed: 15338272]

Brooks DJ. Positron emission tomography and single-photon emission computed tomography in central nervous system drug development. NeuroRx. 2005; 2:226–236. [PubMed: 15897947]

Brooks DJ, Pavese N. Imaging biomarkers in Parkinson's disease. Prog Neurobiol. 2011; 95:614–628. [PubMed: 21896306]

Brunenberg EJL, Moeskops P, Backes W, Pollo C, Cammoun L, Vilanova A, … Platel B. Structural and resting state functional connectivity of the subthalamic nucleus: identification of motor STN parts and the hyperdirect pathway. PLOS ONE. 2012; 7(6):e39061. (**significant contribution). 10.1371/journal.pone.0039061 [PubMed: 22768059]

Bu L, Li R, Liu H, Xiong X, Zhao H, Vollrath D, … Cheng Z. Intrastriatal transplantation of retinal pigment epithelial cells for the treatment of Parkinson disease: in vivo longitudinal molecular imaging with ^{18}F-P3BZA PET/CT. Radiology. 2014; 272:174–183. [PubMed: 24758555]

Bunzeck N, Singh-Curry V, Eckart C, Weiskopf N, Perry RJ, Bain PG, … Husain M. Motor phenotype and magnetic resonance measures of basal ganglia iron levels in Parkinson's disease. Parkinsonism Rel Disord. 2013; 19:1136–1142.

Burciu RG, Ofori E, Shukla P, Planetta PJ, Snyder AF, Li H, … Vaillancourt DE. Distinct patterns of brain activity in progressive supranuclear palsy and Parkinson's disease. Mov Disord. 2015; 30:1248–1258. [PubMed: 26148135]

Burke RE, O'Malley K. Axon degeneration in Parkinson's disease. Exp Neurol. 2013; 246:72–83. [PubMed: 22285449]

Calabresi P, Castrioto A, Di Filippo M, Picconi B. New experimental and clinical links between the hippocampus and the dopaminergic system in Parkinson's disease. Lancet Neurol. 2013; 12:811–821. [PubMed: 23867199]

Calabresi P, Picconi B, Parnetti L, Di Filippo MD. A convergent model for cognitive dysfunctions in Parkinson's disease: the critical dopamine-acetylcholine synaptic balance. Lancet Neurol. 2006; 5:974–983. [PubMed: 17052664]

Campbell MC, Koller JM, Snyder AZ, Buddhala C, Kotzbauer PT, Perlmutter JS. CSF proteins and resting-state functional connectivity in Parkinson disease. Neurology. 2015; 84:2413–2421. (**significant contribution). [PubMed: 25979701]

Campbell MC, Markham J, Flores H, Hartlein JM, Goate AM, Cairns NJ, … Perlmutter JS. Principal component analysis of PiB distribution in Parkinson and Alzheimer diseases. Neurology. 2013; 81:520–527. [PubMed: 23825179]

Carbonell F, Nagano-Saito A, Leyton M, Cisek P, Benkelfat C, He Y, Dagher A. Dopamine precursor depletion impairs structure and efficiency of resting state brain functional networks. Neuropharmacology. 2014; 84:90–100. [PubMed: 24412649]

Carlsson A, Waters NW, Waters S, Carlsson ML. Network interactions in schizophrenia – therapeutic implications. Brain Res Interact. 2000; 31:342–349.

Carriere N, Lopes R, Defebvre L, Delmaire C, Dujardin K. Impaired corticostriatal connectivity in impulse control disorders in Parkinson disease. Neurology. 2015; 84:1–8.

Castellanos G, Fernandez-Seara MA, Lorenzo-Betancor O, Ortega-Cubero S, Puigvert M, Uranga J, … Pastor MA. Automated neuromelanin imaging as a diagnostic biomarker for Parkinson's disease. Mov Disord. 2015; 30:945–52. (*special interest). [PubMed: 25772492]

Chen NK, Chou YH, Song AW, Madden DJ. Measurement of spontaneous signal fluctuations in fMRI: adult age differences in intrinsic functional connectivity. Brain Struct Funct. 2009; 213:571–585. [PubMed: 19727810]

Cherubini A, Morelli M, Nistico R, Salsone M, Gennarina A, Vasta R, … Quattrone A. Magnetic resonance support vector machine discriminates between Parkinson disease and progressive supranuclear palsy. Mov Disord. 2014; 29:266–269. [PubMed: 24323617]

Cho ZL, Oh SH, Kim JM, Park SY, Kwon DH, Jeong HJ, … Jeon BS. Direct visualization of Parkinson's disease by in vivo human brain imaging using 7.0T magnetic resonance imaging. Mov Disord. 2011; 26:713–718. [PubMed: 21506148]

Coakeley S, Strafella AP. Imaging pathological tau in atypical parkinsonian disorders. Curr Opin Neurol. 2015; 28:447–452. [PubMed: 26110795]

Cochrane CJ, Ebmeier KP. Diffusion tensor imaging in parkinsonian syndromes: a systematic review and meta-analysis. Neurology. 2013; 80:857–864. (**significant contribution). [PubMed: 23439701]

Cole DM, Beckmann CF, Oei NYI, Both S, van Gerven JMA, Rombouts SARB. Differential and distributed effects of dopamine neuromodulations on resting-state network connectivity. Neuroimage. 2013; 78:59–67. [PubMed: 23603346]

Colloby SJ, Pakrasi S, Firbank MJ, Perry EK, Piggott MA, Owens J, … O'Brien JT. In vivo SPECT imaging of muscarinic acetylcholine receptors using *(R,R)*^{123}I-QNB in dementia with Lewy bodies and Parkinson's disease dementia. Neuroimage. 2006; 33:423–429. [PubMed: 16959499]

Criswell SR, Perlmutter JS, Videen TO, Moerlein SM, Flores HP, Birke AM, Racette BA. Reduced uptake of [^{18}F]FDOPA PET in asymptomatic welders with occupational manganese exposure. Neurology. 2011; 76:1296–1301. [PubMed: 21471467]

Cropley VL, Fujita M, Bara-Jimenez W, Brown AK, Zhang XY, Sangare J, … Innis RB. Pre- and post-synaptic dopamine imaging and its relation with frontostriatal cognitive function in Parkinson disease: PET studies with [^{11}C]NNC 112 and [^{18}F]FDOPA. Psychiatry Res: Neuroimaging. 2008; 163:171–182. [PubMed: 18504119]

Dager SR, Oskin NM, Richards TL, Posse S. Research applications of magnetic resonance spectroscopy (MRS) to investigate psychiatric disorders. Top Magn Reson Imaging. 2008; 19(2): 81–96.10.1097/RMR.0b01318181e0be [PubMed: 19363431]

Dehorter N, Guigoni C, Lopez C, Hirsch J, Eusebio A, Ben-Ari Y, Hammond C. Dopamine-deprived striatal GABAergic interneurons burst and generate repetitive IPSCs in medium spiny neurons. J Neurosci. 2009; 29:7776–7787. [PubMed: 19535589]

Delong MR. Primate models of movement disorders of basal ganglia origin. Trends Neurosci. 1990; 13:281–285. [PubMed: 1695404]

Detre JA, Rao HR, Wang DJJ, Chen YF, Wang Z. Applications of arterial spin labeled MRI in the brain. J Magn Reson Imaging. 2012; 35:1026–1037. [PubMed: 22246782]

Di X, Kim EH, Huang CC, Tsai SJ, Lin CP, Biswal BB. The influence of the amplitude of low-frequency fluctuations on resting-state functional connectivity. Front Hum Neurosci. 2013; 7:118.10.3389/fnhum.2013.00118 [PubMed: 23565090]

Di Martino A, Scheres A, Margulies DS, Kelly AMC, Uddin LQ, Shehzad Z, … Milham MP. Functional connectivity of human striatum: a resting state fMRI study. Cereb Cortex. 2008; 8:2735–2747. [PubMed: 18400794]

Draganski B, Kherif F, Klöppel S, Cook PA, Alexander DC, Parker GJM, … Frackowiak RSJ. Evidence for segregated and integrative connectivity patterns in the human basal ganglia. J Neurosci. 2008; 28:7143–7152. [PubMed: 18614684]

Du C, Volkow ND, Koretsky AP, Pan Y. Low-frequency calcium oscillations accompany deoxyhemoglobin oscillations in rat somatosensory cortex. Proc Nat Acad Sci. 2014; 111(43):E4677–4686.10.1073/pnas.1410800111 [PubMed: 25313035]

Duncan GW, Firbank MJ, O'Brien JT, Burn DJ. Magnetic resonance imaging: a biomarker for cognitive impairment in Parkinson's disease? Mov Disord. 2013; 28:425–438. (*special interest). [PubMed: 23450518]

Dupre KB, Eskow KL, Steiniger A, Klioueva A, Negron GE, Lormand L, … Bishop C. Effects of coincident 5-HT$_{1a}$ receptor stimulation and NMDA receptor antagonism on L-DOPA-induced dyskinesia and rotational behaviors in the hemi-parkinsonian rat. Psychopharmacol. 2008; 199:99–108.

Duvoisin RC. Variations in the on-off phenomenon. Adv Neurol. 1974; 5:339–340. [PubMed: 4440582]

Düzel E, Bunzcek N, Guitart-Masip M, Wittmann B, Schott BH, Tobler N. Functional imaging of the human dopaminergic midbrain. Trends Neurosci. 2009; 32:321–328. [PubMed: 19446348]

Dydak U, Jiang YM, Long LL, Zhu H, Chen J, Li WM, … Zheng W. *In vivo* measurement of brain GABA concentrations by magnetic resonance spectroscopy in smelters occupationally exposed to manganese. Environ Health Persp. 2011; 119:219–224.

Eckert T, Tang C, Ma Y, Brown N, Lin T, Frucht S, … Eidelberg D. Abnormal metabolic networks in atypical parkinsonism. Mov Disord. 2008; 23:727–733. [PubMed: 18186116]

Eckert T, Van Laere K, Tang C, Lewis DE, Edwards C, Santens P, Eidelberg D. Quantification of Parkinson's disease-related network expression with ECD SPECT. Eur J Nucl Med Mol Imaging. 2007; 34:496–501. [PubMed: 17096095]

Edison P, Ahmed I, Fan Z, Hinz R, Gelosa G, Chaudhuri KR, … Brooks DJ. Microglia, amyloid, and glucose metabolism in Parkinson's disease with and without dementia. Neuropsychopharmacol. 2013; 38:938–949. (*special interest).

Eggers C, Schmidt A, Hagenah J, Brüggemann N, Klein JC, Tadic V, … Klein C. Progression of subtle motor signs in PINK1 mutation carriers with mild dopaminergic deficit. Neurology. 2010; 74:1798–1805. [PubMed: 20513816]

Eidelberg D. Metabolic brain networks in neurodegenerative disorders: a functional imaging approach. Trends Neurosci. 2009; 32:548–557. [PubMed: 19765835]

Emir UE, Tuite PJ, Öz G. Elevated pontine and putamenal GABA levels in mid-moderate Parkinson disease detected by 7 Tesla proton MRS. PLOS ONE. 2012; 7(1):e30918.10.1371/journal.pone.0030918 [PubMed: 22295119]

Erro R, Picillo M, Vitale C, Amboni M, Moccia M, Longo K, … Barone P. Non-motor symptoms in early Parkinson's disease: a 2-year follow-up study on previously untreated patients. J Neurol Neurosurg Psychiatry. 2013; 84:14–17. [PubMed: 22993448]

Esposito F, Tessitore A, Giordano A, De Micco R, Paccone A, Conforti R, … Tedeschi G. Rhythm-specific modulation of the sensorimotor network in drug-naive patients with Parkinson's disease by levodopa. Brain. 2013; 136:710–725. [PubMed: 23423673]

Farquharson S, Tournier JT, Calamante F, Fabinyi G, Schneider-Kolsky M, Jackson GD, Connelly A. White matter fiber tractography: why we need to move beyond DTI. J Neurosurg. 2013; 118:1367–1377. [PubMed: 23540269]

Feigin A, Kaplitt MG, Tang C, Lin T, Mattis P, Dhawan V, … Eidelberg D. Modulation of metabolic brain networks after subthalamic gene therapy for Parkinson's disease. Proc Nat Acad Sci. 2007; 104:19559–19564. (**significant contribution). [PubMed: 18042721]

Fernandez-Seara MA, Mengual E, Vidorreta M, Castellanos G, Irigoyen J, Erro E, Pastor MA. Resting state functional connectivity of the subthalamic nucleus in Parkinson's disease assessed using arterial spin-labeled perfusion fMRI. Human Brain Mapping. 2015; 36:1937–1950. (*special interest). [PubMed: 25641065]

Fioravanti V, Benuzzi F, Codeluppi L, Contardi S, Cavallieri F, Nichelli P, Valzania F. MRI correlates of Parkinson's disease progression: a voxel based morphometry study. Parkinsons Dis. 2015; 2015:378032.10.1155/2015/378032 [PubMed: 25628916]

Fox MD, Snyder AZ, Vincent JL, Corbetta M, Van Essen DC, Raichle ME. The human brain is intrinsically organized into dynamic, anticorrelated functional networks. Proc Natl Acad Sci. 2005; 102:9673–9678. [PubMed: 15976020]

de la Fuente-Fernandez R. Frontostriatal cognitive staging in Parkinson's disease. Parkinson's Dis. 2012; 2012:561046.10.1155/2012/561046 [PubMed: 22191070]

Galvan A, Wichmann T. Pathophysiology of Parkinsonism. Clin Neurophysiol. 2008; 119:1459–1474. [PubMed: 18467168]

Garcia-Lorenzo D, Santos CLD, Ewenczyk C, Leu-Semenescu S, Gallea C, Quattrocchi G, … Lehericy S. The coeruleus/subcoeruleus complex in rapid eye movement sleep behaviour disorders in Parkinson's disease. Brain. 2013; 136:2120–2129. [PubMed: 23801736]

Garraux G, Phillips C, Schrouff J, Kreisler A, Lemaire C, Degueldre C, … Salmon E. Multiclass classification of FDG PET scans for the distinction between Parkinson's disease and atypical parkinsonian syndromes. Neuroimage: Clin. 2013; 2:883–893. [PubMed: 24179839]

Gatto NM, Deapen D, Stoyanoff S, Pinder R, Narayan S, Bordelon Y, Ritz B. Lifetime exposure to estrogens and Parkinson's disease in California teachers. Parkinsonism Relat Disord. 2014; 20:1149–1156. [PubMed: 25179495]

Gerasimou G, Costa DC, Papanastasiou E, Bostanjiopoulou S, Arnaoutoglou M, Moralidis E, … Gotzamani-Psarrakou A. SPECT study with I-123 –Ioflupane (DaTSCAN) inpatients with essential tremor. Is there any correlation with Parkinson's disease? Ann Nucl Med. 2012; 26:337–344. [PubMed: 22382608]

Gjerløff T, Fedorova T, Knudsen K, Munk OL, Nahimi A, Jacobsen S, … Borghammer P. Imaging acetylcholinesterae density in peripheral organs in Parkinson's disease with ^{11}C-donepezil PET. Brain. 2015; 138:653–663. (**significant contribution). [PubMed: 25539902]

Goedert M, Spillantini MG, Tredici KD, Braak H. 100 years of Lewy pathology. Nature Rev Neurosci. 2013; 9:13–24.

Goldstein DS, Holmes C, Bentho O, Sato T, Moak MD, Sharabi Y, … Eldadah BA. Biomarkers to detect central dopamine deficiency and distinguish Parkinson disease from multiple system atrophy. Parkinsonism Rel Disord. 2008; 14:600–607.

Gonzalez-Garcia N, Armony JL, Soto J, Trejo D, Alegria MA, Drucker-Colin R. Effects of rTMS on Parkinson's disease: a longitudinal fMRI study. J Neurol. 2011; 258:1268–1280. [PubMed: 21298283]

Gorges M, Müller HP, Lule D, Ludolph AC, Pinkhardt EH, Kassubek J. Functional connectivity within the default mode network is associated with saccadic accuracy in Parkinson's disease: a resting-state fMRI and videooculographic study. Brain Connect. 2013; 3:265–272. [PubMed: 23627641]

Göttlich M, Münte TF, Heldmann M, Kasten M, Hagenah J, Krämer UM. Altered resting state brain networks in Parkinson's disease. PLOS ONE. 2013; 8(10):e77336.10.1371/journal.pone.0077336 [PubMed: 24204812]

Graff-Radford J, Boeve BF, Murray M, Ferman TJ, Tosakulwong N, Lesnick TG, … Kantarci K. Regional proton magnetic resonance spectroscopy patterns in dementia with Lewy bodies. Neurobiol Aging. 2014; 35:1483–1490. [PubMed: 24468473]

Gröger A, Kolb RK, Schäfer R, Klose U. Dopamine reduction in the substantia nigra of Parkinson's disease patients confirmed by in vivo magnetic resonance spectroscopic imaging. PLOS ONE. 2014; 9(1):e84081.10.1371/journal.pone.0084081 [PubMed: 24416192]

Hacker CD, Perlmutter JS, Criswell SR, Ances BM, Snyder AZ. Resting state functional connectivity of the striatum in Parkinson's disease. Brain. 2012; 135:3699–3711. [PubMed: 23195207]

Hagmann P, Jonasson L, Maeder P, Thiran JP, Wedeen VJ, Meuli R. Understanding diffusion MR imaging techniques: from scalar diffusion-weighted imaging to diffusion tensor imaging and beyond. RadioGraphics. 2006; 26:S205–S223. [PubMed: 17050517]

Haller S, Badoud S, Nguyen D, Garibotto V, Lovblad KO, Burkhard PR. Individual detection of patients with Parkinson disease using support vector machine analysis of diffusion tensor imaging data: initial results. Am J Neuroradiol. 2012; 33:2123–2128. (*special interest). [PubMed: 22653326]

Ham JH, Cha J, Lee JJ, Baek GM, Sunwoo MK, Hong JY, … Lee PH. Nigrostriatal dopamine-independent resting-state functional networks in Parkinson's disease. Neuroimage. 2015; 119:296–304. [PubMed: 26143204]

Hammoud DA, Hoffman JM, Pomper MG. Molecular neuroimaging: from conventional to emerging techniques. Radiol. 2007; 245:21–42.

Hellwig S, Amtage F, Kreft A, Buchert R, Winz OH, Vach W, … Meyer PT. [^{18}F]FDG-PET is superior to [^{123}I]IBZM-SPECT for the differential diagnosis of parkinsonism. Neurology. 2012; 79:1314–1322. [PubMed: 22914831]

Hellwig S, Kreft A, Amtage F, Tüscher O, Winz OH, Hellwig B, … Meyer PT. ^{123}I-iodobenzamide SPECT is not an independent predictor of dopaminergic responsiveness in patients with suspected atypical Parkinsonian syndromes. J Nucl Med. 2013; 54:2081–2086. (**significant contribution). [PubMed: 24115529]

Helmich RC, Derikx LC, Bakker M, Scheeringa R, Bloem BR, Toni I. Spatial remapping of cortico-striatal connectivity in Parkinson's disease. Cereb Cortex. 2010; 20:1175–1186. (**significant contribution). [PubMed: 19710357]

Hely MA, Reid WGJ, Adena MA, Halliday GM, Morris JGL. The Sydney multicenter study of Parkinson's disease: the inevitability of dementia at 20 years. Mov Disord. 2008; 23:837–844. [PubMed: 18307261]

Henkelman RM, Stanisz GJ, Graham SJ. Magnetization transfer in MRI: a review. NMR Biomed. 2001; 14:57–64. [PubMed: 11320533]

Herz DM, Eickhoff SB, Lokkegaard A, Siebner HR. Functional neuroimaging of motor control in Parkinson's disease: a meta-analysis. Hum Brain Mapp. 2014; 35:3227–3237. (**significant contribution). [PubMed: 24123553]

Herz DM, Haagensen BN, Christensen MS, Madsen KH, Rowe JB, Løkkegaard A, Siebner HR. Abnormal dopaminergic modulation of striato-cortical networks underlies levodopa-induced dyskinesias in humans. Brain. 2015; 138:1658–1666. [PubMed: 25882651]

Hickey P, Stacy M. Available and emerging treatments for Parkinson's disease: a review. Drug Des Devel Ther. 2011; 5:241–254.

Hilker R, Pilatus U, Eggers C, Hagenah J, Roggendorf J, Baudrexel S, … Hattingen E. The bioenergetic status related to dopamine neuron loss in familial PD with PINK1 mutations. PLOS ONE. 2012; 7(12):e51308.10.1371/journal.pone.0051308 [PubMed: 23251494]

Hirano S, Asanuma K, Ma Y, Tang C, Feigin A, Dhawan V, … Eidelberg D. Dissociation of metabolic and neurovascular responses to levodopa in the treatment of Parkinson's disease. J Neurosci. 2008; 28:4201–4209. (**significant contribution). [PubMed: 18417699]

Höglinger GU, Huppertz HJ, Wagenpfeil S, Andres MV, Belloch V, Leon TL, del Ser T. Tideglusib reduces progression of brain atrophy in progressive supranuclear palsy in a randomized trial. Mov Disord. 2014; 29:479–487. [PubMed: 24488721]

Holiga S, Mueller K, Möller HE, Sieger T, Schroeter ML, Vymazal J, … Jech R. Motor matters: tackling heterogeneity of Parkinson's disease in functional MRI studies. PLOS ONE. 2013; 8(2):e56133.10.1371/journal.pone.0056133 [PubMed: 23418522]

Holtbernd F, Gagnon JF, Postuma RB, Ma Y, Tang CC, Feigin A, … Montplaisir J. Abnormal metabolic network activity in REM sleep behavior disorder. Neurology. 2014; 82:620–627. (**significant contribution). [PubMed: 24453082]

Honey GD, Suckling J, Zelaya F, Long C, Routledge C, Jackson S, … Bullmore ET. Dopaminergic drug effects on physiological connectivity in a human corticostriato-thalamic system. Brain. 2003; 126:1767–1781. [PubMed: 12805106]

Hou Y, Wu X, Hallett M, Chan P, Wu T. Frequency-dependent neural activity in Parkinson's disease. Hum Brain Mapp. 2014; 35:5815–5833. (*special interest). [PubMed: 25045127]

Hsiao IT, Weng YH, Hsieh CJ, Lin WY, Wey SP, Kung MP, … Lin KJ. Correlation of Parkinson disease severity and ^{18}F-DTBZ positron emission tomography. JAMA Neurol. 2014a; 71:758–66. (**significant contribution). [PubMed: 24756323]

Hsiao IT, Weng YH, Lin WY, Hsieh CJ, Wey SP, Yen TC, … Lin KJ. Comparison of ^{99m}Tc-TRODAT-1 SPECT and ^{18}F-AV-133 PET imaging in healthy controls and Parkinson's disease patients. Nucl Med Biol. 2014b; 41:322–329. [PubMed: 24503330]

Iannaccone S, Cerami C, Alessio M, Garibotto V, Panzacchi A, Olivieri S, … Perani D. *In vivo* microglia activation in very early dementia with Lewy bodies, comparison with Parkinson's disease. Parkinsonism Relat Disord. 2013; 19:47–52. [PubMed: 22841687]

Isaias IU, Spiegel J, Brumberg J, Cosgrove KP, Marotta G, Oishi N, … Samnick S. Nicotinic acetylcholine receptor density in cognitively intact subjects at an early stage of Parkinson's disease. Front Aging Neurosci. 2014; 6:213.10.3389/fnagi.2014.00213 [PubMed: 25177294]

Jadvar H, Colletti PM. Competitive advantage of PET/MRI. Eur J Radiol. 2014; 83:84–94. [PubMed: 23791129]

Jahanshahi M, Jones CRG, Zijlmans J, Katsenschlager R, Lee L, Quinn N, … Lees AJ. Dopaminergic modulation of striato-frontal connectivity during motor timing in Parkinson's disease. Brain. 2010; 133:727–745. (**significant contribution). [PubMed: 20305278]

Jaunarajs KLE, Angoa-Perez M, Kuhn DM, Bishop C. Potential mechanisms underlying anxiety and depression in Parkinson's disease: consequences of L-DOPA treatment. Neurosci Biobehav Rev. 2011; 35:556–564. [PubMed: 20615430]

Jech R, Mueller K, Schroeter ML, Ruzicka E. Letter to the editor: levodopa increases functional connectivity in the cerebellum and brainstem in Parkinson's disease. Brain. 2013; 136:1–2. [PubMed: 23365088]

Ji, L.; Wang, Y.; Zhu, D.; Liu, W.; Shi, J. White matter differences between multiple system atrophy (parkinsonian type) and Parkinson's disease: a diffusion tensor image study. Neuroscience. 2015. http://dx.doi.org/10.1016/j.neuroscience.2015.07.060

Jimenez-Urbieta, H.; Gago, B.; de la Riva, P.; Delgado-Alvarado, M.; Marin, C.; Rodriguez-Oroz, MC. Dyskinesias and impulse control disorders in Parkinson's disease: from pathogenesis to potential therapeutic approaches. Neurosci Biobehav Rev. 2015. http://dx.doi.org/10.1016/j.neubiorev.2015.07.010

Joutsa J, Johansson J, Seppänen M, Noponen T, Kaasinen V. Dorsal-to-ventral shift in midbrain dopaminergic projections and increased thalamic/raphe serotonergic function in early Parkinson disease. J Nucl Med. 2015; 56:1036–1041. [PubMed: 25952735]

Kahan J, Urner M, Moran R, Flandin G, Marreiros A, Mancini L, … Foltynie T. Resting state functional MRI in Parkinson's disease: the impact of deep brain stimulation on 'effective' connectivity. Brain. 2014; 137:1130–1144. (**significant contribution). [PubMed: 24566670]

Kamagata K, Motoi Y, Abe O, Shimoji K, Hori M, Nakanishi A, Sano T, … Hattori N. White matter alteration of the cingulum in Parkinson disease with and without dementia: evaluation by diffusion tensor tract-specific analysis. Am J Neuroradiol. 2012; 33:890–895. [PubMed: 22241380]

Kamagata K, Motoi Y, Tomiyama H, Abe O, Ito K, Shimoji K, … Hattori N. Relationship between cognitive impairment and white-matter alteration in Parkinson's disease with dementia: tract-based spatial statistics and tract-specific analysis. Eur Radiol. 2013; 23:1946–1955. [PubMed: 23404139]

Kamagata K, Tomiyama H, Hatano T, Motoi Y, Abe O, Shimoji K, … Aoki S. A preliminary diffusional kurtosis imaging study of Parkinson disease: comparison with conventional diffusion tensor imaging. Neuroradiol. 2014; 56:251–258.

Kantarci K, Lowe VJ, Boeve BF, Weigand SD, Senjems ML, Przybelski SA, … Jack CR. Multimodality imaging characteristics of dementia with Lewy bodies. Neurobiol Aging. 2012; 33:2091–2105. [PubMed: 22018896]

Kapogiannis D, Reiter DA, Willette AA, Mattson MP. Posteromedial cortex glutamate and GABA predict intrinsic functional connectivity of the default mode network. Neuroimage. 2013; 64:112–119. [PubMed: 23000786]

Kas A, Bottlaender M, Gallezot JD, Vidailhet M, Villafane G, Gregoire MC, … Remy P. Decrease of nicotinic receptors in the nigrostriatal system in Parkinson's disease. J Cereb Blood Flow Metab. 2009; 29:1601–1608. [PubMed: 19491921]

Kelly C, de Zubicaray G, Di Martino A, Copland DA, Reiss PT, Klein DF, … McMahon K. L-DOPA modulates functional connectivity in striatal cognitive and motor networks: a double-blind placebo-controlled study. J Neurosci. 2009; 29:7364–7378. [PubMed: 19494158]

Kepe V, Bordelon Y, Boxer A, Huang SC, Liu J, Thiede FC, … Barrio JR. PET imaging of neuropathology in tauopathies: progressive supranuclear palsy. J Alzheimers disease. 2013; 36:145–153. [PubMed: 23579330]

Kiessling F. Science to practice: cellular therapy of Parkinson disease – a new radiotracer to target transplanted dopaminergic cells with PET. Radiology. 2014; 272:1–3. [PubMed: 24956043]

Kim DJ, Park B, Park HJ. Functional connectivity-based identification of subdivisions of the basal ganglia and thalamus using multilevel independent component analysis of resting state fMRI. Hum Brain Mapp. 2013; 34:1371–1385. [PubMed: 22331611]

Kim HJ, Kim SJ, Kim HS, Choi CG, Kim N, Han S, … Lee CS. Alterations of mean diffusivity in brain white matter and deep gray matter in Parkinson's disease. Neurosci Lett. 2013; 550:64–68. [PubMed: 23831353]

Kim YH, Ma HI, Kim YJ. Utility of the midbrain tegmentum diameter in the differential diagnosis of progressive supranuclear palsy from idiopathic Parkinson's disease. J Clin Neurol. 2015; 11:268–274. [PubMed: 26174787]

Klein C, Westenberger A. Genetics of Parkinson's disease. Cold Spring Harb Perspect Med. 2012; 2:a008888.10.1101/cshperspect.a008888 [PubMed: 22315721]

Ko JH, Feigin A, Mattis PJ, Tang CC, Ma Y, Dhawan V, … Eidelberg D. Network modulation following sham surgery in Parkinson's disease. J Clin Invest. 2014; 124:3656–3666. (**significant contribution). [PubMed: 25036712]

Ko JH, Mure H, Tang CC, Ma Y, Dhawan V, Spetsieris P, Eidelberg D. Parkinson's disease: increased motor network activity in the absence of movement. J Neurosci. 2013; 33:4540–4549. [PubMed: 23467370]

Kotagal V, Albin RL, Müller MLTM, Koeppe RA, Chervin RD, Frey KA, Bohnen NI. Symptoms of rapid eye movement sleep behavior disorder are associated with cholinergic denervation in Parkinson disease. Ann Neurol. 2012; 71:560–568. [PubMed: 22522445]

Kwak Y, Peltier S, Bohnen NI, Müller MLTM, Dayalu P, Seidler RD. Altered resting state cortico-striatal connectivity in mild to moderate stage Parkinson's disease. Front Syst Neurosci. 2010; 4:143.10.3389/fnsys.2010.00143 [PubMed: 21206528]

Kwak Y, Peltier S, Bohnen NI, Müller MLTM, Dayalu P, Seidler RD. L-DOPA changes spontaneous low-frequency BOLD signal oscillations in Parkinson's disease: a resting state fMRI study. Front Syst Neurosci. 2012; 6:52.10.3389/fnsys.2012.00052 [PubMed: 22783172]

Kwon HG, Jang SH. Differences in neural connectivity between substantia nigra and ventral tegmental area in the human brain. Front Hum Neurosci. 2014; 8:41.10.3389/fnhum.2014.00041 [PubMed: 24567711]

Laere KV, Casteels C, Lunskens S, Goffin K, Grachev ID, Bormans G, Vandenberghe W. Regional changes in type 1 cannabinoid receptor availability in Parkinson's disease in vivo. Neurobiol Aging. 2012; 33(3):620.e1–620.e8. [PubMed: 21459482]

Lanciego JL, Luquin N, Obeso JA. Functional neuroanatomy of the basal ganglia. Cold Spring Harb Perspect Med. 2012; 2(12):a009621. [PubMed: 23071379]

Langston JW. The Parkinson's complex: Parkinsonism is just the tip of the iceberg. Ann Neurol. 2006; 59:591–596. [PubMed: 16566021]

Le Bihan DL. Looking into the functional architecture of the brain with diffusion MRI. Nat Rev Neurosci. 2003; 4:469–480. [PubMed: 12778119]

Lebedev AV, Westman E, Simmons A, Lebedeva A, Siepel FJ, Pereira JB, Aarsland D. Large-scale resting state network correlates of cognitive impairment in Parkinson's disease and related dopaminergic deficits. Front Syst Neurosci. 2014; 8:45.10.3389/fnsys.2014.00045 [PubMed: 24765065]

Lee EY, Eslinger PJ, Guangwei D, Kong L, Lewis MM, Huang X. Olfactory-related cortical atrophy is associated with olfactory dysfunction in Parkinson's disease. Mov Disord. 2014; 29:1205–1208. [PubMed: 24482154]

Lee JE, Cho KH, Ham JH, Song SK, Sohn YH, Lee PH. Olfactory performance acts as a cognitive reserve in non-demented patients with Parkinson's disease. Parkinsonism Rel Disord. 2014; 20:186–191.

Lee JY, Seo SH, Kim YK, Yoo HB, Kim YE, Song IC, … Jeon BS. Extrastriatal dopaminergic changes in Parkinson's disease patients with impulse control disorders. J Neurol Neurosurg Psychiatry. 2014; 85:23–30. [PubMed: 24023269]

Lee PH, Lee JE, Kim HS, Song SK, Lee HS, Nam HS, … Sohn YH. A randomized trial of mesenchymal stem cells in multiple system atrophy. Ann Neurol. 2012; 72:32–40. (*special interest). [PubMed: 22829267]

Lees AJ. The on-off phenomenon. J Neurol Neurosurg Psychiatry. 1989; 52(Suppl):29–37. [PubMed: 2666577]

Lemke MR. Depressive symptoms in Parkinson's disease. Eur J Neurol. 2008; 15(Suppl 1):21–25. [PubMed: 18353133]

Lenglet C, Abosch A, Yacoub E, De Martino F, Sapiro G, Harel N. Comprehensive in vivo mapping of the human basal ganglia and thalamic connectome in individuals using 7T MRI. PLOS ONE. 2012; 7(1):e29153. (**significant contribution). 10.1371/journal.pone.0029153 [PubMed: 22235267]

Lenka, A.; Jhunjhunwala, KR.; Saini, J.; Pal, PK. Structural and functional neuroimaging in patients with Parkinson's disease and visual hallucinations: a critical review. Parkinsonism Rel Disord. 2015. http://dx.doi.org/10.1016/j.parkreldis.2015.04.005

Levesque M, Parent A. The striatofugal fiber system in primates: a reevaluation of its organization based on single-axon tracing studies. Proc Natl Acad Sci. 2005; 102:11888–11893. [PubMed: 16087877]

Levin BE, Katzen HL, Maudsley A, Post J, Myerson C, Govind V, … Mittel A. Whole-brain proton MR spectroscopic imaging in Parkinson's disease. J Neuroimaging. 2012; 24:39–44. [PubMed: 23228009]

Lewis SJ, Pavese N, Rivero-Bosch M, Eggert K, Oertel W, Mathias CJ, … Gerhard A. Brain monoamine systems in multiple system atrophy: a positron emission tomography study. Neurobiol Dis. 2012; 46:130–136. [PubMed: 22266105]

LeWitt PA. Norepinephrine: the next therapeutics frontier for Parkinson's disease. Transl Neurodegen. 2012; 1:4.10.1186/2047-9158-1-4

Liang Z, King J, Zhang N. Anticorrelated resting-state functional connectivity in awake rat brain. Neuroimage. 2011; 592:1190–1199. [PubMed: 21864689]

Lin, CH.; Wu, R-M. Biomarkers of cognitive decline in Parkinson's disease. Parkinsonism Rel Disord. 2015. http://dx.doi.org/10.1016/j.parkreldis.2015.02.010

Little S, Brown P. The functional role of beta oscillations in Parkinson's disease. Parkinsonism Rel Disord. 2014; 20S1:S44–S48.

Liu H, Edmiston EK, Fan G, Xu K, Zhao B, Wang F. Altered resting-state functional connectivity of the dentate nucleus in Parkinson's disease. Psychiatry Res: Neuroimaging. 2013; 211:64–71. [PubMed: 23352277]

Liu T, Eskreis-Winkler S, Schweitzer AD, Chen W, Kaplitt MG, Tsiouris AJ, Wang Y. Improved subthalamic nucleus depiction with quantitative susceptibility mapping. Radiology. 2013; 269:216–223. [PubMed: 23674786]

Loftipour AK, Wharton S, Schwarz ST, Gontu V, Schäfer A, Peters AM, … Bajaj NPS. High resolution magnetic susceptibility mapping of the substantia nigra in Parkinson's disease. J Magn Reson Med. 2012; 35:48–55. (*special interest).

Logothetis NK. What we can do and what we cannot do with fMRI. Nature. 2008; 453:869–878. [PubMed: 18548064]

Long D, Wang J, Xuan M, Gu Q, Xu X, Kong D, Zhang M. Automatic classification of Parkinson's disease with multi-modal MR imaging. PLOS ONE. 2012; 7(11):e47714.10.1371/journal.pone.0047714 [PubMed: 23152757]

Lubomski M, Rushworth RL, Lee W, Bertram K, Williams DR. Sex differences in Parkinson's disease. J Clin Neurosci. 2014; 21:1503–1506. [PubMed: 24767694]

Lucero C, Campbell M, Flores H, Maiti B, Perlmutter JS, Foster ER. Cognitive reserve and β-amyloid pathology in Parkinson disease. Parkinsonism Rel Disord. 2015; 21:899–904. (**significant contribution).

Luo CY, Chen Q, Song Q, Chen K, Guo XY, Yang J, … Shang HF. Resting-state fMRI study on drug-naive patients with Parkinson's disease and with depression. J Neurol Neurosurg Psychiatry. 2014a; 85:675–683. [PubMed: 24227759]

Luo CY, Song W, Chen Q, Zheng ZZ, Chen K, Cao B, … Shang HF. Reduced functional connectivity in early-stage drug naive Parkinson's disease: a resting-state fMRI study. Neurobiol Aging. 2014b; 35:431–441. [PubMed: 24074808]

Ma Y, Huang C, Dyke JP, Pan H, Alsop D, Feigin A, Eidelberg D. Parkinson's disease spatial covariance pattern: noninvasive quantification with perfusion MRI. J Cereb Blood Flow Metab. 2010a; 30:505–509. [PubMed: 20051975]

Ma Y, Peng S, Spetsieris PG, Sossi V, Eidelberg D, Doudet DJ. Abnormal metabolic brain networks in a nonhuman primate model of parkinsonism. J Cereb Blood Flow Metab. 2012; 32:633–642. [PubMed: 22126913]

Ma Y, Tang C, Chaly T, Greene P, Breeze R, Fahn S, … Eidelberg D. Dopamine cell implantation in Parkinson's disease: long-term clinical and ^{18}F-DOPA PET outcomes. J Nucl Med. 2010b; 51:7–15. (**significant contribution). [PubMed: 20008998]

Ma Y, Tang C, Spetsieris PG, Dhawan V, Eidelberg D. Abnormal metabolic network activity in Parkinson's disease: test-retest reproducibility. J Cereb Blood Flow Metab. 2007; 27:597–605. (*special interest). [PubMed: 16804550]

MacDonald PA, MacDonald AA, Seergobin KN, Tamjeedi R, Ganjavi H, Provost JS, Monchi O. The effect of dopamine therapy on ventral and dorsal striatum-mediated cognition in Parkinson's

disease: support from functional MRI. Brain. 2011; 134:1447–1463. (**significant contribution). [PubMed: 21596772]

Madden DJ, Bennett IJ, Burzynska A, Potter G, Chen NK, Song AW. Diffusion tensor imaging of cerebral white matter integrity in cognitive aging. Biochim Biophys Acta. 2012; 1822:386–400. [PubMed: 21871957]

Madhyastha TM, Askren MK, Boord P, Zhang J, Leverenz JB, Grabowski TJ. Cerebral perfusion and cortical thickness indicate cortical involvement in mild Parkinson's disease. Mov Disord. 2015; 30:1893–1900. [PubMed: 25759166]

Mak E, Su L, Williams GB, O'Brien JT. Neuroimaging correlates of cognitive impairment and dementia in Parkinson's disease. Parkinsonism Rel Disord. 2015; 21:862–870.

Marreiros AC, Cagnan H, Moran RJ, Friston KJ, Brown P. Basal ganglia-cortical interactions in Parkinsonian patients. Neuroimage. 2013; 66:301–310. [PubMed: 23153964]

Mattis PJ, Tang CC, Ma Y, Dhawan V, Edidelberg D. Network correlates of the cognitive response to levodopa in Parkinson's disease. Neurology. 2011; 77:858–865. [PubMed: 21849641]

Mayer G, Bitterlich M, Kuwert T, Ritt P, Stefan H. Ictal SPECT in patients with rapid eye movement sleep behaviour disorder. Brain. 2015; 138:1263–1270. (**significant contribution). [PubMed: 25732183]

Mazere J, Meissner WG, Mayo W, Sibon I, Lamare F, Guilloteau D, … Allard M. Progressive supranuclear palsy: in vivo SPECT imaging of presynaptic vesicular acetylcholine transporter. Radiol. 2012; 265:537–543.

McCarthy MM, Moore-Kochlacs C, Gu X, Boyden ES, Han X, Kopell N. Striatal origin of the pathologic beta oscillations in Parkinson's disease. Proc Natl Acad Sci. 2011; 108:11620–11625. [PubMed: 21697509]

McNeill A, Wu RM, Tzen KY, Aguiar PC, Arbelo JM, Barone P, … Schapira AHV. Dopaminergic neuronal imaging in genetic Parkinson's disease: insights into pathogenesis. PLOS ONE. 2013; 8(7):e69190. (**significant contribution). 10.1371/journal.pone.0069190 [PubMed: 23935950]

Mehnert S, Reuter I, Schepp K, Maaser P, Stolz E, Kaps M. Transcranial sonography for diagnosis of Parkinson's disease. BMC Neurol. 2010; 10:9. [PubMed: 20089201]

Melzer TR, Watts R, MacAskill MR, Pearson JF, Rüeger S, Pitcher TL, … Anderson TJ. Arterial spin labelling reveals an abnormal cerebral perfusion pattern in Parkinson's disease. Brain. 2011; 134:845–855. [PubMed: 21310726]

Mesulam M. The cholinergic lesion of Alzheimer's disease: pivotal factor or side show? Learn Mem. 2004; 11:43–49. [PubMed: 14747516]

Meyer PM, Strecker K, Kendziorra K, Bevcker G, Hesse S, Woelpl D, … Schwarz J. Reduced α4β2*-nicotinic acetylcholine receptor binding and its relationship to mild cognitive and depressive symptoms in Parkinson disease. Arch Gen Psychiatry. 2009; 66:866–877. [PubMed: 19652126]

Meyer-Lindenberg A. From maps to mechanisms through neuroimaging of schizophrenia. Nature. 2010; 468:194–202. [PubMed: 21068827]

Miller DB, O'Callaghan JP. Biomarkers of Parkinson's disease: present and future. Metabolism. 2015; 64:S40–S46. (*special interest). [PubMed: 25510818]

Mishina M, Ishiwata K, Naganawa M, Kimura Y, Kitamura S, Suzuki M, … Ishii K. Adenosine A_{2A} receptors measured with [^{11}C]TMSX PET in the striata of Parkinson's disease patients. PLOS ONE. 2011; 6(2):e17338.10.1371/journal/pone.0017338 [PubMed: 21386999]

Moran RJ, Mallet N, Litvak V, Dolan RJ, Magill PJ, Friston KJ, Brown P. Alterations in brain connectivity underlying beta oscillations in Parkinsonism. PLOS Comput Biol. 2011; 7(8):e1002124.10.1371/journal.pcbi.1002124 [PubMed: 21852943]

Morelli M, Arabia G, Messina D, Vescio B, Salsone M, Chiriaco C, … Quattrone A. Effect of aging on magnetic resonance measures differentiating progressive supranuclear palsy from Parkinson's disease. Mov Disord. 2014; 29:488–495. [PubMed: 24573655]

Müller MLTM, Bohnen NI. Cholinergic dysfunction in Parkinson's disease. Curr Neurol Neurosci Rep. 2013; 139:377. [PubMed: 23943367]

Murakami Y, Kakeda S, Watanabe K, Ueda I, Ogasawara A, Moriya J, … Korogi Y. Usefulness of quantitative susceptibility mapping for the diagnosis of Parkinson disease. Am J Neuroradiol. 2015 doi:10.3174.ajnr.A4260.

Mure H, Hirano S, Tang CC, Isaias I, Antonini A, Ma Y, … Eidelberg D. Parkinson's disease tremor-related metabolic network: characterization, progression, and treatment effects. Neuroimage. 2011; 54:1244–1253. [PubMed: 20851193]

Mure H, Tang CC, Argyelan M, Ghilardi MF, Kaplitt MG, Dhawan V, Eidelberg D. Improved sequence learning with subthalamic nucleus deep brain stimulation: evidence for treatment-specific network modulation. J Neurosci. 2012; 32:2804–2813. (**significant contribution). [PubMed: 22357863]

Narayanan NS, Rodnitzky RL, Uc E. Prefrontal dopamine signaling and cognitive symptoms of Parkinson's disease. Rev Neurosci. 2013; 24:267–278.10.1515/revneuro-2013-0004 [PubMed: 23729617]

New AB, Robin DA, Parkinson AL, Eickhoff CR, Reetz K, Hoffstaedter F, … Eickhoff SB. The intrinsic resting state voice network in Parkinson's disease. Human Brain Mapping. 2015; 36:1951–1962. (*special interest). [PubMed: 25627959]

Niethammer M, Feigin A, Eidelberg D. Functional neuroimaging in Parkinson's disease. Cold Spring Harb Perspect Med. 2012; 2:a009274. [PubMed: 22553499]

Niethammer M, Tang CC, Ma Y, Mattis PJ, Ko JH, Dhawan V, Eidelberg D. Parkinson's disease cognitive network correlates with caudate dopamine. Neuroimage. 2013; 78:204–209. [PubMed: 23578575]

O'Callaghan C, Bertoux M, Hornberger M. Beyond and below the cortex: the contribution of striatal dysfunction to cognition and behaviour in neurodegeneration. J Neurol Neurosurg Psychiatry. 2014; 85:371–378. [PubMed: 23833269]

Oh M, Kim JS, Kim JY, Shin KH, Park SH, Kim HO, … Lee CS. Subregional patterns of preferential striatal dopamine transporter loss differ in Parkinson disease, progressive supranuclear palsy, and multiple-system atrophy. J Nucl Med. 2012; 53:399–406. [PubMed: 22323779]

Olde Dubbelink KTE, Hilllebrand A, Stoffers D, Berend Deijen J, Twisk JR, Stam CJ, Berendse HW. Disrupted brain network topology in Parkinson's disease: a longitudinal magnetoencephalography study. Brain. 2014a; 137:197–207. [PubMed: 24271324]

Olde Dubbelink KTE, Hilllebrand A, Twisk JW, Deijen JB, Stoffers D, Schmand, … Berendse HW. Predicting dementia in Parkinson disease by combining neurophysiologic and cognitive markers. Neurology. 2014b; 82:263–270. [PubMed: 24353335]

Olde Dubblelink KTE, Stoffers D, Deijen JB, Twisk JWR, Stam CJ, Hillebrand A, Berendse HW. Resting-state functional connectivity as a marker of disease progression in Parkinson's disease: a longitudinal MEG study. Neuroimage Clin. 2013; 2:612–619. [PubMed: 24179812]

Oliveira FPM, Castelo-Branco M. Computer-aided diagnosis of Parkinson's disease based on [^{123}I]FP-CIT SPECT binding potential images, using the voxels-as-features approach and support vector machines. J Neural Eng. 2015 Apr.12(2):026008. (*special interest). 10.1088/1741-2560/12/2/026008 [PubMed: 25710187]

O'Sullivan SS, Williams DR, Gallagher DA, Massey LA, Silveira-Moriyama L, Lees A. Nonmotor symptoms as presenting complaints in Parkinson's disease: a clinicopathological study. Mov Disord. 2008; 23:101–106. [PubMed: 17994582]

Pahapill PA, Lozano AM. The pedunculopontine nucleus and Parkinson's disease. Brain. 2000; 123:1767–1783. [PubMed: 10960043]

Palmer SJ, Li J, Wang ZJ, McKeown MJ. Joint amplitude and connectivity compensatory mechanisms in Parkinson's disease. Neurosci. 2010; 166:1110–1118.

Park E, Hwang YM, Lee CN, Kim S, Oh SY, Kim YC, … Park KW. Differential diagnosis of patients with inconclusive parkinsonian features using [^{18}F]FP-CIT PET/CT. Nucl Med Mol Imaging. 2014; 48:106–113. [PubMed: 24900150]

Pavese N, Moore RY, Scherfler C, Khan NL, Hotton G, Quinn NP, … Piccini P. In vivo assessment of brain monoamine systems in *parkin* gene carriers: a PET study. Exp Neurol. 2010; 222:120–124. [PubMed: 20043906]

Pavese N, Rivero-Bosch M, Lewis SL, Whone AL, Brooks DJ. Progression of monoaminergic dysfunction in Parkinson's disease: a longitudinal ^{18}F-dopa PET study. Neuroimage. 2011; 56:1463–1468. [PubMed: 21396455]

Pavese N, Simpson BS, Metta V, Ramlackansingh A, Chaudhuri KR, Brooks DJ. [^{18}F]FDOPA uptake in the raphe nuclei complex reflects serotonin transporter availability. A combined [^{18}F]FDOPA and [^{11}C]DASB PET study in Parkinson's disease. Neuroimage. 2012; 59:1080–1084. [PubMed: 21963917]

Perlmutter JS, Norris SA. Neuroimaging biomarkers for Parkinson disease: facts and fantasy. Ann Neurol. 2014; 76:769–783. [PubMed: 25363872]

Peterson DS, Fling BW, Mancini M, Cohen RG, Nutt JG, Horak FB. Dual-task interference and brain structural connectivity in people with Parkinson's disease who freeze. J Neurol Neurosurg Psychiatry. 2015; 86:786–792. [PubMed: 25224677]

Petrou M, Dwamena BA, Foerster BR, MacEachern MP, Bohnen NI, Müller MLTM, … Frey KA. Amyloid deposition in Parkinson's disease and cognitive impairment: a systematic review. Mov Disord. 2015; 30:928–935. [PubMed: 25879534]

Picillo M, Erro R, Amboni M, Longo K, Vitale C, Moccia M, … Pellecchia MT. Gender differences in non-motor symptoms in early Parkinson's disease: a 2-years follow-up study on previously untreated patients. Parkinsonism Relat Disord. 2014; 20:850–854. [PubMed: 24842702]

Politis M. Neuroimaging in Parkinson disease: from research setting to clinical practice. Nat Rev Neurol. 2014; 10:708–722. (*special interest). [PubMed: 25385334]

Politis M, Wu K, Loane C, Brooks DJ, Kiferle L, Turkheimer FE, … Piccini P. Serotonergic mechanisms responsible for levodopa-induced dyskinesias in Parkinson's disease patients. J Clin Investig. 2014; 124:1340–1349. (**significant contribution). [PubMed: 24531549]

Politis M, Wu K, Loane C, Quinn NP, Brooks DJ, Oertel WH, … Piccini P. Serotonin neuron loss and nonmotor symptoms continue in Parkinson's patients treated with dopamine grafts. Sci Transl Med. 2012 Apr 4.4(128):128ra41. (**significant contribution). 10.1126/scitranslmed.3003391

Ponsen MM, Stam CJ, Bosboom JLW, Berendse HW, Hillebrand A. A three dimensional anatomical view of oscillatory resting-state activity and functional connectivity in Parkinson's disease related dementia: an MEG study using atlas-based beamforming. Neuroimage: Clin. 2013; 2:95–102. [PubMed: 24179762]

Posse S, Otazo R, Dager SR, Alger J. MR spectroscopic imaging: principles and recent advances. J Magn Reson Imag. 2013; 37:1301–1325.

Poston KL, Tang CC, Eckert T, Dhawan V, Frucht S, Vonsattel JP, … Eidelberg D. Network correlates of disease severity in multiple system atrophy. Neurology. 2012; 78:1237–1244. [PubMed: 22491861]

Postuma RB, Dagher A. Basal ganglia functional connectivity based on meta-analysis of 126 positron emission tomography and functional magnetic resonance imaging publications. Cereb Cortex. 2006; 16:1508–1521. (**significant contribution). [PubMed: 16373457]

Price JC. Molecular brain imaging in the multimodality era. J Cereb Blood Flow Metab. 2012; 32:1377–1392. [PubMed: 22434068]

Prodoehl J, Li H, Planetta PJ, Goetz C, Shannon KM, Tangonan R, … Vaillancourt DE. Diffusion tensor imaging of Parkinson's disease, atypical Parkinsonism, and essential tremor. Mov Disord. 2013; 28:1816–1822. [PubMed: 23674400]

Putcha D, Ross RS, Cronin-Golomb A, Janes AC, Stern CE. Altered intrinsic functional coupling between core neurocognitive networks in Parkinson's disease. Neuroimage: Clin. 2015; 7:449–455. (**significant contribution). [PubMed: 25685711]

Pyatigorskaya N, Gallea C, Garcia-Lorenzo D, Vidailhet M, Lehericy S. A review of the use of magnetic resonance imaging in Parkinson's disease. Ther Adv Neurol Disord. 2014; 7:206–220. [PubMed: 25002908]

Qamhawi Z, Towey D, Shah B, Pagano G, Seibyl J, Marek K, … Pavese N. Clinical correlates of raphe serotonergic dysfunction in early Parkinson's disease. Brain. 2015; 138:2964–2973. [PubMed: 26209314]

Rae CL, Correia MM, Altena E, Hughes LE, Barker RA, Rowe JB. White matter pathology in Parkinson's disease: the effect of imaging protocol differences and relevance to executive function. Neuroimage. 2012; 62:1675–1684. [PubMed: 22713671]

Raichle ME. The restless brain. Brain Connect. 2011; 1:3–12.10.10189/brain.2011.0019 [PubMed: 22432951]

Ramlackhansingh AF, Bose SK, Ahmed I, Turkheimer FE, Pavese N, Brooks DJ. Adenosine 2A receptor availability in dyskinetic and nondyskinetic patients with Parkinson disease. Neurology. 2011; 76:1811–1816. [PubMed: 21606452]

Rice ME, Patel JC, Cragg SJ. Dopamine release in the basal ganglia. Neurosci. 2011; 198:112–137.

Riedl V, Bienkowska K, Strobel C, Tahmasian M, Grimmer T, Förster S, … Drzezga A. Local activity determines functional connectivity in the resting human brain: a simultaneous FDG-PET/fMRI study. J Neurosci. 2014; 34:6260–6266. [PubMed: 24790196]

Russo SJ, Nestler EJ. The brain reward circuitry in mood disorders. Nat Rev Neurosci. 2013; 14:609–625. [PubMed: 23942470]

Sahuquillo P, Tembl JI, Parkhutik V, Vazquez JF, Sastre I, Lago A. The study of deep brain structures by transcranial duplex sonography and imaging resonance correlation. Ultrasound Med Biol. 2013; 39:226–232. [PubMed: 23257352]

Salvatore C, Cerasa A, Castiglioni I, Gallivanone F, Augimeri A, Lopez M, … Quattrone A. Machine learning on brain MRI data for differential diagnosis of Parkinson's disease and progressive supranuclear palsy. J Neurosci Methods. 2014; 222:230–237. [PubMed: 24286700]

Schapira AHV. Recent developments in biomarkers in Parkinson disease. Curr Opin Neurol. 2013; 26:395–400. (*special interest). [PubMed: 23823465]

Schapira AHV, Tolosa E. Molecular and clinical prodrome of Parkinson disease; implications for treatment. Nat Rev Neurol. 2010; 6:309–317. [PubMed: 20479780]

Scherfler C, Esterhammer R, Nocker M, Mahlknecht P, Stockner H, Warwitz B, … Sepi K. Correlation of dopaminergic terminal dysfunction and microstructural abnormalities of the basal ganglia and the olfactory tract in Parkinson's disease. Brain. 2013; 136:3028–3037. (**significant contribution). [PubMed: 24014521]

Schwarz ST, Abaei M, Gontu V, Morgan PS, Bajaj N, Auer DP. Diffusion tensor imaging of nigral degeneration in Parkinson's disease: A region-of-interest and voxel-based study at 3T and systematic review with meta-analysis. Neuroimage: Clin. 2013; 3:481–488. (**significant contribution). [PubMed: 24273730]

Schwarz ST, Afzal M, Morgan PS, Bajaj N, Gowland PA, Auer DP. The 'swallow tail' appearance of the healthy nigrosome – a new accurate test of Parkinson's disease: a case control and retrospective cross-sectional MRI study at 3T. PLOS ONE. 2014; 9(4):e93814.10.1371/journal.pone.0093814 [PubMed: 24710392]

Sharma S, Moon CS, Khogali A, Haidous A, Chabenne A, Ojo C, … Ebadi M. Biomarkers in Parkinson's disease (recent update). Neurochem Int. 2013; 63:201–229. [PubMed: 23791710]

Sharman M, Valabregue R, Perlbarg V, Marrakchi-Kacem L, Vidailhet M, Benali H, … Lehericy S. Parkinson's disease patients show reduced cortical-subcortical sensorimotor connectivity. Mov Disord. 2013; 28:447–454. (**significant contribution). [PubMed: 23144002]

Sheng K, Fang W, Su M, Li R, Zou D, Han Y, … Cheng O. Altered spontaneous brain activity in patients with Parkinson's disease accompanied by depressive symptoms, as revealed by regional homogeneity and functional connectivity in the prefrontal-limbic system. PLOS ONE. 2014; 9(1):e84705.10.1371/journal.pone.0084705 [PubMed: 24404185]

Shine JM, Halliday GM, Gilat M, Matar E, Bolitho SJ, Carlos M, … Lewis SJ. The role of dysfunctional attentional networks in visual misperceptions in Parkinson's disease. Hum Brain Mapp. 2014; 35:2206–2219. [PubMed: 23760982]

Shine JM, Mata E, Ward PB, Bolitho SJ, Pearson M, Naismith SL, Lewis SJG. Differential neural activation patterns in patients with Parkinson's disease and freezing of gait in response to concurrent cognitive and motor load. PLOS ONE. 2013; 8(1):e52602.10.1371/journal.pone.0052602 [PubMed: 23382821]

Siebert TM, Murphy EA, Kaestner EJ, Brewer JB. Interregional correlations in Parkinson disease and Parkinson-related dementia. Radiol. 2012; 263:226–234.

Siegel, A.; Sapru, HN. Essential Neuroscience. Lippincott Williams & Wilkins; Philadelphia: 2006.

Skidmore F, Korenkevych D, Liu Y, He G, Bullmore E, Pardalos PM. Connectivity brain networks based on wavelet correlation analysis in Parkinson fMRI data. Neurosci Lett. 2011; 499:47–51. [PubMed: 21624430]

Skidmore FM, Yang M, Baxter L, von Deneen KM, Collingwood J, He G, … Liu Y. Reliability analysis of the resting state can sensitively and specifically identify the presence of Parkinson disease. Neuroimage. 2013a; 75:249–261. [PubMed: 21924367]

Skidmore FM, Yang M, von Deneen K, Collingwood J, He G, Tandon R, … Liu Y. Apathy, depression, and motor symptoms have distinct and separable resting activity patterns in idiopathic Parkinson disease. Neuroimage. 2013b; 81:484–495. [PubMed: 21782030]

Smith Y, Wichmann T, Factor SA, DeLong MR. Parkinson's disease therapeutics: new developments and challenges since the introduction of levodopa. Neuropsychopharmacol. 2012; 37:213–246.

Smith R, Wu K, Hart T, Loane C, Brooks DJ, Björklund A, … Politis M. The role of pallidal serotonergic function in Parkinson's disease dyskinesias: a positron emission tomography study. Neurobiol Aging. 2015; 36:1736–1742. (**significant contribution). [PubMed: 25649022]

Song IU, Chung YA, Oh JK, Chung SW. An FP-CIT PET comparison of the difference in dopaminergic neuronal loss in subtypes of early Parkinson's disease. Acta Radiologica. 2014; 55:366–371. [PubMed: 23943629]

Stagg CJ, Bachtiar V, Amadi U, Gudberg CA, Ilie AS, Sampaio-Baptista C, … Johansen-berg H. Local GABA concentration is related to network-level resting functional connectivity. eLife. 2014; 3:e01465.10.7554/eLife.01465 [PubMed: 24668166]

Stam CJ. Use of magnetoencephalography (MEG) to study the functional brain networks in neurodegenerative disorders. J Neurol Sci. 2010; 289:128–134. [PubMed: 19729174]

Stamelou M, Hoeglinger GU. Atypical parkinsonism: an update. Curr Opin Neurol. 2013; 26:401–405. [PubMed: 23812308]

Stenc BI, Mihaljevic I, Butkovic-Soldo S, Kadojic D, Titlic M, Bradvica M, Kralik K. Transcranial sonography and the pocket smell test in the differential diagnosis between Parkinson's disease and essential tremor. Neurol Sci. 2015; 36(8):1403–1410. [PubMed: 25787809]

Stoessl AJ. Imaging in Parkinson's disease: time to look below the neck. Brain. 2015; 138:512–514. [PubMed: 25713402]

Su M, Wang S, Weidong F, Zhu Y, Li R, Sheng K, … Cheng O. Alterations in the limbic/paralimbic cortices of Parkinson's disease patients with hyposmia under resting-state functional MRI by regional homogeneity and functional connectivity analysis. Parkinsonism Rel Disord. 2015; 21:698–703.

Sulzer D, Surmeier DJ. Neuronal vulnerability, pathogenesis and Parkinson's disease. Mov Disord. 2013; 28:41–50. [PubMed: 22791686]

Surdhar I, Gee M, Bouchard T, Coupland N, Malykhin N, Camicioli R. Intact limbic-prefrontal connections and reduced amygdala volumes in Parkinson's disease with mild depressive symptoms. Parkinsonism Rel Disord. 2012; 18:809–813.

Surmeier DJ, Sulzer D. The pathology roadmap in Parkinson disease. Prion. 2013; 7:85–91. [PubMed: 23324593]

Suwijn S, van Boheemen CJM, de Haan R, Tissingh G, Booij J, de Bie RMA. The diagnostic accuracy of dopamine transporter SPECT imaging to detect nigrostriatal cell loss in patients with Parkinson's disease or clinically uncertain parkinsonism: A systematic review. EJNMMI (2015). 2015; 5:12.10.1186/s13550-015-0087-1

Sweet JA, Walter BL, Gunalan K, Chaturvedi A, McIntyre CC, Miller JP. Fiber tractography of the axonal pathways linking the basal ganglia and cerebellum in Parkinson disease: implications for targeting in deep brain stimulation. J Neurosurg. 2014; 120:988–996. [PubMed: 24484226]

Sydoff M, Lizana H, Mattson S, Stabin M, Leide-Svegborn S. Determination of the biodistribution and dosimetry of ^{123}I-FP-CIT in male patients with suspected Parkinsonism or Lewy body dementia using planar and combined planar and SPECT/CT imaging. Applied Radiation and Isotopes. 2013; 82:300–307. [PubMed: 24135637]

Szewczyk-krolikowski K, Menke RAL, Rolinski M, Duff E, Salimi-Khorshidi G, Filippini N, … Mackay CE. Functional connectivity in the basal ganglia network differentiates PD patients from controls. Neurology. 2015; 83:208–214. (** significant contribution). [PubMed: 24920856]

Tabbal SD, Tian LL, Karimi M, Brown CA, Loftin SK, Perlmutter JS. Low nigrostriatal reserve for motor parkinsonism in nonhuman primates. Exp Neurol. 2012; 237:355–362. [PubMed: 22836146]

Tambasco N, Nigro P, Romoli M, Simoni S, Parnetti L, Calabresi P. Magnetization transfer MRI in dementia disorders, Huntington's disease and parkinsonism. J Neurol Sci. 2015; 353:1–8. [PubMed: 25891828]

Tang CC, Poston KL, Eckert T, Feigin A, Frucht A, Guidesblatt M, … Eidelberg D. Differential diagnosis of parkinsonism: a metabolic imaging study using pattern analysis. Lancet Neurol. 2010; 9:149–158. (**significant contribution). [PubMed: 20061183]

Tessitore A, Amboni M, Esposito F, Russo A, Picillo M, Marcuccio L, … Barone P. Resting-state brain connectivity in patients with Parkinson's disease and freezing of gait. Parkinsonism Rel Disord. 2012a; 18:781–787.

Tessitore A, Esposito F, Vitale C, Santangelo C, Amboni M, Russo A, … Tedeschi G. Default-mode network connectivity in cognitively unimpaired patients with Parkinson's disease. Neurology. 2012b; 79:2226–2232. [PubMed: 23100395]

Teune LK, Renken RJ, de Jong BM, Willemsen AT, van Osch MJ, Roerdink JBTM, … Leenders KL. Parkinson's disease-related perfusion and glucose metabolic brain patterns identified with PCASL-MRI and FDG-PET imaging. Neuroimage: Clin. 2014; 5:240–244. [PubMed: 25068113]

Teune LK, Renken RJ, Mudali D, De Jong BM, Dierckx RA, Roerdink JBTM, Leenders KL. Validation of parkinsonian disease-related metabolic brain patterns. Mov Disord. 2013; 28:547–551. [PubMed: 23483593]

Thaler A, Artzi M, Mirelman A, Jacob Y, Helmich RC, Van Nuenen BFL. … LRRK2 Ashkenazi Jewish Consortium. A voxel-based morphometry and diffusion tensor imaging analysis of asymptomatic Parkinson's disease-related G2019S LRRK2 mutation carriers. Mov Disord. 2014; 29:823–827. (**significant contribution). [PubMed: 24482120]

Thiriez C, Itti E, Fenelon G, Evangelista E, Meignan M, Cesaro P, Remy P. Clinical routine use of dopamine transporter imaging in 516 consecutive patients. J Neurol. 2015; 262:909–915. [PubMed: 25649832]

Tinazzi M, Morgante F, Matinella A, Bovi T, Cannas A, Solla P, … Barbui C. Imaging of the dopamine transporter predicts pattern of disease progression and response to levodopa in patients with schizophrenia and parkinsonism: a 2-year follow-up multicenter study. Schizophr Res. 2014; 152:344–349. [PubMed: 24369987]

Troeung L, Egan SJ, Gasson N. A meta-analysis of randomised placebo-controlled treatment trials for depression and anxiety in Parkinson's disease. PLOS ONE. 2013; 8(11):e79510. (*special interest). 10.1371/journal.pone.0079510 [PubMed: 24236141]

Tuite PJ, Mangia S, Michael S. Magnetic resonance imaging (MRI) in Parkinson's disease. J Alzheimer's Dis Suppl. 2013; 1:001.

Tuite PJ, Mangia S, Tyan AE, Lee MK, Garwood M, Michaeli S. Magnetization transfer and adiabatic $R_{1\rho}$ MRI in the brainstem of Parkinson's disease. Parkinsonism Relat Disord. 2012; 18:623–625. [PubMed: 22265140]

Tziortzi AC, Haber SN, Searle GE, Tsoumpas C, Long CJ, Shotbolt P, … Gunn RN. Connectivity-based functional analysis of dopamine release in the striatum using diffusion-weighted MRI and positron emission tomography. Cereb Cortex. 2014; 24:1165–1177. [PubMed: 23283687]

Van den Heuvel MP, Hulshoff Pol HE. Exploring the brain network: a review on resting-state fMRI functional connectivity. Eur Neuropsychopharmacol. 2010; 20:519–534. [PubMed: 20471808]

Van Mierlo TJ, Chung C, Foncke EM, Berendse H, van den Heuvel OA. Depressive symptoms in Parkinson's disease are related to decreased hippocampus and amygdala volume. Mov Disord. 2015; 30:245–252. [PubMed: 25600157]

Van Nuenen BFL, van Eimeren T, van der Vegt JPM, Buhmann C, Klein C, Bloem BR, Siebner HR. Mapping preclinical compensation in Parkinson's disease: an imaging genomics approach. Mov Disord. 2009; 24:S703–S710. [PubMed: 19877238]

Vercruysse S, Leunissen I, Vervoort G, Vandenberghe W, Swinnen S, Nieuwboer A. Microstructural changes in white matter associated with freezing of gait in Parkinson's disease. Mov Disord. 2015; 30:567–576. [PubMed: 25640958]

Vernon AC, Ballard C, Modo M. Neuroimaging for Lewy body disease: is the in vivo molecular imaging of α-synuclein neuropathology required and feasible? Brain Res Rev. 2010; 65:28–55. [PubMed: 20685363]

Villemagne VL, Okamura N. In vivo tau imaging: Obstacles and progress. Alzheimer's & Dementia. 2014; 10:S254–264.

Vriend C, Pattij T, van der Werf YD, Voorn P, Booij J, Rutten S, … van den Heuvel OA. Depression and impulse control disorders in Parkinson's disease: Two sides of the same coin? Neurosci Biobehav Rev. 2014a; 38:60–71. [PubMed: 24239733]

Vriend C, Raijmakers P, Veltman DJ, van Dijk KD, van der Werf YD, Foncke EM, … van den Heuvel OA. Depressive symptoms in Parkinson's disease are related to reduced [^{123}I]FP-CIT binding in the caudate nucleus. J Neuro Neurosur Psychiatry. 2014b; 85:159–164.

Wakana S, Jiang H, Nagae-Poetscher LM, van Zijl PCM, Mori S. Fiber tract-based atlas of human white matter anatomy. Radiology. 2004; 230:77–87. [PubMed: 14645885]

Weiduschat N, Mao X, Beal MF, Nirenberg MJ, Shungu DC, Henchcliffe C. Sex differences in cerebral energy metabolism in Parkinson's disease: a phosphorus magnetic resonance spectroscopic imaging study. Parkinsonism Rel Disord. 2014; 20:545–548. (*special interest).

Weintraub D, Dietz N, Duda JE, Wolk DA, Doshi J, Xie SX, … Siderow A. Alzheimer's disease pattern of brain atrophy predicts cognitive decline in Parkinson's disease. Brain. 2012; 135:170–180. (**significant contribution). [PubMed: 22108576]

Weintraub D, Papay K, Siderowf A. Screening for impulse control symptoms in patients with de novo Parkinson disease: a case-control study. Neurology. 2013; 80:176–180.10.1212/WNL.0b013e31827b915c [PubMed: 23296128]

Weiss PH, Herzog J, Pötter-Nerger M, Falk D, Herzog H, Deuschl G, … Fink GR. Subthalamic nucleus stimulation improves parkinsonian gait via brainstem locomotor centers. Mov Disord. 2015; 30:1121–1125. [PubMed: 25914247]

Wen X, Wu X, Liu J, Li K, Yao L. Abnormal baseline brain activity in non-depressed Parkinson's disease and depressed Parkinson's disease: a resting-state functional magnetic resonance imaging study. PLOS ONE. 2013; 8(5):e63691.10.1371/journal.pone.0063691 [PubMed: 23717467]

Werner P, Barthel H, Drzezga A, Sabri O. Current status and future role of brain PET/MRI in clinical and research settings. Eur J Nucl Med Mol Imaging. 2015; 42:512–526. [PubMed: 25573629]

Wichmann T, Dostrovsky JO. Pathological basal ganglia activity in movement disorders. Neurosci. 2011; 198:232–244.

Wing Y, Lam SP, Zhang J, Leung E, Ho CL, Chen S, … Ho CKW. Reduced striatal dopamine transmission in REM sleep behavior disorder comorbid with depression. Neurology. 2015; 84:516–522. (**significant contribution). [PubMed: 25568298]

Wu P, Yu H, Peng S, Dauvilliers Y, Wang J, Ge J, … Zuo C. Consistent abnormalities in metabolic network activity in idiopathic rapid eye movement sleep behaviour disorder. Brain. 2014; 137:3122–3128. [PubMed: 25338949]

Wu T, Hallett M. The cerebellum in Parkinson's disease. Brain. 2013; 136:696–709. [PubMed: 23404337]

Wu T, Long X, Wang L, Hallett M, Zang Y, Li K, Chan P. Functional connectivity of cortical motor areas in the resting state in Parkinson's disease. Hum Brain Mapp. 2011a; 32:1443–1457. [PubMed: 20740649]

Wu T, Long X, Zang Y, Wang L, Hallett M, Li K, Chan P. Regional homogeneity changes in patients with Parkinson's disease. Hum Brain Mapp. 2009; 30:1502–1510. [PubMed: 18649351]

Wu T, Ma Y, Zheng Z, Peng S, Wu X, Eidelberg D, Chan P. Parkinson's disease-related spatial covariance pattern identified with resting-state functional MRI. J Cereb Blood Flow Metab. 2015; 35:1764–1770. (**significant contribution). [PubMed: 26036935]

Wu T, Wang L, Hallett M, Chen Y, Li K, Chan P. Effective connectivity of brain networks during self-initiated movement in Parkinson's disease. Neuroimage. 2011b; 55:204–215. [PubMed: 21126588]

Wu T, Wang C, Wang J, Hallett M, Zang Y, Chan P. Preclinical and clinical neural network changes in SCA2 parkinsonism. Parkinsonism Rel Disord. 2013; 19:158–164.

Wu T, Wang J, Wang C, Hallett M, Zang Y, Wu X, Chan P. Basal ganglia circuits in Parkinson's disease patients. Neurosci Lett. 2012; 524:55–59. [PubMed: 22813979]

Yao N, Cheung C, Pang S, Chang RS-k, Lau KK, Suckling J, … McAlonan GM. Multimodal MRI of the hippocampus in Parkinson's disease with visual hallucinations. Brain Struct Func. 201410.1007/s00429-014-0907-5

Yao N, Pang S, Cheung C, Shek-kwan C, Lau KK, Suckling J, … Chua S-e. Resting activity in visual and corticostriatal pathways in Parkinson's disease with hallucinations. Parkinsonism Rel Disord. 2015; 21:131–137.

Yarnall AJ, Breen DP, Duncan DP, Khoo TK, Coleman SY, Firbank MJ, … Burn DJ. Characterizing mild cognitive impairment in incident Parkinson disease: the ICICLE-PD study. Neurology. 2014; 82:308–316. (**significant contribution). [PubMed: 24363137]

Yoon RG, Kim SJ, Kim HS, Choi CG, Kim JS, Oh J, … Lee CS. Parkinsonism-predominant multiple system atrophy from Parkinson's disease: correlation with ^{18}F-flurodeoxyglucose positron emission tomography. Neurosci Lett. 2015; 584:296–301. [PubMed: 25450142]

Yu F, Barron DS, Tantiwongkosi B, Fox P. Patterns of gray matter atrophy in atypical parkinsonism syndromes: aVBM meta-analysis. Brain Behav. 2015 Jun.5(6):e00329. (**significant contribution). 10.1002/brb3.329 [PubMed: 26085961]

Yu R, Liu B, Wang L, Chen J, Liu X. Enhanced functional connectivity between putamen and supplementary motor area in Parkinson's disease patients. PLOS ONE. 2013; 8(3):e59717.10.1371/journal.pone.0059717 [PubMed: 23555758]

Zhang J, Bi W, Zhang Y, Zhu M, Zhang Y, Feng H, … Jiang T. Abnormal functional connectivity density in Parkinson's disease. Behav Brain Res. 2015; 280:113–118. [PubMed: 25496782]

Zhang J, Wei L, Hu X, Zhang Y, Zhou D, Li C, … Wang J. Specific frequency band of amplitude low-frequency fluctuation predicts Parkinson's disease. Behav Brain Res. 2013; 252:18–23. [PubMed: 23727173]

Zhang L, Liu J. The role of neuroimaging in the diagnosis of Parkinson's disease. Int J Integ Med 2013. 2013; 1:11. 2013.

Zhao P, Zhang B, Gao S. ^{18}[F]-FDG PET study on the Idiopathic Parkinson's disease from several parkinsonian-plus syndromes. Parkinsonism Rel Disord. 2012; 18(Suppl 1):S60–S62.

Zheng Z, Shemmassian S, Wijekoon C, Kim W, Bookheimer SY, Pourtian N. DTI correlates of distinct cognitive impairments in Parkinson's disease. Hum Brain Mapp. 2014; 35:1325–1333. [PubMed: 23417856]

- PD neuroimaging is revealing a rapidly expanding range of findings
- Studies of diagnosis, co-morbidity, treatments, and other topics are increasing
- Advances in neuroimaging of clinically useful biomarkers are needed

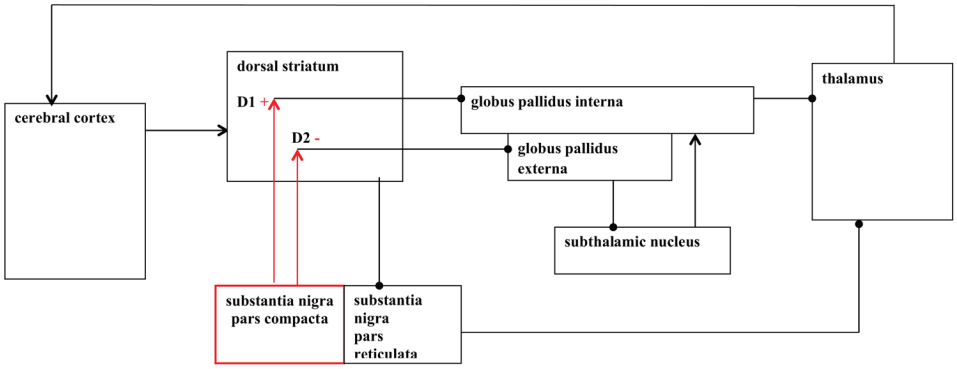

Fig. 1.

Simplified schema of the cortico-basal ganglia-thalamocortical circuit with direct and indirect pathways from the dorsal striatum. Black arrows with triangle heads: Glutamatergic excitatory projection neurons. Black arrows with circle heads: GABAergic inhibitory projection neurons. Red arrows: Dopaminergic projection neurons. Dopamine excites GABAergic medium spiny neurons (MSN) via D1 receptors; dopamine inhibits GABAergic MSNs via D2 receptors. (Delong, 1990; Galvan & Wichmann, 2008; Honey et al., 2003; Lanciego et al., 2012; Siegel & Sapru, 2006).

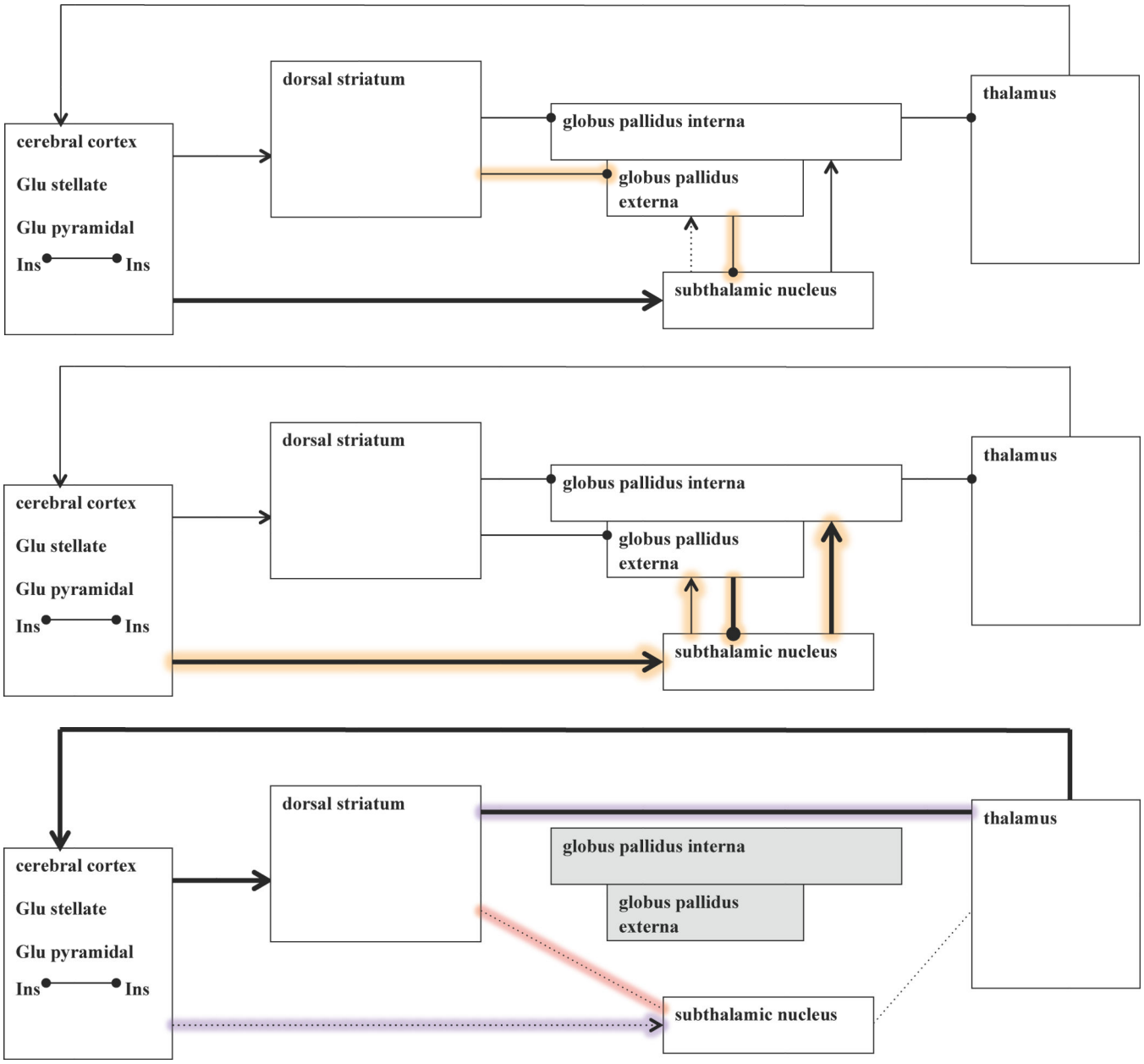

Fig. 2.

Dynamic causal model (DCM) of cortico-basal ganglia-thalamocortical circuit with direct, indirect, and hyperdirect pathways, and three cortical subpopulations: excitatory glutamatergic stellate cells, excitatory glutamatergic pyramidal projection neurons, and inhibitory GABAergic interneurons (adapted from Moran et al., 2011). Black arrows with triangle heads: Glutamatergic exhitatory projection neurons. Black arrows with circle heads: GABAergic inhibitory projection neurons. Black arrow with double circles: GABAergic interneurons. Glu=glutamatergic; Ins=interneurons. (top) DCM study by Moran et al. (2011). Bold arrows: effective connectivity was greater in Parkinsonian versus control animals. Dotted arrows: effective connectivity was less in Parkinsonian versus control animals. Glowing arrows: increasing these connections increased beta oscillations. (Note

that the entopeduncular nucleus in Moran et al.'s (2011) model is homologous to the primate globus pallidus interna shown here.) (middle) DCM and electrophysiological study of Parkinson's patients by Marrieros et al. (2013). Bold arrows: effective connectivity was greater in OFF versus ON L-DOPA state. Glowing arrows: these connections increased beta oscillations in the OFF state. (bottom) DCM and resting-state functional connectivity study of Parkinson's patients by Kahan et al. (2014). The earlier DCM model was simplified by eliminating globus pallidum (gray filled boxes) and adding connections between putamen (dorsal striatum), subthalamic nucleus, and thalamus (lines without arrowheads). Bold arrows: deep brain stimulation (DBS) increased strength of these pathways. Dotted arrows: DBS decreased strength of these pathways. Glowing arrows: these connections predicted motor function both OFF and ON stimulation. Lavendar glow: increasing strength of these connections predicted decreased motor impairment. Red glow: increasing strength of these connections predicted increased motor impairment. (Adapted from Kahan et al., 2014).

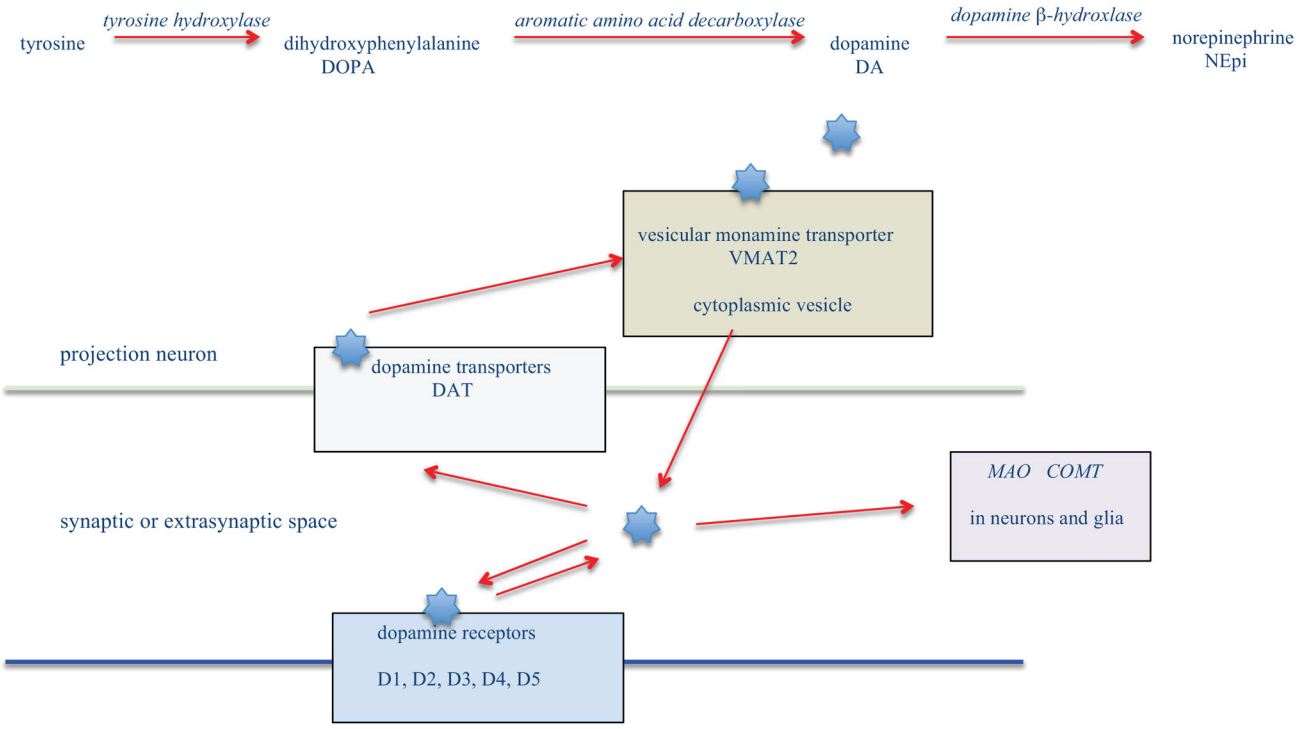

Fig. 3.

Dopamine biochemistry. Some common abbreviations are given. Italics: enzymes. COMT: catechol-O-methyl transferase; MAO: monoamine oxidase. (Hammoud et al. 2007; Rice et al.; 2011).

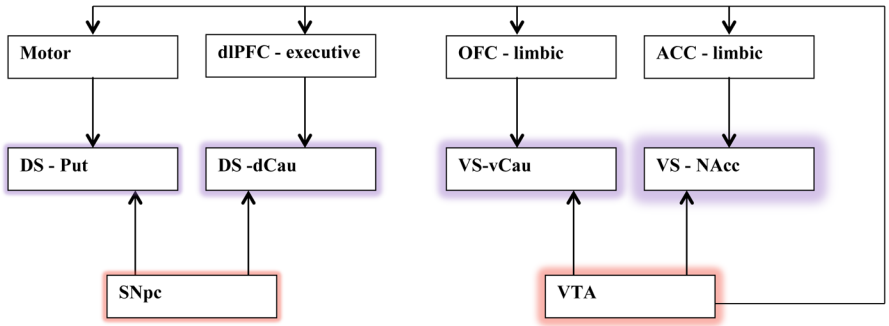

Fig. 4.

Simplified schema of corticostriatal loops and dopaminergic input to the striatum. A direct connection between ventral tegemental area (VTA) and the cortex (mesocortical pathway) is also shown. Glow indicates progression of dopaminergic dysfunction: lowest glow indicates earliest dysfunction; lavendar highlights striatal regions and red highlights sources of dopaminergic projection neurons. ACC=anterior cingulate cortex; dCau=dorsal caudate; dlPFC=dorsolateral prefrontal cortex; DS=dorsal striatum; NAcc=nucleus accumbens; OFC=orbitofrontal cortex; Put=putamen; SNpc=substantia nigra pars compacta; vCau=ventral caudate; VS=ventral striatum. (Adapted from Alexander et al., 1986; Fuente-Fernandez, 2012; O'Callaghan et al., 2014).

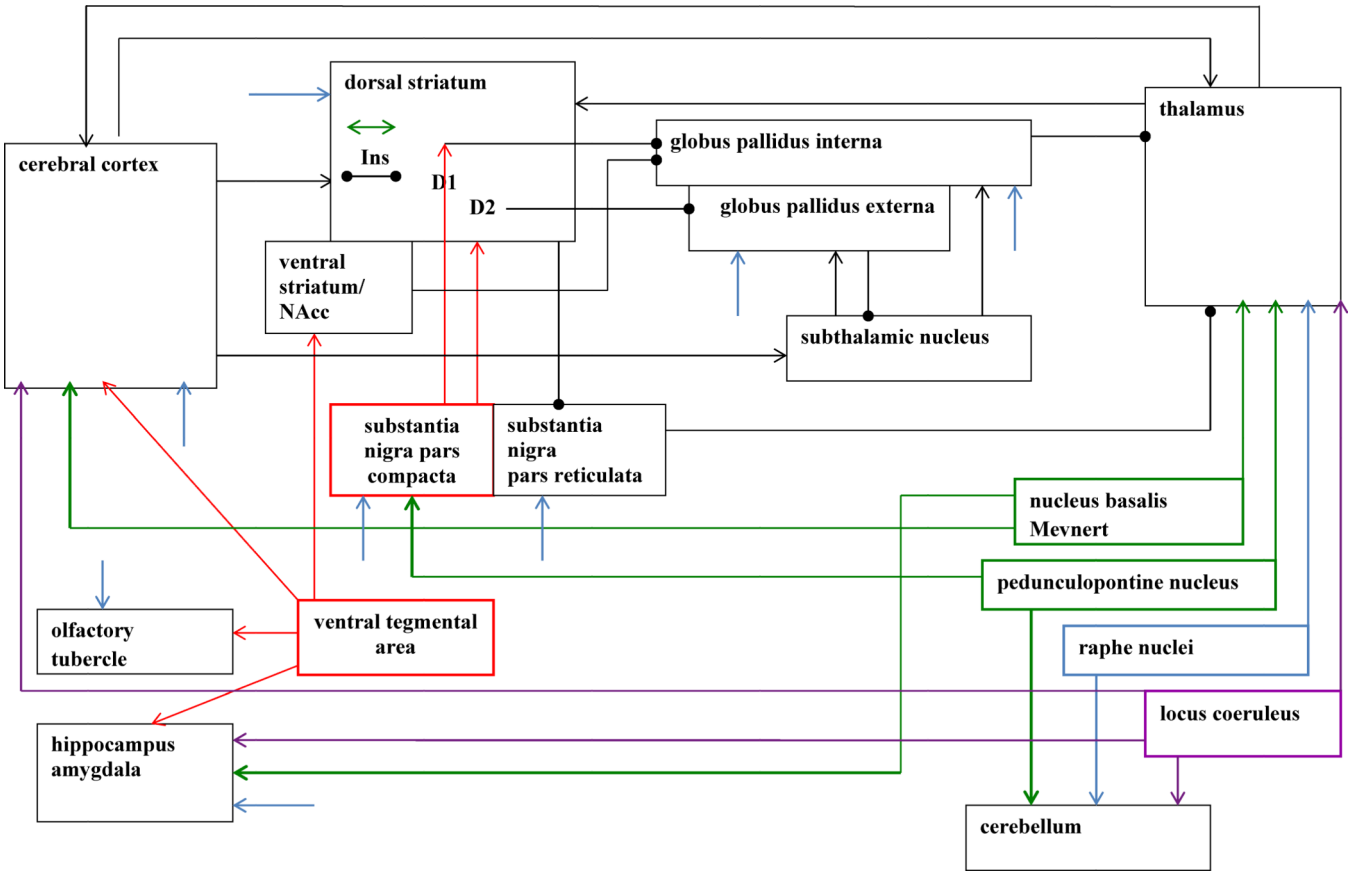

Fig. 5.

Some important brain regions and neurotransmitters in PD. Pathways of the cortico-basal ganglia-thalamocortical circuit are included. D1, D2= dopamine receptors; Ins=interneurons; NAcc=nucleus accumbens. Black arrows with triangle heads: glutamatergic excitatory projection neurons. Black arrows with circle heads: GABAergic inhibitory projection neurons. Colored arrows and boxes: projection neurons and their sources respectively for acetylcholine (green), dopamine (red), norepinephrine (lavendar), and serotonin (blue). For clarity, only the heads of blue arrows portraying serotonergic projection neurons are shown for most locations.

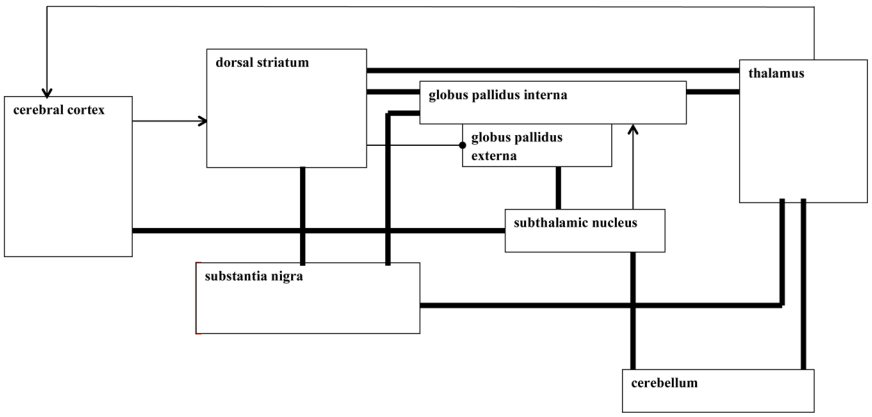

Fig. 6.

Corticobasal ganglia-thalamocortical circuit with pathways that were recently observed in vivo in humans (adapted from Lenglet et al. (2012)). Bold: neuroimaging of structural connections in humans in vivo by Brunenberg et al. (2012; hyperdirect pathway), Sweet et al. (2014; subthalamopontocerebellar and dentothalamic tracts), and Lenglet et al. (2012; other bold pathways).

Table 1

Brain regions in Parkinson's disease

Forebrain
Cortex – all lobes[5–6]
Caudate
Putamen
Globus pallidus externa
Globus pallidus interna
Nucleus accumbens
Ammon's Horn [4]
Hippocampus [4]
Nucleus basalis of Meynert (ACh)[3]
Magnocellular nucleus (ACh)[3]
Olfactory bulb[1]
Diencephalon
Thalamus [4]
Hypothalamus [4]
Subthalamic nucleus
Brainstem
Midbrain
Ventral tegmental area (DA)
Substantia nigra pars compacta (DA)[3]
Substantia nigra pars reticularis
Pons
Pedunculopontine tegmental nucleus (ACh)[3]
Raphe nuclei (Ser) [2]
Locus coeruleus (NEpi) [2]
Medulla
Raphe nuclei (Ser) [2]
Gigantocellular reticular nucleus [2]
Dorsal motor nucleus X of the vagus nerve [1]
Cerebellum

Notes: Some of the brain regions involved in Parkinson's disease. **Bold**: regions of the basal ganglia; *italics*: lenticular/lentiform nucleus. Neurotransmitters are indicated in parentheses ( ) for regions that are a source of neurotransmitter projection neurons: acetylcholine (ACh); dopamine (DA); norepinephrine (NEpi); serotonin (Ser). Superscripts: Braak stage in which the region is noted (Goedert et al., 2013; Braak et al., 2004).

Table 2

Molecular neuroimaging of Parkinson's disease

Study	Imaging	Radioligands/metabolites	Condition/contrast	Results	
A. Neurotransmitters					
Acetylcholine					
acetylcholine vesicular transporter					
Mazere 2012	SPECT	^{123}I-IBVM	PSP vs HC	↓	ACC, Tha
			PSP	pos	IBVM bp Tha with IBVM bp PPN
acetylcholinesterase					
Kotagal* 2012	PET	^{11}C-PMP	PD-RBD vs PD-nRBD	↓	neocortex, limbic (Hip, Amg), Tha
Müller* 2013	PET	^{11}C-PMP	PD	neg	AChe activity Tha with postural sway
muscarinic receptors					
Colloby 2006	SPECT	^{123}I-QNB	PD-D vs HC	↑	lingual g, Cun, mid occipital g,
			PD-D vs HC	↓	mid temporal g, FFG, IFG
			DLB vs HC	↑	mid occipital g, lingual g
nicotinic receptors					
Isaias 2014	SPECT	^{123}I-5IA	PD vs HC	↑	Put, Ins, SMA
				↓	Cau, OFC, mid temporal g
Kas* 2009	PET	2-^{18}F-FA	PD vs HC	↓	Cau, Put, SN
Meyer 2009	PET	2-^{18}F-FA	PD vs HC	↓	cerebellum, midbrain, pons, frontal, parietal, temporal, occipital, ACC, PCC, Hip, Amg
			PD	neg	BDI with 2-FA bp in ACC, midbrain, Put, occipital
Adenosine					
adenosine A_{2A}receptor					
Mishina* 2011	PET	^{11}C-TMSX	PD-Dyskinesia vs HC	↑	Put
			PD-Rx vs PD-nRx	↑	Put
Ramlackhansingh 2011	PET	^{11}C-SCH442416	PD-LID vs PD-nLID or HC	↑	Cau, Put
Cannabinoid					
cannabinoid receptor					
Laere 2012	PET	^{18}F-MK-9470	lPD vs HC	↑	Put, anteIns, PFC, Hip, midcingulate
			ePD vs HC	↑	contra Put, anteIns, Hip, PFC, midcingulate

Study	Imaging	Radioligands/metabolites	Condition/contrast	Results	
A. Neurotransmitters					
			PD	↓	SN
Dopamine					
aromatic amino acid decarboxylase (DOPA decarboxylase)					
Cropley* 2008	PET	^{18}F-FDOPA	PD vs HC	↓	Put, Cau
			PD		Put < Cau; contra striatum < ipsi striatum
			PD	pos	FDOPA uptake Put with WiCST
Goldstein 2008	PET	^{18}F-FDOPA	PD or MSA vs HC	↓	Put/occipital, Cau/occipital, SN/occipital
			PD vs MSA	↓	Put/Cau, Put/SN
			MSA-P vs MSA-C	↓	Put/occipital
Kas* 2009	PET	^{18}F-FDOPA	PD	ns	FDOPA uptake with nAChR in Put and Cau
Lewis 2012	PET	^{18}F-FDOPA	PD vs HC	↓	Put, Cau, ventral striatum
			PD vs HC	↑	LC
			MSA vs HC	↓	Put, Cau, ventral striatum, GPe, red n
			MSA-OH vs MSA-nOH	↓	LC
Pavese* 2010	PET	^{18}F-FDOPA	heteroParkin vs HC	↓	Cau, Put
			ParkinPD vs HC	↓	Cau, Put, GP, ventral striatum, LC, midbrain raphe, GP
			IPD vs HC	↓	Cau, Put, GP, ventral striatum, LC, midbrain raphe, GP, Hyp, vaTha, pineal
			ParkinPD vs IPD		Parkin < IPD midbrain raphe; IPD < Parkin Hyp
			PINK1PD vs HC	↓	Cau, Put, ventral striatum
Pavese* 2011	PET	^{18}F-FDOPA	PD-baseline vs HC	↓	Put, vaTha
			PD-baseline vs HC	↑	GPi, midbrain raphe, ns trend LC
			PD over time	↓	Put, Cau, Hyp, vaTha, GPe, LC, ventral striatum
Pavese* 2012	PET	^{18}F-FDOPA	PD	pos	FDOPA uptake with DASB in med raphe; trend to significance in Hyp, ACC
Politis* 2012	PET	^{18}F-FDOPA	PD after dopamine graft	↑	normal basal ganglia (Cau, Put, GP, STN, SN); normal LC
Scherfler* 2013	PET	^{18}F-FDOPA	PD	pos	odor function with FDOPA uptake Put
				neg	MD SN with FDOPA uptake Put; MD olfactory tract with FDOPA uptake Put
Wing* 2015	PET	^{18}F-FDOPA	RBD-MDD vs MDD or HC	↓	Put, Cau
D1 dopamine receptors					
Cropley* 2008	PET	^{11}C-NNC	PD vs HC	ns	NNC bp Cau, Put, Tha, frontal g

Study	Imaging	Radioligands/metabolites	Condition/contrast	Results	
A. Neurotransmitters					
D2/D3 dopamine receptors					
Hellwig* 2012	SPECT	^{123}I-IBZM	APS, LBD		FDG PET better than IBZM SPECT for dx (LBD, APS); dx (MSA, PSP, CBD)
Hellwig 2013	SPECT	^{123}I-IBZM	APS		IBZM SPECT not additive for predicting response to dopaminergic treatment
Mishina* 2011	PET	^{11}C-RAC	PD-Dyskinesia vs HC	↓	Put, Cau
			PD-Rx vs PD-nRx	↓	Put, Cau
Politis* 2012	PET	^{11}C-RAC	PD after dopamine graft		normalized RAC binding in basal ganglia after methamphetamine
Politis* 2014	PET	^{11}C-RAC	PD-LID vs PD-stable	↓	L-DOPA challenge RAC bp striatum
			PD-LID: Bu+L-DOPA vs L-DOPA	↑	RAC bp striatum
			PD-LID	pos	DASB bp with % change RAC bp in Cau, Put after buspirone
Wing* 2015	PET	^{11}C-RAC	RBD-MDD vs MDD or HC	ns	Put, Cau
dopamine					
Gröger* 2014	MRSI 3T	^{1}H dopamine	PD vs HC	↓	SN
			PD		caudal SN < rostral SN
dopamine transporter					
Baik* 2014	PET	^{18}F-FP-CIT	PD-nRx	pos	dopamine postPut with rsfc{antePut-dlfrontal area}, {Cau-postCG; Cau-preCG}, {postPut-cerebellum}, {postPut -R dlfrontal area}
				neg	dopamine postPut with rsfc {antePut- med frontal area}
Gerasimou 2012	SPECT	^{123}I-FP-CIT	PD vs ET, HC	↓	Put
Ham* 2015	PET	^{18}F-FP-CIT	PD vs DIP or HC	↓	DAT activity postPut (either MAS or LAS)
Hsiao* 2014b	SPECT	^{99m}Tc-TRODAT	PD		F-AV striatal asymmetry correlated better than TRODAT with clinical laterality
Joutsa 2015	SPECT	^{123}I-FP-CIT	PD vs HC	↓	striatum, ventral midbrain
			PD vs HC	↑	Tha, raphe nuclei
			HC	pos	FP-CIT binding ventral midbrain with Put
			PD	pos	FP-CIT binding ventral midbrain with antePut, Cau, PFC, Ins, MTL, ACC, PCC
Lebedev* 2014	SPECT	^{123}I-FP-CIT	PD-nRx	pos	DAT binding Cau with global increase of rsfc nodal strength
				neg	DAT binding Cau with network modularity
Lee, J.-Y. 2014	PET	^{18}F-FP-CIT	PD vs HC		FP-CIT bp ratios (NAcc/Put, Amg/Put, OFC/Put, vmPFC/Put) 3–6 times higher
			PD-ICD vs PD-nICD	↑	FP-CIT bp vmPFC
			PD-ICD vs PD-nICD	↓	FP-CIT bp NAcc

Study	Imaging	Radioligands/metabolites	Condition/contrast	Results	
A. Neurotransmitters					
McNeill 2013	SPECT	^{123}I-FP-CIT	GBA, LRRK2		Cau and Put, bilaterally asymmetric binding observed for GBA or LRRK2, but symmetric binding for α-synuclein, PINK1, Parkin mutations
			α-synuclein, PINK1, Parkin PD		
Mishina* 2011	PET	^{11}C-CFT	PD-Dyskinesia vs HC	↓	Cau, Put
			PD-Rx vs PD-nRx	↓	Cau, Put
Niethammer 2013*	PET	^{18}F-FP-CIT	PD-nD vs HC	↓	Cau, Put
			PD-nD	neg	DAT binding Cau with FDG-PET PDCP expression
Oh 2012	PET	^{18}F-FP-CIT	PD, PSP, or MSA vs HC	↓	ventral striatum, Cau, Put
			PSP vs PD	↓	anteCau
			MSA vs PD	↓	ventral Put
Oliveira 2015	SPECT	^{123}I-FP-CIT	PD vs HC		FP-CIT bp voxels-as-feature SVM: 98% accuracy, sensitivity, specificity
Vriend 2014b	SPECT	^{123}I-FP-CIT	PD	neg	depression BDI with DAT binding Cau
				neg	motor UPDRS-III with DAT binding Put
vesicular monoaminergic transporter					
Bohnen 2011	PET	^{11}C-DTBZ	PD		denervation postPut > Cau
			PD	neg	VMAT2 binding with UPDRS motor
Kotagal* 2012	PET	^{11}C-DTBZ	PD-RBD vs PD-nRBD	ns	striatum
Hsiao 2014a	PET	^{18}F-DTBZ	PD, HC		VMAT2 density in Cau, Put, SN decreased as disease severity increased
Hsiao* 2014b	PET	^{18}F-F-AV-133	PD vs HC		discriminating power of postPut > antePut > Cau
			PD		F-AV striatal asymmetry correlated better than TRODAT with clinical laterality
Müller* 2013	PET	^{11}C-DTBZ	PD	ns	DTBZ DVR with postural sway
γ-aminobutyric acid (GABA)					
Emir* 2012	MRS 7T	^{1}H GABA	PD vs HC	↑	pons, Put; greater increase in pons than Put
Gröger* 2014	MRSI 3T	^{1}H GABA	PD vs HC	↑	SN; rostral SN > caudal SN
Glutamate					
glutamate					
Emir* 2012	MRS 7T	^{1}H Glu	PD vs HC	ns	pons, Put, SN
Gröger* 2014	MRSI 3T	^{1}H Glu+Gln	PD vs HC	↑	SN
glutamate NMDA receptor					
Ahmed 2011	PET	^{11}C-CNS 5161	PD-LID vs PD-nLID:OFF	ns	basal ganglia, preCG

Study	Imaging	Radioligands/metabolites	Condition/contrast	Results	
A. Neurotransmitters					
			PD-LID vs PD-nLID:ON	↑	Cau, Put, preCG
Norepinephrine					
aromatic amino acid decarboxylase (DOPA decarboxylase)					
Pavese* 2010	PET	^{18}F-FDOPA	see above: Pavese 2010, LC results		
Pavese* 2011	PET	^{18}F-FDOPA	see above: Pavese 2011, LC results		
Politis* 2012	PET	^{18}F-FDOPA	see above: Politis 2012, LC results		
Serotonin					
aromatic amino acid decarboxylase					
Pavese* 2010	PET	^{18}F-FDOPA	see above: Pavese 2010, midbrain raphe results		
Pavese* 2011	PET	^{18}F-FDOPA	see above: Pavese 2011, midbrain raphe results		
serotonin transporter					
Bohnen 2013	PET	^{11}C-DASB	PD	ns	SERT binding raphe n, Amg, Hip, striatum with smell test
Kotagal* 2012	PET	^{11}C-DASB	PD-RBD vs PD-nRBD	ns	DASB binding brainstem, striatum
Pavese* 2012	PET	^{11}C-DASB	see above: Pavese 2012		
Politis* 2012	PET	^{11}C-DASB	PD after dopamine graft	↓	raphe n, Amg, Tha, Hyp, Ins, ACC, PCC, PFC
Politis* 2014	PET	^{11}C-DASB	see above: Politis 2014		
Qamhawi 2015	SPECT	^{123}I-FP-CIT	PD-nRx vs HC or SWEDD	↓	brainstem raphe, but only in 13% of PD-nRX individuals
			PD-nRx	neg	FP-CIT binding in raphe with measures of resting tremor

Study	Imaging	Radioligands/metabolites	Condition/contrast	Results	
B. Other biochemicals					
Amyloid					
Campbell 2013	PET	^{11}C-PiB	PD-cog, AD, HC		PiB binding patterns AD vs HC, AD vs PD; ns for PD vs HC
Campbell* 2015	PET	^{11}C-PiB	PD vs HC	↑	PiB binding in cortex only observed in 16% PD individuals
			PD or HC	ns	PiB binding in cortex with rsfc DMN
Edison* 2013	PET	^{11}C-PiB	PD-D or PD-nD vs HC	↑	small increases in PCC, Tha, frontal c, parietal c, occipital c
Lucero 2015	PET	^{11}C-PiB	PD		<16 yr education: PiB binding correlated positively with cognitive impairment ≥16 yr education: PiB binding did not correlate with cognitive impairment
MRS metabolites					
Emir* 2012	MRS 7T	^{1}H multiple	PD vs HC	↑	GABA in pons, Put, but ns in SN. No other neurochemical abnormalities.

Study	Imaging	Radioligands/metabolites	Condition/contrast	Results	
B. Other biochemicals					
Graff-Radford 2014	MRS 1.5T	^{1}H multiple	DLB vs CN	↓	NAA/Cr occipital
			AD vs CN	↓	NAA/Cr PCC, frontal
			DLB vs CN	↑	Cho/Cr PCC, frontal
			AD vs CN	↑	Cho/Cr PCC
			DLB vs CN	↑	myo-inositol/Cr PCC, occipital
			AD vs CN	↑	myo-inositol/Cr PCC, frontal l
Gröger* 2014	MRSI 3T	^{1}H multiple	PD vs HC	↓	dopamine, NAA, Cho, Cr, myo-inositol, GSH in SN
				↑	Glu-Gln, GABA, HVA in SN
Levin 2012	MRSI 3T	^{1}H multiple	PD vs HC	↓	GM: NAA and/or NAA/Cr in temporal l, occipital l, total cerebrum
				↓	WM: Cr in temporal l, parietal l
				↑	GM: Cr in temporal l
Weiduschat 2014	MRS 3T	^{31}P multiple	PD: men vs women	↓	ATP, HEP in striatum, temperoparietal GM
			HC: men vs women	ns	striatum, GM
Tau					
Kepe 2013	PET	^{18}F-FDDNP	PSP vs PD or HC	↑	subthalamic area, midbrain, WM cerebellum
Translocator protein					
Edison* 2013	PET	^{11}C-PK11195	PD-D vs HC	↑	ACC, PCC, striatum, frontal c, temporal c, parietal c, occipital c
			PD-nD vs HC	↑	temporal c, occipital c
			PD-D	neg	PK bp cortical regions with MMSE
Iannaccone 2013	PET	^{11}C-PK11195	PD vs HC	↑	SN, Put
			DLB vs HC	↑	SN, Put, Cau, Tha, cerebellum, ACC, PCC, preCun, occipital med c, and lat frontal, temporal, and parietal c

Study	Imaging	Radioligands/metabolites	Condition/contrast	Results	
C. Cerebral glucose metabolism and cerebral blood flow					
Borghammer 2012	PET	^{18}F-FDG	PD vs HC	↑	GPe, GPi, Put, Tha
				↓	med and lat frontal c, med and lat parieto-occipital c, lat temporal c, Ins
Eckert 2008	PET	^{18}F-FDG	MSA, PSP		MSARP: (↓ Put, cerebellum) PSPRP: (↓ med PFC, FEF, vlPFC, Cau, med Tha, upper brainstem)
Edison* 2013	PET	^{18}F-FDG	PD-D vs HC	↓	PCC, temporal, parietal, occipital
			PD-D vs PD	↓	frontal, temporal, parietal, occipital c

Study	Imaging	Radioligands/metabolites	Condition/contrast	Results	
C. Cerebral glucose metabolism and cerebral blood flow					
				pos	glucose metabolism in temperoparietal and occipital regions with MMSE
Garraux 2013	PET	^{18}F-FDG	PD vs APS		RVM Excess network (↑ glucose metabolism indicates PD): upper brain stem, med Tha, ventral striatum, headCau, med temporal, ACC, mid cingulate, med frontal/preSMA, Ins, dorsal frontal regions. Deficit network: preCun/PCC, occipital, lat temporal, lat parietal, inf frontal (subgenual, OFC, inf lateral PFC), lat Tha
Hellwig* 2012	PET	^{18}F-FDG	LBD		↑ Put; ↓ temperoparietal c, occipital c
			MSA		↓ Put, pons, cerebellum
			PSP		↓ midline frontal, premotor/motor c, Cau, upper brainstem
			CBD		↓ contralateral (to affected side) striatum, frontoparietal c
Holtbernd 2014	PET	^{18}F-FDG	RBD vs HC	↑	PDRP: (↑ pons, cerebellum, GPi, Put, ventral Tha, primary motor; ↓ lateral premotor, parietal association c)
	SPECT	^{99m}Tc-ECD	RBD vs HC	↑	PDRP
	SPECT	^{99m}Tc-ECD	RBD, HC		PDRP + age predicted phenoconversion to PD or DLB
Ma 2007	PET	^{18}F-FDG	PD vs HC	↑	PDRP: (↑ GP/Put, Tha, pons, cerebellum; ↓ premotor, post parietal)
	PET	^{15}O-H_2O	PD vs HC	↑	PDRP
Mayer 2015	SPECT	^{99m}Tc-ECD	RBD, PD-RBD, narcolepsy-RBD	↑	ictal results: premotor, interhemispheric cleft, periaqueductal, dorsal pons, ventral pons, ante lobe cerebellum
Niethammer* 2013	PET	^{18}F-FDG	PD-nD		PDCP: (↑ cerebellar vermis, dentate n; ↓ PMC, rostral SMA/preSMA, preCun) PDCP expression negatively correlated with DAT binding Cau No correlation between PDRP and DAT binding Cau
Poston 2012	PET	^{18}F-FDG	PD		PDRP: (↑ GP, Tha, pons, cerebellum, sensorimotor; ↓ lateral premotor, parieto- occipital c)
			MSA		MSARP: (↓ Put, cerebellum)
Tang 2010	PET	^{18}F-FDG	PD, MSA, PSP		FDG PET imaging automated classification showed high specificity for PD, MSA, PSP
Teune 2013	PET	^{18}F-FDG	PD, MSA, PSP, HC		PD pattern: (↑GP, Tha, pons, dorsalPut, primary motor c, SMA; ↓lateral premotor, prefrontal association c, post parietal association c, visual c) MSA pattern: (↑subcortical WM, mid temporal c; ↓ Put, Cau, premotor c, primary visual c) PSP pattern: (↑ inferior and mid temporal c, subcortical WM, sensorimotor c, pons, vermis; ↓ prefrontal c, cingulate, FEF, post parietal association c, Cau, ventralPut, cerebellum crus)
Wing* 2015	PET	^{18}F-FDG	RBD-MDD vs MDD or HC	ns	Put, Cau
Wu 2014	PET	^{18}F-FDG	RBD or PD vs HC	↑	RBDRP: (↑ pons, Tha, precentral g, SMA, med frontal g, Hip/paraHip, supramarginal g, inf temporal g, post cerebellar tonsil; ↓ occipital, red n, sup/mid temporal).
			RBD or PD vs HC	↑	PDRP: (↑ sensorimotor, GP, Tha, pons, cerebellum; ↓ premotor, post parietal-occipital)
Zhao 2012	PET	^{18}F-FDG	PD, MSA, PSP, CBD, DLB, NPH		Comparisons between groups highlighted these regions: PD: ↓ bilateral parietal l MSA-P: ↓ bilateral basal ganglia MSA-C: ↓ bilateral cerebellum PSP: ↓ midbrain, middle frontal c CBD: ↓ asymmetrical hypometabolism cortex and BG

Study	Imaging	Radioligands/metabolites	Condition/contrast	Results
C. Cerebral glucose metabolism and cerebral blood flow				
				DLB: ↓ bilateral occipital and parieto-occipital c

Notes: Recent molecular neuroimaging studies of Parkinson's disease. The first author of each study is given. Some examples of results from each study are given. All results reported here were from studies obtained during the resting-state unless a task is specified. *: study appears more than once in Table 2 and/or 3. A. Studies grouped according to neurotransmitters, enzymes, receptors, or transporters that were investigated. B. Studies grouped according to other biochemicals that were investigated. C. Studies of cerebral glucose metabolism and cerebral blood flow.

*Abbreviations.***Imaging:** MRS=magnetic resonance spectroscopy; MRSI= MRS imaging; PET=positron emission tomography; SPECT=single photon emission computed tomography; T=Tesla. **Radioligands/metabolites:** CFT= 2β-carbomethoxy-3*β*-(4-fluorophenyl)tropane; CNS=[N-methyl-3(thyomethylphenyl)cyanamide; DASB=3-amino-4-(2-dimethylaminomethylphenylthio)benzonitrile; DTBZ=dihydrotetrabenazine; ECD=ethylcysteinate dimer; FA=fluoro-3-(2[S]-2-azetidinylmethoxy)-pyridine; F-AV= fluoropropyl-(+)-dihydrotetrabenazine; FDDNP=2-(1-{6-[(2-[F-18]fluoroethyl)(methyl)amino]-2-naphthyl}ethylidene)malononitrile; FDG=fluorodeoxyglucose; FDOPA=fluoro-dihydroxyphenylalanine; FP-CIT=ioflupane=*N*-*ϖ*-flouro-propyl-2*β*-carbomethoxy-3*β*-(4-iodophenyl)nortropane; GABA= γ-aminobutyric acid; Gln=glutamine; Glu=glutamate; 5IA=5-iodo-3-[2(*S*)-2-azetidinylmethoxy]pyridine; IBVM =iodobenzovesamicol; IBZM=iodobenzamide; MK-9470=(*N*-[2-(3-cyanophenyl)-3-(4-(2-[18F]fluorethoxy)phenyl)-1-methylpropyl]-2-(5-methyl-2-pyridyloxy)-2-methylproponamide); NNC=(+)-8-chloro-5-(7-benzofuranyl)-7-hydroxy-3-methyl-2,3,4,5-tetrahydro-1H-3-benzazepine; PiB=Pittsburgh Compound B= (N-methyl-2[(4-methylaminophenyl)-6-hydroxybenzothiazole); PK11195=1-(2-chlorophenyl)-*N*-methyl-*N*-(1-methylpropyl)-3-isoquinoline carboxamide; PMP=methyl-4-piperidinyl propionate; QNB=quinuclidinyl-benzilate; RAC= raclopride; SCH442416=5-amino-7-(3-(4- methoxyphenyl)propyl)-2-(2-furyl)pyrazolo[4,3-*e*]-1,2,4-triazolo[1,5-*c*]pyrimidine; TMSX=[7-methyl-11C]-(E)-8-(3,4,5-trimethoxystyryl)-1,3,7-trimethylxanthine; TRODAT=2-[[2-[[[3-(4-chlorophenyl)-8-methyl-8-azabicyclo[3,2,1]oct-2-yl]methyl](2-mercaptoethyl)amino]-ethyl]amino]ethanethiolate(3-)-N2,N2′,S2,S2′]oxo-[1R-(*exo*-*exo*).

Condition: AD=Alzheimer's disease; APS=atypical Parkinson's syndromes; Bu=buspirone; CBD=corticobasal degeneration; CN=cognitively normal; DIP=drug induced parkinsonism; DLB=dementia with Lewy bodies; ePD=early PD; ET=essential tremor; GBA=glucosidase, beta, acid gene; HC=healthy controls; heteroParkin=heterozygous carrier of Parkin mutation; IPD=idiopathic PD; LBD=Lewy body disease; L-DOPA=L-3,4-dihydroxyphenylalanine; lPD=latePD; LRRK2=leucine-rich repeat kinase 2; MDD= major depressive disorder; MSA=multiple system atrophy; MSA-C=MSA with cerebellar features; MSA-OH=MSA with orthostatic hypotension; MSA-nOH=MSA without orthostatic hypotension; MSA-P=Parkinsonian form MSA; NPH=normal pressure hydrocephalus; PD=Parkinson's disease; PD-cog=PD with cognitive impairment; PD-D=PD with dementia; PD-ICD=PD with impulse control disorder; PD-LID=PD with levodopa induced dyskinesias; PD-nD=PD without dementia; PD-nICD=PD without impulse control disorder; PD-nLID=PD without levodopa induced dyskinesias; PD-nRBD= PD without RBD; PD-nRx=PD medication naive; PD-RBD=PD with RBD; PD-Rx=PD taking medications; PINK1=PTEN induced putative kinase 1; PSP=progressive supranuclear palsy; RBD=rapid eye movement sleep behavior disorder; RBD-MDD=RBD plus MDD; SWEDD=subjects without evidence of dopaminergic deficit.

Results:↓ or ↑ = significant decrease or increase of the measure was observed in the given brain region(s); neg=negative correlation; ns=not significant; pos=positive correlation. {X-Y}=connectivity between X and Y. ACC= anterior cingulate cortex; AChe=acetylcholinesterase; Amg=amygdala; ante=anterior; ATP= adenosine triphosphate; BDI=Beck depression index; bp=binding potential; c=cortex; Cau=caudate; Cho=choline; contra=contralateral; Cr=creatine; Cun=cuneus; DAT=dopamine transporter; dlfrontal=dorsolateral frontal; DVR=distribution volume ratio; dx=diagnosis; FEF=frontal eye fields; FFG=fusiform gyrus; g=gyrus; GM=gray matter; GP=globus pallidus; GPe=Gp externa; GPi=GP interna; GSH=glutathione; HEP=high energy phosphate; Hip=hippocampus; HVA=homovanillic acid; Hyp=hypothalamus; IFG=inferior frontal gyrus; inf=inferior; Ins=insula; ipsi=ipsilateral; l=lobe; LAS=less affected side; lat=lateral; LC=locus coeruleus; MAS=more affected side; MD=mean diffusivity; med=medial; mid=middle; MMSE=Mini Mental State Examination; MSARP=multiple system atrophy related pattern; MTL=medial temporal lobe; n=nucleus; NAA= N-acetylaspartate; nAChR= nicotinic acetylcholine receptors; OFC=orbital frontal c; paraHip=parahippocampus; PCC=posterior cingulate cortex; PDCP=Parkinson's disease cognition related pattern; PDRP=Parkinson's disease related pattern; PFC=prefrontal cortex; PMC=premotor c; post=posterior; postCG=postcentral gyrus; PPN=pedunculopontine nucleus; preCG=precentral gyrus; preCun=precuneus; PSPRP=progressive supranuclear palsy related pattern; Put=putamen; RBDRP=rapid eye movement sleep behavior disorder related pattern; rsfc=resting-state functional connectivity; RVM=relevance vector machine; SERT=serotonin transporter; SMA=supplementary motor area; SN=substantia nigra; STN=subthalamic nucleus; SVM=support vector machine; Tha= thalamus; UPDRS=Unified Parkinson's Disease Rating Scale; vaTha=ventral anterior thalamus; vlPFC=ventrolateral PFC; VMAT2=vesicular monoaminergic transporter type 2; vmPFC=ventromedial prefrontal cortex; WiCST=Wisconsin Card Sort Test; WM=white matter; yr=years.

Table 3

MRI neuroimaging in PD

Study	B_0	Condition/contrast	Results	
A. Diffusion imaging				
Agosta 2014	1.5T	PD-MCI vs HC	↓	FA ACR, SCR, bCC, anteSLF
		PD-MCI vs PD-nMCI	↓	FA ACR, SCR, gCC, bCC, anteIFOF/Unc, anteSLF
Aquino 2014	1.5T	ePD, lPD, HC	ns	FA, MD, R2* in SN ns for all contrasts
		ePD vs HC	↓	area SN
		lPD vs ePD	↓	area, vol SN
		ePD, lPD	neg	area or vol SN with UPDRS
Auning 2014	1.5T	PD-nD vs HC	↑	RD WM: paraHip (temporal), lingual g (occipital), preCun (parietal)
		PD-nD vs HC	↓	FA WM: frontoparietal, CC, postCG
		PD-nD vs MCI(AD)	↑	RD WM: frontoparietal (CST)
		PD-nD	neg	RD WM: rostral mid frontal c with executive function
Cherubini 2014	3T	PD, PSP		SVM: WM atrophy, GM atrophy, and DTI parameters used to classify PSP and PD
Garcia-Lorenzo 2013	3T	PD-RBD vs HC	↑	FA midbrain tegmentum, rostral pons
		PD-RBD or PD-nRBD vs HC	↑	ADC pontine tegmentum, midbrain cerebral peduncles region, SN
		PD-RBD vs PD-nRBD or HC	↓	NMS intensity locus coeruleus/subcoeruleus
Haller 2012	3T	PD vs Other Parkinsonism		SVM analysis of DTI results classified PD patients individually
Ji 2015	3T	PD vs HC	↓	FA bCC
		MSA-P vs PD	↓	FA CST, ATR
		MSA-P vs PD	↑	RD CST, ATR
Kamagata 2012	3T	PD-D vs HC	↓	FA anteCFT, postCFT
		PD-nD vs HC	↓	FA anteCFT
		PD-D	pos	MMSE with FA anteCFT
Kamagata 2013	3T	PD-D vs HC	↓	FA SLF, ILF, IFOF, UF, Cg, ALIC, SN
		PD-D vs HC	↑	MD similar tracts as for FA results, with addition of PLIC
		PD-D vs PD-nD	↓	FA anteIFOF, gCC
		PD-D and PD-nD	pos	MMSE with FA anteIFOF, gCC, anteSLF, postSLF, CC
Kamagata 2014	3T	PD vs HC	↓	FA frontal WM
			↓	MK frontal, parietal, occipital, temporal WM; PCRand SLF fiber crossing

Neurosci Biobehav Rev. Author manuscript; available in PMC 2016 December 01.

Study	B_0	Condition/contrast	Results	
A. Diffusion imaging				
Kim, H. 2013	3T	PD vs HC	↑	MD WM: corticofugal pathway (CR, IC, cerebral peduncle), Cg, UF, fornix/ST, CC, EC, SLF, PTR (optic radiation), sup cerebellar peduncle, WM near preCun and SMG; GM:Cau, Put, GP, Tha
Peterson 2015	3T	PD-nFOG vs PD-FOG	↑	PPN tract quantity
		PD-FOG	pos	dual-task walking interference with PPN structural connectivity laterality
Prodoehl 2013	3T	PD, MSA, PSP, ET, HC		SVM distinguished these diagnoses using FA, MD, RD, LD in Cau, Put, GP, SN, red n, inf CP, mid CP, sup CP, dentate n. Cau, Put, SN, mid CP appeared frequently in the findings
Rae 2012	3T	PD vs HC	↑	MD FMi, FMa, CC, ATR, UF, IFOF, IC, EC, CST, SLF, ILF
		PD vs HC	↓	FA FMi, FMa, CC, ATR, UF, IFOF, CST, SLF, ILF
		PD	pos	executive function (phonemic fluency) with ↑ FA or ↓MD in above tracts except FMa, CST, ILF
Scherfler* 2013	1.5T	PD vs HC	↑	MD Olf tract, SN
			↓	FA SN
			neg	MD SN, Olf tract with PET FDOPA uptake Put
Schwarz 2013	3T	PD vs PSP	↑	MD SN; meta-analysis indicated not a useful biomarker
Sharman* 2013	3T	PD vs HC	↓	{SM c-Put}, {SM c-Tha}, {GP-Tha}, {SN-Tha}
Surdhar 2012	1.5T	PD-Depr or PD-nDepr vs HC	ns	FA, MD, length UF, CC
		PD-Depr vs HC	↓	vol Amg
Thaler 2014	3T	LLRK2car vs LLRK2ncar	ns	nonsignificant trend ↑ FA ↓MD in ATR, CST, SLF, IFOF, Cg, FMa, SN; ↓MD NAcc
Vercruysse 2015	3T	PD-FOG vs PD-nFOG	↓	FA cerebellum, temporal SLF
		PD-FOG vs PD-nFOG	↑	MD anteIC, ACR, ATR, sup frontal c, cerebellum
			neg	FA cerebellum VIIIb with L-DOPA equiv Rx; {Cau-ACC}with UPDRS motor
			pos	MD anteIC,{Cau-ACC}, {Cau-SFG}, {Cau-preSMA}, {GP-ACC} with UPDRS motor
Zheng 2014	3T	PD	pos	executive function with FA ACR, ALIC, gCC, PTR
			neg	executive function with MD ACR, ALIC, gCC, PCR, SS, SFOF
			pos	linguistic function with FA ALIC, SS
			neg	linguistic function with MD ACR, gCC, SS, SFOF
			pos	attention with FA Cg, EC, PTR, RLIC, SS, SFOF
			neg	attention with MD ACR, ALIC, CST, Cg, Hip, PCR, PTR, RLIC, SS, sCC, SCR, SFOF
			neg	short-term memory with MD fornix
			neg	long-term memory with MD R ACR

Study	B_0	Condition/contrast	Results	
B. Functional MRI (fMRI): amplitude of low frequency fluctuations (ALFF), functional connectivity (fc), and task-based fMRI				
Baggio 2014	3T	PD-MCI vs HC	↓	long-range connections (wide-spread); centrality, degree
			↑	connectivities for shorter connections in frontal and temporal lobes
			↑	clustering, small-worldness, modularity (frontal, temporal) reorganization of network nodes (e.g. some PD prefrontal nodes not observed in HC)
			neg	VS/VP, memory with global measures of clustering, small-worldness, modularity
			neg, pos	VS/VP, memory, A/E with network parameters at regional level
Baik* 2014	3T	PD-nRx	pos	dopamine postPut with rsfc {antePut-R dlfrontal area}, {Cau-postCG/preCG}
			neg	dopamine postPut with rsfc {antePut-med frontal area}
			pos	dopamine postPut with rsfc {postPut-[cerebellum, dlfrontal area]}
Baudrexel 2011	3T	ePD-Tr vs HC	↑	{STN-[preCG, postCG]}
		ePD-nTr vs HC	↑	{STN-[paracentral lobule, SMA, MCC, inf parietal l/SMG, inf parietal l/STG]}
		ePD-Tr vs HC	↑	{motor hand area-[sup/med frontal g, cerebellum, STN]}
		ePD-Tr vs HC	↓	{motor hand area-[M1/S1, mid/sup occipital g, mid temporal g]}
Borroni 2015	1.5T	PD vs HC	ns	VBM vol
		PD-D vs HC	↓	VBM frontal, subcortical
		DLB vs HC	↓	VBM parietal, occipital, subcortical
		PD or PD-D vs HC	↓	ReHo frontal regions
		DLB vs HC	↓	ReHo FFG, pons
Burciu 2015	3T	PD, PSP, HC		VBM and fMRI (hand force generation task) results in multiple regions of the basal ganglia, cerebellum, and cortex are different for PSP vs PD
Campbell* 2015	3T	PD vs HC	↓	rsfc SMN
		PD vs HC	↑	rsfc DMN
		PD or HC	ns	PET PiB binding with rsfc DMN
		PD		rsfc SMN correlated positively and DAN negatively with CSF α-synuclein
Carriere 2015	3T	PD-nICD vs HC	ns	rsfc corticostriatal
		PD-nICD vs PD-ICD	↑	{antePut-[ITG, ACG]}
Gorges 2013	1.5T	PD vs HC	↓	{medPFC-PCC}
			↑	{left HF – right HF}
			neg	horizontal and vertical saccadic accuracy with {PCC- MTL}
			pos	vertical saccadic accuracy with {left inf parietal c-right HF} and {right inf parietal c-left HF}
Göttlich 2013	1.5T	PD vs HC	↑	characteristic path length
		PD vs HC	↓	rsfc degree med OFC, mid OFC, Cun, Cal

Study	B_0	Condition/contrast	Results	
B. Functional MRI (fMRI): amplitude of low frequency fluctuations (ALFF), functional connectivity (fc), and task-based fMRI				
		PD vs HC	↑	rsfc degree sup parietal c, PCC, SMG, SMA
Hacker 2012	3T	PD vs HC	↓	{EBS (contiguous Tha, midbrain, pons, cerebellum)-[Cau, antePut, postPut]} Cau-EBS < antePut-EBS < postPut-EBS
		PD vs HC	↑	anticorrelated (negative) striatal rsfc with sensori-motor, visual, and subgenual frontal regions was observed in HC but absent in PD, leading to↑ (more positive) results for these connections in PD
		PD vs HC	↓	{Put-SMG}
		PD	neg	striatal-EBS with UPDRS-motor
Ham* 2015	3T	PD vs DIP	↑	{cerebellum-[MASCau, LASantePut, LASpostPut]},{anteprefrontal-[MASantePut, LASpostPut]},
		PD vs DIP	↓	rsfc {PCC-temporal}
		DIP vs PD	↓	{dlPFC-[frontal, parietal]}
Helmich 2010	3T	PD or HC		{postPut –[primary motor, primary somatosensory, premotor, cerebellum, inf parietal c, dlPFC, extrastriate visual c]}
		PD or HC		{antePut-[preSMA, ACC, mid frontal g, mid temporal, mid cingulate c, STN region]}
		PD or HC		{anteCau-[dmPFC, dlPFC, ITG, inf parietal c, paraHip, cerebellum]}
		PD vs HC	↓	{postPut- [CMA, postCG, parietal operculum (S2), SMG/inf parietal c]}
		PD vs HC	↑	{antePut-[parietal operculum (S2), SMG/inf parietal c]}
Hou 2014	3T	PD vs HC	↓	slow-4 (0.027–0.073) or slow-5 (0.010–0.027 Hz) ALFF striatum; slow-4 > slow-5
		PD vs HC	↑	slow-4 or slow-5 ALFF midbrain; slow-4 > slow-5
		PD	neg	UPDRS motor score with ALFF Put, preSMA, CMA in slow-4 or slow-5
		PD	neg	UPDRS motor score with ALFF SN, GP only in slow-4
		PD	pos	UPDRS motor score with ALFF cerebellum only in slow-5
		PD	neg	bradykinesia with ALFF preSMA in slow-4 or slow-5
Lebedev* 2014	3T	PD-nRx	pos	DAT binding Cau with global increase of nodal strength
			neg	DAT binding Cau with cognitive network modularity
Liu, H. 2013	3T	PD vs HC	↑	pos rsfc {dentate n-cerebellar post l}; neg rsfc {dentate n-preCUN}
		PD vs HC	↓	pos rsfc {dentate n-IPL}; neg {rsfc dentate n-medPFC}
		PD-Tr vs PD-AR	↓	pos rsfc {dentate n-cerebellar post l}
Luo 2014a	3T	PD-nRx-Depr vs PD–nDepr or HC	↑	ALFF OFC
		PD-nRx-Depr or PD–nDepr vs HC	↓	rsfc {Put-[Amg, Hip, Olf, post rectus]}
		PD-nRx-Depr vs PD-nRx-nDepr	↓	rsfc {Ins-OFC}; {postPut-MTG}
		PD-nRx-Depr	pos	ALFF OFC with HRDS
Luo 2014b	3T	PD-nRx vs HC	↓	{antePut-[Put, Amg, Hip, Olf, rectus]; {postPut-[Put, Amg, Hip, Olf, rectus, postCG, SMG]}
		PD-nRx right onset vs HC	↓	postPut on the left, but not right, showed ↓ rsfc with left preCG and postCG

Study	B_0	Condition/contrast	Results	
B. Functional MRI (fMRI): amplitude of low frequency fluctuations (ALFF), functional connectivity (fc), and task-based fMRI				
		PD-nRx	neg	{right Amg-[left postPut, right postPut]} with nonmotor symptom scores
		PD-nRx vs HC	ns	VBM GM
New 2015	3T	PD vs HC		rsfc {subcortical (Put, Tha, cerebellum) - cortical (frontal, temporal)} absent in PD
		PD		rsfc between many regions of vocalization network significantly correlated with PDQ and UPDRS communication related scores
Palmer 2010	3T	PD vs HC	↓	visuomotor task activation in striato-TC; fc in striato-TC and DMN (preCun, PCC)
			↑	visuomotor task activation in cerebellar-TC, DMN (preCun, PCC); fc in cerebello-TC
Putcha 2015	3T	PD vs HC	↓	rsfc coupling SaN-CEN
		PD		pos rsfc coupling DMN-CEN
		HC		neg rsfc coupling DMN-CEN
		PD vs HC	↑	rsfc coupling DMN-CEN
Sharman* 2013	3T	PD vs HC	↓	{SM c-Tha}, {GP-[Put, Tha]}, {SN-[GP, Put, Tha]}
			↑	{As c- Put}, {Lb c-Tha}, {Put-Tha}
Sheng 2014	3T	PD-Depr vs PD-nDepr	↓	ReHo Amg, lingual g
		PD-Depr vs PD-nDepr	↑	mid frontal g, IFG
		PD-Depr vs PD-nDepr	↑↓	rsfc of multiple regions with mid frontal g, IFG, Amg, lingual g
Shine 2013	3T	PD-FOG vs PD-nFOG	↓	activation in Ins, ventral striatum, preSMA, STN during virtual reality task with motor and cognitive loads
Shine 2014	3T	PD-VH vs PD-nVH	↓	activation during visual perception tasks in FEF, dlPFC, SPL, midbrain, preSMA, V2
		PD-VH vs PD-nVH	↓	rsfc {anteIns-FEF}, {dorsal ACC-FEF}
		PD-VH vs PD-nVH	↓	vol GM anteIns
		PD	pos	vol GM anteIns with rsfc {dorsal ACC-FEF}
			neg	vol GM anteIns with task error score
Siebert 2012	1.5T	PD-D vs HC	ns	DMN (isthmus cingulate seed)
		PD-D vs HC	↓	{Cau-[Put, sup frontal, mid frontal]}
Skidmore 2011	3T	PD vs HC	↓	0.06–0.12 Hz wavelet analysis nodal efficiency, global efficiency
Skidmore 2013b	3T	PD		↑ ALFF subgenual cingulate predicted depression ↑ ALFF OFC and ↓ ALFF SMA predicted apathy ↓ ALFF Put predicted UPDRS-motor
Su 2015	3T	PD-OH vs PD-nOH	↓	ReHo Amg, Ins, paraHip, OFC, IFG, Olf, RG, sup temporal pole
		PD-OH vs PD-nOH	↑	ReHo lingual, Cal, Cun, postCG, ACC/PCC, mid/sup temporal g, mid occiptal g
		PD-OH vs PD-nOH	↓	{left RG-[bilateral RG, OFC, paraHip, mid occipital g, lingual g, cerebellum, Ins, sup temporal pole, PCC, Cun, Amg, temporal l]}
		PD	neg	ReHo OFC, Ins with threshold of olfactory detection

Study	B_0	Condition/contrast	Results	
B. Functional MRI (fMRI): amplitude of low frequency fluctuations (ALFF), functional connectivity (fc), and task-based fMRI				
Tessitore 2012a	3T	PD-FOG vs PD-nFOG	↓	rsfc mid frontal g, Ang (executive-attention network); occipitotemporal g (visual network)
			neg	FOG-Q with ICA scores mid frontal g, Ang, occipito-temporal g
Tessitore 2012b	3T	PD vs HC	↓	DMN ICA components MTL, IPC
			pos	ICA score MTL with memory scores; IPC with visuospatial
			ns	VBM GM, WM, CSF
Wu 2015	3T	PD vs HC		PDRP-ALFF: ↑Tha, cerebellum, med frontal/RG, preCun, SPL, temporal/postIns; ↓ Cau, antePut, mid frontal g, preSMA, lingual, mid occipital g, preCun, ITG, SMG, PCC
Yao 2015	3T	PD-VH vs PD-nVH or HC	↓	ALFF lingual, Cun
		PD-VH vs PD-nVH or HC	↑	ALFF tempero-parietal, MTL, cerebellum
		PD-VH or PD-nVH vs HC	↓	rsfc occipital
		PD-VH vs PD-nVH	↑	{occipital-corticostriatal}
Yu 2013	1.5T	PD vs HC	↑	{Put-SMA} with Put seed; PD had pos while HC had neg rsfc {Put-SMA}
			↓	{Cau-OFC}with Cau seed
			↑	{SMA-[Put, Amg]} with SMA seed; PD had pos but HC had neg rsfc SMA-[Put, Amg]}
Zhang 2013	3T	PD vs HC	↑	slow-5 band (0.010–0.027 Hz) ALFF Cau, Hip, STG, ITG, FFG, IFG
			↓	slow-5 band ALFF cerebellum, mid temporal g, mid occiptal g, Cun, Cal
			↓	slow-4 band (0.027–0.073) cerebellum, Tha, mid occipital g, inf occipital g
			neg	slow-5 ALFF IFG with UPDRS-III; ns slow-4 band with UPDRS-III
Zhang 2015	3T	PD vs HC	↓	short-range rsfc densities ventral visual pathway; long-range rsfc densities mid and sup frontal g
			↑	short and long-range rsfc densities preCun, PCC

Notes: Recent MRI studies of Parkinson's disease. The first author of each study is given. Some examples of results from each study are given. All results reported here were from studies obtained during the resting-state unless a task is specified. B_0=magnetic field strength. T=Tesla. A. Diffusion imaging: diffusion weighted imaging, diffusion tensor imaging (DTI), and diffusion kurtosis imaging (DKI). B. Functional MRI (fMRI): amplitude of low frequency fluctuations (ALFF), functional connectivity (fc), and task-based fMRI studies. *: study appears more than once in Table 2 and/or 3.
Abbreviations: **Condition:** AD=Alzheimer's dementia; DIP=drug induced parkinsonism; DLB=dementia with Lewy bodies; ePD=early PD; ET=essential tremor; HC=healthy controls; lPD=late PD; LRRK2car=leucine-rich repeat kinase 2 mutation carrier; LRRK2ncar=not carrier of leucine-rich repeat kinase 2 mutation; MSA=multiple system atrophy; MSA-P=Parkinsonian form MSA; PD=Parkinson's disease; PD-AR=PD akinetic rigid; PD-D=PD with dementia; PD-Depr=PD with depression; PD-FOG= PD freezing-of-gait; PD-ICD=PD with impulse control disorder; PD-MCI=PD with mild cognitive impairment; PD-nD=PD without dementia; PD-nDepr=PD without depression; PD-nFOG= PD without freezing-of-gait; PD-nICD=PD without impulse control disorder; PD-nMCI=PD without mild cognitive impairment; PD-nOH=PD with none/less obvious hyposmia; PD-nRBD=PD without RBD; PD-nRx=PD medication naive; PD-nTr=PD without tremor; PD-nVH=PD without visual hallucinations; PD-OH=PD with obvious hyposmia; PD-RBD=PD with RBD; PD-Tr=PD with tremor; PD-VH=PD with visual hallucinations; PSP=progressive supranuclear palsy.

Results:↓ or ↑ = significant decrease or increase of the measure was observed in the given brain region(s); neg=negative correlation; ns=not significant; pos=positive correlation. {X-Y}=connectivity between X and Y; {X-[Y1,Y2…]}= connectivity between X and Y1, X and Y2, etc. {X-Y} describes anatomical connectivity in (A) or resting-state functional connectivity in (B) unless otherwise noted. ACC=anterior cingulate cortex; ACG=anterior cingulate gyrus; ACR=anterior corona radiata; ADC=apparent diffusion coefficient; A/E=attention/executive; ALIC=anterior limb of internal capsule; Amg=amygdala; Ang=angular gyrus; ante=anterior; As= associative; ATR=anterior thalamic radiation; bCC=body of corpus callosum; c=cortex; Cal=calcarine; Cau=caudate; CC=corpus callosum; CEN=central executive network; CFT=cingulate fiber tract; Cg=cingulum/cingulate; CMA=cingulate motor area; CP=cerebellar peduncle; CR=corona radiata; CSF=cerebrospinal fluid; CST=corticospinal tract; Cun=cuneus; DAN=dorsal attention network; DAT=dopamine transporter; dlfrontal=dorsal lateral frontal; dlPFC=dorsolateral prefrontal cortex; DMN=default mode network; dmPFC=dorsomedial

prefrontal cortex; EBS=extended brainstem; EC=external capsule; FA=fractional anisotropy; fc=functional connectivity; FDOPA= fluoro-dihydroxyphenylalanine; FEF=frontal eye fields; FFG=fusiform gyrus; FMa=forceps major; FMi=forceps minor; FOG-Q=freezing-of-gait questionnaire; g=gyrus; gCC=genu corpus callosum; GM=gray matter; GP=globus pallidus; HDRS=Hamilton Depression Rating Scale; HF=hippocampal formation; Hip=hippocampus; IC=internal capsule; ICA=independent component analysis; IFG=inferior frontal gyrus; IFOF=inferior fronto-occipital fasciculus; ILF=inferior longitudinal fasciculus; inf=inferior; Ins=insula; IPC=inferior parietal cortex; IPL=inferior parietal lobule; ITG=inferior temporal gyrus; l=lobe; LAS=less affected side; Lb=limbic; LD=longitudinal diffusivity; L-DOPA=L-3,4-dihydroxyphenylalanine; M1=primary motor cortex; MAS=more affected side; MCC=middle cingulate cortex; MD=mean diffusivity; med=medial; medPFC=medial prefrontal cortex; mid=middle; MK=mean kurtosis; MMSE=Mini Mental State Examination; MTG=middle temporal gyrus; MTL=medial temporal lobe; n=nucleus; NAcc=nucleus accumbens; neg=negative; NMS=neuromelanin-sensitive T1-weighted; ns=not significant; OFC= orbitofrontal cortex; Olf=olfactory area; paraHip=parahippocampus; PCC=posterior cingulate cortex; PCR=posterior corona radiata; PDQ=Parkinson's disease questionnaire; PDRP=Parkinson's disease related pattern; PET=positron emission tomography; PiB=Pittsburgh Compound B; PLIC=posterior limb of internal capsule; pos=positive; post=posterior; postCG=postcentral gyrus; PPN=pedunculopontine nucleus; preCG=precentral g; preCun=precuneus; preSMA=pre-supplementary area; PTR=posterior thalamic radiation; Put=putamen; R=right; RD=radial diffusivity; ReHo=regional homogeneity; RG=rectal gyrus; RLIC=retrolenticular limb of internal capsule; rsfc=resting-state functional connectivity; Rx=medication; S1=primary sensory cortex; SaN=salience network; sCC=splenium corpus callosum; SCR=superior corona radiata; SFG=superior frontal gyrus; SFOF=superior fronto-occipital fasciculus; SLF=superior longitudinal fasciculus; SM=sensorimotor; SMA=supplementary motor area; SMG=supramarginal gyrus; SMN=sensorimotor network; SN=substantia nigra; SPL=superior parietal lobule; SS=sagittal stratum; ST=stria terminalis; STG=superior temporal gyrus; STN=subthalamic nucleus; sup=superior; SVM=support vector machine; TC=thalamo-cortical loop; Tha=thalamus; UF=uncinate fasciculus; Unc=uncinate; UPDRS=Unified Parkinson's Disease Rating Scale; VBM=voxel based morphometry; vol=volume; VS/VP=visuospatial/visuoperceptual; WM=white matter.

Table 4

Genetic Parkinsons's disease

Study	Gene	Role	Imaging
Anders 2012	Parkin	mitochondrial autophagy	fMRI of affective face-processing task
Castellanos 2015	Parkin	mitochondrial autophagy	neuromelanin sensitive MRI
	LRRK2	leucine rich repeat kinase	
Eggers 2010	PINK1	mitochondrial kinase	^{18}F-FDOPA PET
Hilker 2012	PINK1	mitochondrial kinase	^{31}P MRSI, ^{1}H MRSI, ^{18}F-FDOPA PET
McNeill 2013	GBA	lysosomal glucocerebrosidase	DaTSCAN (^{123}I-FP-CIT) SPECT
	SNCA	α-synuclein	
	LRRK2	leucine rich repeat kinase	
	PINK1	mitochondrial kinase	
	Parkin	mitochondrial autophagy	
Pavese 2010	Parkin, PINK1	mitochondrial autophagy, mitochondrial kinase	^{18}F-FDOPA PET
Thaler 2014	LRRK2	leucine rich repeat kinase	DTI, VBM MRI
Van Nuenen 2009	Parkin, PINK1	mitochondrial autophagy, mitochondrial kinase	fMRI of motor sequence and internal movement selection tasks
Wu 2013	SCA2	spinocerebellar ataxia type 2 gene	rsfc MRI, fMRI of motor task

Notes: Examples of neuroimaging studies of genetic Parkinson's disease. The first author of each study is listed. All results reported here were from studies obtained during the resting-state unless a task is specified. *Abbreviations:* DTI=diffusion tensor imaging; FDOPA=fluoro-dihydroxyphenylalanine; fMRI=functional MRI; 123I-FP-CIT=FP-CIT=*N*-ϖ-flouro-propyl-2*β*-carbomethoxy-3*β*-(4-iodophenyl)nortropane; MRI=magnetic resonance imaging; MRSI=magnetic resonance spectroscopy imaging; PET=positron emission tomography; rsfc=resting-state functional connectivity; SPECT=single photon emission computed tomography; VBM=voxel-based morphometry.

Neurosci Biobehav Rev. Author manuscript; available in PMC 2016 December 01.

Table 5

Neuroimaging of treatment effects in PD

Study	Treatment	Imaging	Results
Ahmed 2011	L-DOPA	^{11}C-CNS PET (Glu NMDA receptor)	**OFF:** PD-nLID and PD-LID showed similar glutamatergic activity. **ON vs OFF:** PD-nLID showed decreased glutamatergic activity in Cau, Put, preCG; PD-LID showed increased glutamatergic activity in Put, preCG.
Black 2005	L-DOPA	^{15}O-H_2O PET	**ON vs OFF:** PD-nMF showed decreased rCBF in med frontal (BA6) and PCC after L-DOPA, while PD-MF did not. **ON:** PD-MF vs PD-nMF showed increased rCBF in med frontal g, PCC.
Esposito 2013	L-DOPA	rsfc MRI	**OFF**: Drug naive PD vs HC showed decreased rsfc in sensorimotor network. **ON**: rsfc in SMA normalized. Slow-5 band (0.01-.0027 Hz): a spectral peak between 0.015–0.020 Hz was observed for drug naive (**OFF, ON**, placebo) and HC subjects; a second peak between 0.020–0.30 Hz appeared for drug naive **ON** but not other groups.
Feigin 2007	AAV-GAD	^{18}F-FDG PET	**OFF:** PD baseline showed increased PDRP and PDCP activity. PDRP decreased after AAV-GAD; PDCP activity did not change.
Gonzalez-Garcia 2011	rTMS	fMRI	PD rTMS to motor cortex: increased activation in Cau, primary motor, dorsal premotor cortex, and temporal and parietal lobes during simple motor task, or cerebellum and dlPFC in complex motor task; decreased activation in primary somatosensory cortex in simple task or SMA in complex task.
Hellwig 2013	L-DOPA	^{123}I-IBZM SPECT (D2/D3 receptor)	LBD (with PD) or APS: D2 binding in striatum did not independently predict response to dopaminergic therapy
Herz 2015	L-DOPA	DCM, fMRI	**ON**: PD-LID but not PD-nLID showed increased connectivity between Put and M1 during motor task after L-DOPA
Hirano 2008	L-DOPA, STN DBS	^{15}O-H_2O and ^{18}F-FDG PET	**ON vs OFF L-DOPA:** PD showed decreased PDRP CMR but increased CBF; CMR CBF dissociation in Put/GP, ventral Tha, dorsal pons/midbrain (locus coeruleus, PPN, dorsal raphe, STN). PD-LID showed greater CBF changes in Put and pons than PD-DYS-. **ON vs OFF DBS:**PD showed decreased PDRP CMR and CBF - no dissociation.
Jahanshahi 2010	apomorphine (dopamine agonist)	^{15}O-H_2O PET	Brain activations during two types of motor timing tasks: **OFF:** HC showed increased activation in mPFC, Hip, ANG, PCC, NAcc/Cau. PD showed increased activation in cerebellum, Tha, lateral-caudal SN **OFF vs ON**: PD showed pallidal overactivation and cortical underactivation **ON vs OFF**: PD showed effective connectivity increased between Cau and PFC **OFF vs ON**: Red n and habenular n (epithalamus) also showed increased activation for some types of motor timing tasks.
Jech 2013	L-DOPA	rsfc MRI	**ON vs OFF**: PD showed increased rsfc in posterior mesencephalon/PPN, inferior pons, and cerebellar vermis/hemispheres (V, IX)
Kahan 2014	STN-DBS	DCM, rsfc MRI	**STN-DBS stimulation:** PD showed increased effective connectivity of corticostriatal, and thalamocortical, direct connections; decreased STN effective connectivity in hyperdirect, striatal, and thalamus connections. Increasing strength of the direct and hyperdirect connections predicted clinical improvement; increased strength of the striato-STN connection predicted more clinical impairment.
Ko 2013	L-DOPA, STN-DBS	^{15}O-H_2O and ^{18}F-FDG PET	NMRP (↑ L sensorimotor c, premotor c, IPC, cerebellum vermis/paramedian) **OFF:** PD vs HC showed increased resting NMRP expression.

Study	Treatment	Imaging	Results
			ON vs OFF DBS: decreased resting NMRP. **ON vs OFF L-DOPA:** no effect for resting NMRP.
Ko 2014	SHAM (burr hole), AAV-GAD	^{18}F-FDG PET	SSRP (↑ ACC, subgenual cingulate, inferior temporal c, Hip/paraHip, Amg, post cerebellar vermis) in PD patients ↑ SSRP in blinded SHAM-R but not SHAM-nR. 6 months after SHAM, blinded SHAM-R SSRP correlated with motor scores. Baseline SSRP predicted blinded 6 months motor scores. After unblinding, SHAM-R but not GAD-R showed ↓ SSRP.
Kwak 2010	L-DOPA	rsfc MRI	**OFF:** PD vs HC showed increased rsfc{VSi-dmTha}; {dcPut- [ACC,ITG]}; {drPut-[RG, MTG, ACC, vmPFC]}; {vrPut-IFG}. **OFF vs ON:** PD showed increased rsfc {VSi-[SFG, vlPFC, vmPFC, OFC]}; {VSs-[M1, SFG, dlPFC, dmTha, STG]; dCau-[FEF, dlPFC, dmTha]; dcPut-{[M1, FEF, MTG, Cun]}; {drPut-[FEF, M1, dmTha, MTG]}; {vrPut-[M1, postCG, preCun, IPL, cerebellum]}. Frequency band analysis showed increased power in 0.02–0.05 Hz band for PD-OFF vs HC or PD-OFF vs PD-ON.
Kwak 2012	L-DOPA	ALFF MRI	**ON:** PD-ON vs HC showed increased ALFF in preSMA on less affected side; but decreased ALFF in Tha on more affected side and bilateral mid frontal g. **ON vs OFF:** PD showed decreased ALFF in premotor (preCG), SMA, mid frontal g, med frontal g. No increases were observed.
Lee 2012	MSC	^{18}F-FDG PET; MRI 3T T1, DWI	MSA: decreased metabolism and GM density in cerebellum after MSC or placebo; more cortical regions with decreased metabolism and GM density after placebo than MSC. DWI ischemic lesions observed after placebo or MSC.
Ma 2010b	fetal dopamine graft	^{18}F-FDOPA PET	PD: increased FDOPA uptake in Put after graft; baseline FDOPA uptake in ventrorostral putamen correlated with motor scores.
MacDonald 2011	L-DOPA	fMRI	PD: with respect to performance of selection task, dopaminergic treatment impaired encoding and facilitation consistent with role for ventral striatum; but improved interference consistent with a role for dorsal striatum. HC: fMRI of selection task showed dorsal and ventral striatal involvement consistent with hypotheses about PD patients.
Mattis 2011	L-DOPA	^{18}F-FDG PET	**ON vs OFF:** PD without dementia showed decreased PDCP levels that correlated with improvement in verbal learning. Baseline PDCP levels correlated with verbal learning L-DOPA response.
Mishina 2011	L-DOPA	^{11}C-TMSX PET (A_{2A} receptor) ^{11}C-CFT PET (DAT) ^{11}C-RAC PET (D2 receptor)	**OFF:** Drug naive PD vs HC in bilateral Put showed similar TMSX or RAC binding while CFT binding was decreased. Drug naive PD showed asymmetric findings in Put: TMSX, CFT binding was lower and RAC binding increased on more vs less affected side. PD-LID vs HC: TMSX binding was increased. **ON**: Drug naive after treatment showed TMSX binding increased while CFT and RAC binding decreased.
Mure 2011	STN-DBS, Vim-DBS	^{18}F-FDG PET	PDTP: increased activity in primary motor c, Cau/Put, anterior cerebellum (IV–V), dentate n, dorsal pons. PDTP expression progressed more slowly than PDRP expression. PDRP decreased by STN-DBS but not VimDBS. PDTP decreased by STN-DBS or Vim-DBS: effects of Vim-DBS > STN-DBS
Mure 2012	STN-DBS, L-DOPA	^{15}O-H_2O PET	Motor-sequence learning-related network pattern: increased activity in lateral cerebellum, dorsal premotor c, paraHip, and decreased activity in SMA, OFC. **ON vs OFF L-DOPA:** PD no change in learning-related network activity **On vs OFF DBS**: learning-related pattern abnormalities at baseline improved with STN-DBS

Study	Treatment	Imaging	Results
Politis 2012	fetal dopamine graft	^{18}F-FDOPA PET (dopamine, NEpi) ^{11}C-DASB PET (SERT) ^{11}C-RAC PET (D2 receptor)	PD after graft: dopaminergic function normalized in basal ganglia; noradrenergic function normal in locus coeruleus; serotonergic function was decreased in raphe n, Amg, Tha, Hyp, ACC, PCC, PFC.
Politis 2014	L-DOPA, buspirone (serotonin receptor agonist)	^{11}C-DASB PET (SERT) ^{11}C-RAC PET (D2 receptor)	**Off:** PD-LID vs PD-stable showed ns difference serotonin function in striatum. **ON:** PD-LID vs PD-stable showed increased dopamine release in striatum. PD-LID showed buspirone pretreatment before L-DOPA decreased LIDs and decreased dopamine release in striatum. In striatum, increased striatal serotonergic function correlated with larger buspirone dopamine decrease.
Smith 2015	L-DOPA	^{11}C-DASB PET (SERT) ^{11}C-RAC PET (D2 receptor)	**OFF:** PD-stable vs HC showed decreased GP serotonin transporter binding; PD-LID GP serotonin transporter binding normal GP serotonin transporter binding positively correlated with dyskinesia scores **ON:** PD-LID showed increased GP synaptic dopamine; PD-stable ns change
Sweet 2014	STN-DBS	DTI	ns trend increased tremor control with DBS electrode closer to DTT than SPCT
Szewczyk-krolikowski 2015	L-DOPA	rsfc MRI	**OFF:** PD vs HC showed decreased basal ganglia network rsfc in Put, Cau, midbrain, STG, dlPFC, mPFC, preCun **ON vs OFF:** increased rsfc in basal ganglia **ON:** PD vs HC showed ns rsfc
Tinazzi 2014	L-DOPA	^{123}I-FP-CIT SPECT (DAT)	SZ with Parkinsonism: abnormal FP-CIT uptake in Put and Cau predicted motor impairment and response to L-DOPA treatment.
Weiss 2015	STN-DBS	^{15}O-H_2O PET	**OFF or ON:** Imagery of gait vs stance showed activity in SMA, SPL **ON:** Imagery of gait vs stance showed activity in PPN/MLR
Wu 2009	L-DOPA	ReHo fMRI	**OFF:** PD vs HC showed decreased ReHo in Put, Tha, SMA; increased in cerebellum, primary sensorimotor c, premotor c. UPDRS correlated negatively with ReHo Put; positively with ReHo cerebellum **ON:** PD ReHo normalized
Wu 2012	L-DOPA	resting and task-based fcMRI	**OFF:** In HC, SNpc activity predicted activity in SMA, DMN, and dlPFC; in PD, SNpc activity predicted decreases in these structures. PD vs HC showed decreased fc {SNpc-[striatum, GP, STN, Tha, SMA, dlPFC, Ins, DMN, temporal lobe, cerebellum, pons]}. **ON:** L-DOPA normalized many of the abnormalities.
Wu 2013	L-DOPA	rsfc MRI	**OFF:** For asymptomatic SCA2 carriers vs HC, rsfc was decreased {postPut-[antePut, Cau, GP, Ins, temporal c, preSMA]}; increased {postPut-[M1, postCG, preCun, SPL, IPL, ACC, PFC, pons]}; increased {preSMA-[SMA, M1, PMC, ACC, Cau, cerebellum, pons]}. For symptomatic SCA2 carriers vs HC, rsfc decreased {postPut-[pons, Cau, Put, GP, Ins, Tha, preSMA, SMA, postCG]}; no rsfc increases observed. **ON vs OFF:** For asymptomatic carriers and patients there was "increased connectivity of putamen-thalamo-cortical, putamen-cerebellar, and cortical motor circuits in both asymptomatic carriers and patients, and increased putamen-pons connectivity in the patients" (2013: 161).

Notes: Neuroimaging studies of treatment of Parkinson's disease. The first author of each study is listed. Some examples of results from each study are given. All results reported here were from studies obtained during the resting-state unless a task is specified. Studies used longitudinal design.

Abbreviations: **Treatment:** AAV-GAD=adenoassociated virus vector expressing glutamic acid decarboxylase; DBS=deep brain stimulation; L-DOPA= L-3,4-dihydroxyphenylalanine or L-DOPA equivalent; MSC=mesenchymal stem cells; rTMS=repetitive transcranial magnetic stimulation; SHAM=sham surgery; STN=subthalamic nucleus; Vim=ventral intermediate thalamic nucleus.

Imaging: A2A= adenosine receptor; ALFF=amplitude of low frequency fluctuations; CFT= 2β-carbomethoxy-3*β*-(4-fluorophenyl)tropane; CNS=CNS 5161 [N-methyl-3(thyomethylphenyl)cyanamide]; D2 or D3=dopamine receptor; DASB=3-amino-4-(2-dimethylaminomethylphenylthio) benzonitrile; DAT=dopamine transporter; DCM=dynamic causal model; DTI=diffusion tensor imaging; DWI=diffusion weighted imaging; FDG=fluorodeoxyglucose; FDOPA=fluoro-dihydroxyphenylalanine; fMRI=functional MRI; FP-CIT=Ioflupane=*N*-*ϖ*-flouro-propyl-2*β*-carbomethoxy-3*β*-(4-iodophenyl)nortropane; Glu=glutamate; IBZM=iodobenzamide; MRI=magnetic resonance imaging; NEpi=norepinephrine; NMDA=N-methyl-D-aspartate; PET=positron emission tomography; RAC= raclopride; ReHo=regional homogeneity; rsfc=resting state functional connectivity; SERT=serotonin transporter; SPECT=single photon emission computed tomography; TMSX=[7-methyl-11C]-(E)-8-(3,4,5-trimethoxystyryl)-1,3,7-trimethylxanthine.

Results: {X-Y}=functional connectivity between X and Y; {X-[Y1,Y2…]}= functional connectivity between X and Y1, X and Y2, etc. ACC=anterior cingulate cortex; Amg=amygdala; ANG=angular gyrus; antePut=anterior putamen; APS=atypical Parkinson's syndromes; BA=Brodmann area; c=cortex; Cau=caudate; CBF=cerebral blood flow; CMR=cerebral metabolic rate for glucose; Cun=cuneus; dCau=dorsal caudate; dcPut=dorsal caudal putamen; dlPFC=dorsolateral prefrontal cortex; DMN=default mode network; dmTha=dorsomedial thalamus; drPut=dorsal rostral putamen; DTT=dentothalamic tract; fc=functional connectivity; FEF=frontal eye fields; g=gyrus; GAD-R=AAV-GAD gene therapy responders; GM=gray matter; GP=globus pallidus; HC=healthy controls; Hip=hippocampus; Hyp=hypothalamus; IFG=inferior frontal gyrus; Ins=insula; IPC=inferior parietal cortex; IPL=inferior parietal lobule; ITG=inferior temporal gyrus; LBD=Lewy body disease; LID=levodopa induced dykinesia; M1=primary motor cortex; med=medial; mid=middle; MLR=mesencephalic locomotor region; mPFC=medial prefrontal cortex; MSA=multiple system atrophy; MTG=middle temporal gyrus; n=nucleus; NAcc=nucleus accumbens; NMRP=normal movement-related activation pattern; ns= not significant; OFC=orbitofrontal cortex; OFF=scanned when off treatment; ON=scanned when on treatment; paraHip=parahippocampus; PCC=posterior cingulate cortex; PD=Parkinson's disease; PDCP=Parkinson's disease related cognitive pattern; PD-DYS-=PD without dyskinesias; PD-LID=PD with levodopa induced dyskinesias; PD-MF=PD with levodopa-related mood fluctuations; PD-nLID=PD without levodopa induced dyskinesias; PD-nMF=PD without levodopa-related mood fluctuations; PDRP=PD related pattern; PDTP=PD tremor related pattern; PFC=prefrontal cortex; PMC=premotor cortex; post=posterior; postCG=postcentral gyrus; PPN=pedunculopontine nucleus; preCG=precentral gyrus; preCun=precuneus; preSMA=pre-supplementary area; Put=putamen; rCBF=regional cerebral blood flow; RG=rectal gyrus; SCA2= spinocerebellar ataxia type 2 gene; SFG=superior frontal gyrus; SHAM-nR=sham surgery nonresponders; SHAM-R=sham surgery responders; SMA=supplementary motor area; SN=substantia nigra; SNpc=substantia nigra pars compacta; SPCT=subthalamopontocerebellar tract; SPL=superior parietal lobule; SSRP=sham-related metabolic covariance pattern; STG=superior temporal gyrus; STN=subthalamic nucleus; SZ=schizophrenia; Tha=thalamus; UPDRS=Unified Parkinson's Disease Rating Scale; vlPFC=ventrolateral PFC; vmPFC=ventromedial prefrontal cortex; vrPut=ventral rostral putamen; VSi=inferior ventral striatum; VSs=superior ventral striatum.

Neurosci Biobehav Rev. Author manuscript; available in PMC 2016 December 01.